# Critical Compilation of Surface Structures Determined by Low-Energy Electron Diffraction Crystallography

**Philip R. Watson**

*Department of Chemistry, Oregon State University, Corvallis, Oregon 97331*

Received April 15, 1987; revised manuscript received July 16, 1987

This review critically compiles all surface structures derived from low-energy electron diffraction (LEED) crystallography reported in the refereed literature prior to January 1986. Over 250 investigations have been analyzed covering all types of surfaces including clean and adsorbate-covered metal, semiconductor and other nonmetallic substrates. Particular attention is paid to developing and applying objective criteria that allow an estimation of the reliability of a particular structural determination. The important experimental and theoretical aspects of such investigations have been extracted into easily understood tabular form supplemented by many figures and ancillary tables and complete references. It is hoped that this compilation will provide a valuable resource both for the surface science specialist and for those nonspecialists in other areas who need surface crystallographic data.

Key words: critically reviewed data; LEED, low-energy electron diffraction; reliability factor; surface crystallography; surface structure.

## Contents



### List of Tables

### List of Figures



## 1. Introduction

### 1.1. Background

In recent years there has been a trend towards an increasing sophistication of research methods in fields as diverse as catalyst research, microelectronics, metallurgy, and tribology. Many of the most dramatic advances in these areas have come from the development of microscopic theories of behavior resulting from the application of the methods and results of fundamental surface science studies.

The most basic information that we must acquire in order to understand the surface characteristics of materials is a detailed description of the geometrical arrangement of atoms in a surface or adsorbed layer. Only when we know the structure of the surface that we are dealing with can we embark on an exploration of, for instance, its electronic properties. Such surface crystallographic data forms the cornerstone upon which we can build the fundamental relationships between structure and properties.

The premier technique for the determination of such surface structures over the last decade has been low-energy electron diffraction (LEED).[1,2] LEED patterns, which only reveal the symmetry of the surface, and not the arrangement of atoms within the surface unit cell, have been reported frequently in the literature. However, it was only after the development of new theoretical tools and more powerful computers that it became possible to extract structural information from the intensities of the diffracted beams on a routine basis.

From its beginnings in the early 1970s, LEED crystallography has grown steadily in both the number of structural determinations (well over 250 at the time of writing), and in the complexity of the systems studied. As Fig. 1 shows, studies of complex reconstructed surfaces of metals, semiconductors and alloys, and molecular adsorption systems are becoming increasingly frequent. These types of systems require more accurate and faster data collection methods, and often approximate theoretical approaches that allow us to reduce the possible number of model structures.

Although other surface sensitive techniques are con-

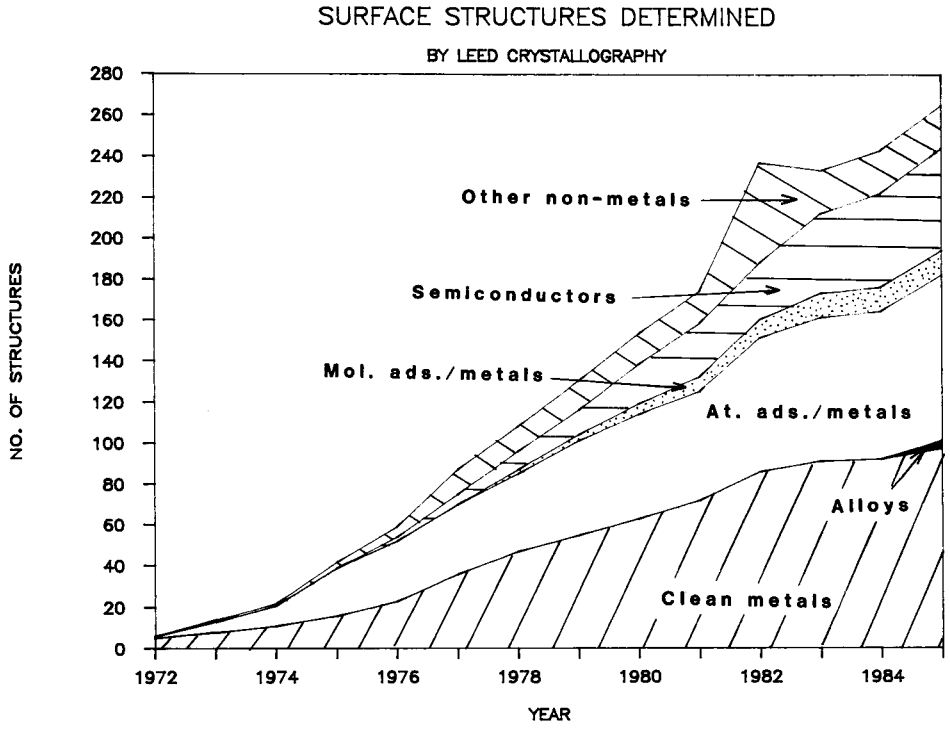


FIG. 1. Growth of LEED crystallographic determinations 1970–1985.

stantly being developed,[3] in terms of the existing database LEED has provided more surface structures than all the other methods combined.

As we shall see, there are many aspects of the LEED experiment, both practical and computational, that affect the confidence level of the result. Unfortunately, unlike x-ray diffraction, the experimental data cannot be directly inverted to yield a unique solution, and one must rely on trial and error search procedures to find the best fit between experimental data and postulated models of the surface structure. Furthermore, there is as yet little agreement within the LEED community as to the best way to compare theory and experiment.

The literature contains several reviews, of varying degrees of completeness, listing the surface structures derived from LEED measurements known at the time.[4–16] Nearly all these compilations, however, are lists of structures with little attempt to assess the reliability of the result. A notable exception to this generalization is a 1978 publication by Jona[10] which details some of the difficulties of this type of work, and attempts some critical examination of published data. This paper is limited in the amount of discussion possible due to its brevity and tutorial nature and, of course, in the eight years since its publication many new structures have been announced.

The present critical compilation summarizes a large amount of literature in an easily accessible and condensed form. It provides a survey of surface structural results derived from LEED data that has been critically examined, based upon objective criteria, as to the accuracy and internal consistency of the quoted results. It is hoped that this survey will be a valuable resource not only for specialists in LEED and other areas of surface science, but also for workers in other disciplines that need surface structural data to understand and extend their work, but lack the expertise to evaluate the complex and interrelating factors that contribute to the reliability of a structure quoted in the literature.

### 1.2. Scope and Organization

This review critically evaluates surface structures determined by LEED crystallography reported in the refereed literature since the inception of modern investigations, roughly 1970, until January 1986. Articles published in unrefereed conference proceedings or society bulletins are not included. Investigations that reported LEED patterns but made no intensity measurements, and hence cannot yield definite structural information, are not considered. The only exceptions to this latter rule are for certain complex semiconductor surfaces where full-scale LEED investigations are not practical and semiquantitative intensity measurements have value.

The main part of the review (Sec. 4) is divided into four parts: A. Clean surfaces of metals and alloys; B. Adsorbate-covered metal surfaces; C. Nonmetallic clean surfaces; and D. Nonmetal/adsorbate systems.

The bulk of the information is presented in the form of large tables, showing the most important experimental and theoretical parameter values and a brief description of the results of the study. This division allows a rather natural separation such that no one Table becomes too unwieldy and difficult to use. Part C covers nonmetallic elements, insulators such as binary metal oxides, and simple and compound semiconductors. Each part also has a number of accompany-

ing notes, figures, and ancillary tables. These serve to amplify and clarify the brief descriptions given in the main tables.

For those readers who are not well versed in the practice of LEED crystallography, a brief review precedes the main body of text. Readers not familiar with the fundamentals of LEED are referred to standard texts.[1,2]

## 2. LEED Crystallography

A proper critical evaluation of a LEED crystallographic study involves a consideration of many different factors, which may have complex interrelationships, that can affect our confidence in the reported result. In order to best appreciate the origins and effects of these influences, we will briefly review the method of LEED crystallography in order to illustrate the sort of difficulties that may arise. Many more detailed reviews exist for the interested reader.[1,2,4,5,10,11]

Determining a surface structure by LEED crystallography proceeds naturally in three stages: measurement, calculation, and comparison. Each of these stages has associated with it certain problems that may affect the reliability of the result and may involve judgements that may be open to more than one interpretation.

### 2.1. The LEED Experiment

The LEED experiment is, at first glance, a rather simple procedure. A beam of low-energy electrons, typically 25–250 eV in energy, is directed from an electron gun onto the surface of interest. Only those electrons that are elastically reflected are allowed by a set of retarding grids to be displayed, most usually on a fluorescent screen. The difficulty in the experiment arises in the process of preparing the surface, choosing the experimental conditions and recording the data.

The first goal of any surface science experiment is to prepare the surface under consideration in the required form. The single-crystal sample is usually cut from a rod or boule, oriented and polished using standard metallographic methods, and mounted on a manipulator. With care the orientation of the polished crystal should be within 1°, or less, of the desired plane. Few workers, however, explicitly state that they check that the x-ray face, as found from a back-reflection Laué photograph, is parallel to the polished optical face. This can be easily done using a small He–Ne alignment laser.[17]

The damage introduced during the cutting and polishing processes is usually removed by cleaning the surface to below some acceptable level of contamination, using thermal, chemical, or ion-bombardment techniques. Chemisorbed structures can then be obtained by adsorption. Analytical techniques such as Auger electron spectroscopy (AES) or x-ray photoelectron spectroscopy (XPS)[18] can reveal adatom concentrations at the level of a few percent of a monolayer coverage and are indispensible adjuncts to the LEED experiment. For the purposes of LEED crystallography, however, the surface must be well crystallized in addition to being clean. In the absence of any well-defined quantitative measure of surface crystallinity, workers generally rely on a visual judgement of a low background coupled with small, sharp diffraction spots to indicate a well-crystallized surface.

The diffracted LEED beams are usually displayed on the fluorescent screen of a typical postacceleration LEED optics. Measurement of the display can be done in several ways using the following:

(1) a Faraday cup; little used now because of its slow and cumbersome nature, but it has the advantage of measuring absolute intensities;

(2) a spot-photometer; has similar problems to the Faraday cup;

(3) photographs digitized by a densitometer,[19] or T.V. camera[20,21]; care is needed for accurate film response;

(4) direct recording by a T.V. camera[22,23] or a resistive anode coupled to a microchannel plate[24]; very fast and easily linked to computer supervision.

It is very important that the method of data collection should be suitable to the problem under study. Increased speed of data collection is increasingly becoming an important goal, especially for the study of reactive and electron beam sensitive adsorbate systems where the LEED data must be collected within a short time period before the integrity of the system is lost. Once collected, the data should be normalized to constant incident beam current and be background subtracted.

### 2.2. Calculation of Diffracted Beam Intensities

The analysis of a surface structure is a trial and error process involving a comparison of beam intensities calculated for a particular postulated surface model with those found experimentally. Attempts to find a data inversion procedure that will result in a unique structural solution have not met with great success.[25–28] Accordingly then, one constructs a model that is consistent with the symmetry and periodicity of the observed LEED pattern. Usually, Occam's Razor is applied and the initial models chosen are those in which atoms occupy positions found in the bulk structure or other high-symmetry environments. In cases where the positions of the atoms in the subsurface layers are not unique, or reconstructions occur, then the situation is not so straightforward.

The nonstructural parameters that go into the theory of low-energy electron scattering—phase shifts, inner potential, absorption, and Debye–Waller factors, also need to be calculated or estimated. Phase shifts can be calculated easily for a given potential, although the precise form of the potential that should be used is not always clear. Standard band-structure potentials have been tabulated for most elements.[29] Fortunately, the sensitivity of the calculated diffracted intensities to the values of the other nonstructural parameters is not very high, and in practice, frequently only the inner potential is included as a fitting variable.

Several computational schemes exist to find the energy dependence of the intensities of diffracted LEED electrons. The reader is referred to the many extensive reviews available.[1,2,5,11] Comparisons of the different major methods show that they are in satisfactory agreement.[30]

Table 1 lists those schemes in common use. In the main

TABLE 1. Schemes for the calculation of theoretical LEED beam intensities

| Basic scheme | Examples in Tables | Reference |
|---|---|---|
| Exact | KKR | 1,31 |
| | CHANGE | 32 |
| | THIN | 33 |
| | IS | 34 |
| | MI | 35,36 |
| Approximate | RFS | 1,11,37 |
| | LD | 1,11,37 |
| | RSP | 38 |
| | CSM | 39 |
| | BSN | 40 |
| | QSD | 41 |
| Kinematical | KIN | 1,2 |
| | CMTA | 42 |
| | CT | 43 |

BSN—beam set neglect
CHANGE/THIN—IBM program suite
CMTA—constant momentum transfer averaging
CSM—combined space method
CT—convolution-transform
IS—inelastic scattering
KIN—kinematical theory
KKR—Korringa–Kohn–Rostoker
LD—layer doubling
MI—matrix inversion
RFS—renormalized forward scattering
RSP—reverse scattering perturbation
QSD—quasidynamical method

they can be grouped into types based on kinematics, exact, and approximate approaches. The kinematical methods have the virtue of simplicity but are only suitable for certain limited situations where a single-scattering approach is justified. The use of exact band structure methods have been largely restricted to the IBM group. The approximate methods, most commonly seen in the CAVLEED and Van Hove-Tong (VHT) embodiments, are popular because of their speed and flexibility. Special precautions, such as the combined-space method (CSM), allow them to be used in situations involving closely spaced atomic layers. The accuracy of these methods does depend upon the choice of certain conditions, such as the number of beams allowed to propagate through the lattice, and must be borne in mind when assessing such calculations. Some approximate methods have been developed [e.g., quasidynamical method (QSD) and beam set neglect (BSN)] to deal with complex adsorbates and large unit cells.

### 2.3. Evaluation of Structural Models

Once the experimental data has been collected and the corresponding calculations completed, it remains to decide which model best fits the measured data. In the early days of the technique, visual comparison was the norm. While the eye has excellent sensitivity for distinguishing small details between a pair of calculated and observed curves, it is very difficult to assess the cumulative fit of many such pairs and it can be hard to obtain agreement between different judges.

Several workers have attempted to construct reliability, or R-factors that can provide a more quantitative description of the degree of fit between theory and experiment.[44–52] These are listed in Table 2. While these factors go some way to providing a reliable indicator of the quality of fit, they all suffer from one or more shortcomings—in that they overemphasize or ignore certain features of the data—such that there is no agreed standard among workers in the field. In a rather thorough analysis of the operation of ten different R-factors, including the popular ones due to Zanazzi and Jona[48] and Pendry,[49] Van Hove and Koestner[52] showed that none alone was really satisfactory. They showed that probably the best course is to apply several different R-factors, which may be picked for their tendency to emphasize certain aspects of the data, to the same data set and look for trends of agreement between the various factors.

TABLE 2. Reliability (R-) factors developed for LEED crystallography

| R-factor | Type | Authors | Reference |
|---|---|---|---|
| VHT | Several | Van Hove, Tong, Elconin | 46 |
| $R_x$ | x ray | Duke *et al.* | 47 |
| ZJ | Complex | Zanazzi and Jona | 48 |
| P | Log. deriv. | Pendry | 49 |
| A | x-ray | Adams *et al.* | 50 |
| R2 | Metric dist. R2 | Phillip and Rundgren | 51 |
| M | Other metrics | Phillip and Rundgren | 51 |

Despite this rather unsatisfactory state of affairs, it is clear that use of such quantitative measures does allow for a consistent evaluation of competing structural models and of comparison of results from one laboratory to another. There is little doubt that this is the way of the future and that there will not only be improvements in the design of R-factors themselves, but that predictor methods will be developed that will allow us to find the global minimum R-factor, corresponding to the best-fit structure, with a minimum of computational effort and maximum confidence.[52]

## 3. Evaluation Criteria

The methodology for critically evaluating LEED crystallographic data will focus principally on the most critical areas of the technique, the collection of data and comparison of theory with experiment. With a few exceptions, most workers have used tested and reliable computational schemes, hence the exact method of calculation is not often a strong determinant of reliability.

Given the many diverse components that go into a complete LEED crystallographic study, and the many factors that can influence the reliability of a given result, it is difficult to come up with some simple numerical index that would signify a "good" or "bad" structure. The most realistic solution to providing a confidence level for a given result is to draw up a list of criteria which would define a very reliable study. In some instances such a criterion might indeed be numerical—a contamination level in percent of a monolayer, or the number of independent beams used in a comparison of theory and experiment. In other instances we might be able to give a yes/no answer to questions like *Is a reliability factor used* ?. Sometimes it may only be possible to

reveal unquantifiable misgivings about some aspect of the procedures—for instance doubts as to a careful avoidance of disturbing effects such as electron beam damage.

Therefore, we will now examine the criteria to be used in assessing the reliability of the experimental and model evaluation procedures before attempting a synthesis of these various factors into a confidence level for a given result.

## 3.1. Experimental Aspects

The preparation of the surface under study and collection of diffraction data are such a fundamental part of the LEED experiment that it is incumbent upon us to make a critical examination of the described procedures. As the metallographic techniques for preparing a polished crystal slice of a particular orientation are standard procedures, we assume that the sample is oriented to within 1°, unless the authors note otherwise.

### 3.1.a. Criteria for Effective Surface Preparation

(1) Is AES, XPS or other surface analytical technique used to monitor surface cleanliness, and/or adsorption?

(2) Is the contamination level below 5% of a monolayer? Are actual spectra shown, or, e.g., Auger peak ratios noted, to backup this value?

(3) Is the surface highly crystalline? Are photographs of LEED patterns provided?

To be fully assured of adequate surface preparation we should be able to give an affirmative answer to all these questions. In fairness, however, it would be sufficient for an author to refer to a previous paper in which these details have been covered.

### 3.1.b. Criteria for Reliable Data Collection

(1) Is the method of data collection suitable for the system under study?

(2) Are contaminant buildup, electron beam effects, etc., seen to be avoided?

(3) Has identical data been obtained from more than one sample?

In reviewing both data collection and cleaning procedures, it is somewhat difficult to know how to weight any deficiencies found in these areas in the context of the whole study. How much effect would a certain level of contamination have on the observed data and derived structure? How much electron-stimulated desorption can we tolerate before the results are invalidated? These questions are difficult to answer with any degree of assurance and hence, while we should record misgivings, it is unlikely that any but the most major shortcomings could seriously compromise a structural result. It is particularly reassuring to find that closely similar sets of experimental data have been measured from more than one separately prepared sample.

## 3.2. Criteria for Comparison of Theory with Experiment

It is in the area of the comparison of the LEED intensities predicted from a model surface with experimental observations that we come to the criteria that, perhaps, might most clearly distinguish between various studies. The majority of recent work uses reliable calculations and good experimental practice, yet frequently there are noticeable variations in the amount, and the characteristics of the data used for comparison with theory. In order to assess how variations of this nature affect our reliance in the derived result, we shall present more criteria and then some arguments in justification. These are the following:

(1) A numerical reliability factor or index used.

(2) Data taken for at least two angles of incidence.

(3) At each angle at least five distinct experimental beams used for comparison, including a high percentage of nonintegral beams, if present.

(4) Only beams with at least an energy range of 40 eV and having some structure included in the analysis.

(5) At least one beam at each angle should have a beam index greater than 1.

(6) The inner potential should be varied systematically in combination with structural parameters.

(7) Several surface structural models should be examined, possibly including changes in more than one interlayer spacing, registry shifts and, in molecular systems, adsorbate stoichiometry.

(8) Any estimated error should be consistent with the demonstrated procedures.

Let us review these criteria in some detail; they are based upon the author's own experience and the work of Jona[10] and Van Hove and Koestner.[52] First, it is clearly preferable to have the work of comparing many sets of experimental and theoretical data done in an objective and consistent manner by computer. The lack of agreement between LEED workers as to what constitutes a good reliability factor means that it is difficult to find many studies that use exactly the same index. Hence it is not usually possible to use R-factor values to distinguish between differing results found by different groups. However, R-factors do have a very important role to play in finding an internally consistent best-fit structure for a particular set of experimental data.

Regardless of the form of any factor, or factors, used, there will be some sort of linkage between the total amount of data compared and the reliance that we can place on the answer having the best fit. Criteria 2–4 above attempt to define the minimum amount of data that is needed in to reach a reasonable confidence level in a structure determination. These criteria are arbitrary but are based on the results of personal experience and conform with published ideas.[10]

Many studies rely heavily on data taken at normal incidence. Using such data is convenient computationally, because of the savings in time and storage possible due to symmetry. However, the number of independent sets of data that can be extracted from normal incidence data is far smaller than that at some arbitrary angle because many beams are made identical to one another by these same symmetry elements. Thus, in order to obtain a sufficiently large data set, it is really necessary to take data, at the least, at two angles of incidence.

However, this criterion must be used with some care as occasions arise where the surface structure is too complex for full-blown dynamical LEED calculations except under

conditions of optimal symmetry. In such cases there is little point in recording data at off-normal incidence.

We use a lower limit of ten distinct beams as representing a criterion for a reasonable dataset. In the cases where fractional-order beams exist from, e.g., an overlayer, a high proportion, such as half, of the measured data should be such beams. This will ensure that the analysis reflects properties of the overlayer, and not primarily the substrate, which may be the case if predominantly integral-order data is analyzed. Furthermore, it is obvious, but bears restating, that there is little point in analyzing beams that are of extremely short range, or possess little in the way of structural features that can be matched to theory.

In criterion 5, we take account of the fact that higher order beams are generally more difficult to match during a structure analysis.[10] Hence, this criterion suggests that at least one beam at a given angle should be from beyond the first shell in reciprocal space.

The sixth criterion is to check that the fit between theory and experiment is not distorted by an improper treatment of the inner potential. As this nonstructural parameter is unknown *a priori*, it is generally estimated as the sum of the Fermi energy plus the work function. To a good approximation, the effect of varying this parameter upon intensity-energy curves is to produce a rigid shift of the energy scale. Hence, the elaborate LEED calculations need not be repeated for different values of the inner potential, but the effect can be simulated during comparison of theory and experiment by translating the intensity-energy curve along the energy axis.

The problem that frequently arises is that changes in this nonstructural parameter, and changes in a structural quantity, such as a bond length, are coupled together. Thus the value of the structural parameter producing the best fit between the observed and calculated data may change if the value of the inner potential is altered. What is more, this change may vary in unpredictable ways between different beams. Thus it is important that this parameter is varied over a wide range of values during the comparison stage of analysis. Contour plots having the inner potential as the $y$ axis, the structural parameter as the $x$ axis, and the degree of fit, as measured by an R-factor, as the contour, work very well for this purpose.[53]

Criterion 7 is intended to address the difficult problem of deciding when enough different structural models have been tested to give us confidence that we are not resting in some local minimum of the parameter space, but are truly at the global minimum of the system. In the simpler systems we have some guides. For example, for a FCC(100) surface that shows a $(1\times1)$ LEED pattern, experience has shown that it is unlikely, but possible, that the surface is reconstructed. Even in such simple systems, complications such as variations of the interlayer spacings of the second or deeper layers deserve to be tested. The more complex the system under study, the more structural models that need to be tried, particularly in molecular adsorbate systems in which we may not be sure of the stoichiometry. Once again, we cannot, in reality, assign any hard and fast numbers to this criterion. Its role will be essentially a negative one; in cases where, for instance, only a very small number of models were tested, it would have an impact in the total estimation of the reliability of the determination.

An eighth possible criterion refers to the error limits on their results quoted by some authors; thus a bond length may be reported as being within 0.1 Å of a certain value. This value may result from the step used in the variation of a structural parameter such as a layer spacing or bond length, or may be derived from an interpolation of a grid of $R$-factor results. Here this criterion will again be used in a negative sense; that is, it will be noted if the quoted error does not appear to be consistent with the data and procedures described in the paper.

### 3.3. Overall Assessment of Reliability—a Caveat

Having enunciated several criteria for estimating the degree of confidence we find in a particular structure determination, it remains to try to find a way to wrap all these different factors into one overall assessment of the confidence level of the structure. As discussed earlier, this is very difficult to do because of the varied nature of the different criteria and the lack of a numerical basis for distinguishing conflicting results.

Accordingly, as detailed below, this critical compilation presents the reader with a rather complete picture of a study in a very condensed form in a series of tables. Each table is arranged so as to allow the reader to easily and quickly find a structure. Furthermore each table is accompanied by a large number of explanatory notes, figures, and ancillary tables. Thus, at a glance, the reader will be able to tell to what extent this study has fulfilled the criteria laid out above.

Cognizant of the difficulties already alluded to in formulating an overall level of confidence in a study, the reviewer has attempted an objective synthesis of the many factors contributing to the reliability of a LEED analysis. This overall rating system ranks as follows.

A—the large majority of the criteria listed above were met.

B—most of the criteria were met but the study has some shortcomings that lessen its reliability.

C—a number of serious omissions or deficiencies sufficient to cast doubt on the reliability of the study.

The user of this compilation should be wary of taking these ratings as more than a guide. It is possible that the structures produced by some studies rated as C may well be correct. Our experience and knowledge of related systems, or corroborating evidence from other techniques, may lessen the need for, for instance, a large database in some investigations. What the rating in such a case shows is that this particular study does not meet the criteria laid down above. These criteria are intended as a generally applicable set that allow us to assess *the methodology of the experiment, not the accuracy of the final result.*

It is equally possible that some studies that fulfill all the criteria necessary for an A rating in this compilation may not derive the correct surface structure. This is a particular problem in LEED investigations where trial and error searches for the best-fit structure are the order of the day. An

A-rated study may have been superbly performed, but simply have not covered a sufficiently large fraction of the volume of model parameter space to discover the structure that lies at the global minimum.

## 4. Surface Structure Compilations

### 4.1. Organization of the Tables

The Summary Tables A–D (Tables 3, 8, 13, and 20) are organized so that a particular structure can be readily found. Within each Table the entries are arranged with the following priorities:

(1) alphabetically by substrate;

(2) numerically by the surface plane Miller indices, i.e. (100) before (110) before (111);

(3) alphabetically by adsorbate, when present;

(4) size of the unit cell, i.e. (1×1) before (2×1) before (2×2). [Here, we arbitrarily assign p(2×2) higher priority than c(2×2).]; and

(5) chronologically by date of publication.

When an entry contains a dash, this indicates that this information was not specified. A query indicates that the value of the parameter in question was discussed but not clearly defined.

To avoid confusion, the references for each Table are arranged immediately following and are labeled by the identification letter of the Table. Hence the tenth reference for Table 8 (Summary Table B) would be referred to in the text as B10. The general references for the review are separately gathered together at the end of the review in Sec. 6, and do not carry any identifying letter.

As some structures are too complex to be easily summarized in a table, the reader is then directed from the main tables to an associated set of explanatory notes, figures, and ancillary tables.

Below are listed explanations of some of the symbols used as table headings and abbreviations that may be encountered in the body of the tables.

*Number of samples:* (S)

The number of experimental samples from which data was taken.

*Crystallinity:* (Crys.)

The degree of surface crystallinity reported as high (H), moderate (M), or low (L). When photographs are reproduced then P appears in parentheses.

*Analytical method:* (Anal. method or Anal. meth.)

AES—Auger electron spectroscopy.

EELS—Electron energy loss spectroscopy.

XPS—X-ray photoelectron spectroscopy.

When spectra are reproduced then S appears in parentheses.

*Contamination level:* (Contamn. level or Cont. level)

The reported level of surface contamination in percent of a monolayer. Low indicates an unspecified "clean" state.

*Data collection:* (Data coll.)

F—Faraday cup; SP—spot photometer; P-MD—photographic/microdensitometer; P-TV—photographic/TV; and TV—direct TV.

*Number of angles:* (Angs.)

The number of angles of incidence at which data was taken.

*Normal (Off norm.):*

The number of beams measured at normal (off-normal) incidence, first integral, then fractional-order beams. In parentheses the number of beams measured with an index $>1$.

*Range:*

The total number of beams used with an energy range $>40$ eV.

*Calculation:* (Calc.)

Some of the less common methods are listed below. Others are listed in Table 1 and discussed in Sec. 2.2.

CAVLEED = Cavendish Laboratory Suite.

DLEED = diffuse LEED.[54]

SPLEED = spin-polarized LEED.[55]

VHT = Van Hove/Tong Suite.[11]

*Number of models:* (Mods.)

The number of models explored. Here, we take one model to be distinguished from another by an atomic arrangement in which something other than a vertical interlayer separation has changed. As interlayer separations are trivial to vary, it makes little sense to count structures that differ only by a small change in such a spacing as a "model."

*R-factor:*

See Sec. 2.3 and Table 2.

*Inner potential:* (Vor)

The value of the best fit, or assumed, inner potential in electron volts. A notation of E-dep indicates an energy dependent inner potential was used.

*Overall rating:* (Rating)

A—C as described above.

*Adsorption site:* (Ads. site)

See Sec. 4.3.b and Fig. 7.

4-F = fourfold coordinate site, e.g., FCC(100).

3-F(1) = threefold coordinate site with an atom directly below in the next layer, e.g., FCC(111).

3-F(2) = threefold coordinate site with no atom directly below in the next layer, e.g., FCC(111).

2-F(S) = twofold coordinate short-bridge site, e.g., FCC(110).

2-F(L) = twofold coordinate long-bridge site, e.g., FCC(110).

1-F = onefold coordinate site.

*Bulk interlayer spacing:* (Bulk d)

The value of the inner layer spacing in the bulk material (Å).

*Overlayer spacing:* (d0)

The value of the distance of an overlayer from the substrate in the normal direction (Å). Error in parentheses where given.

*Interlayer spacings:* ($\delta$di%)

The value of the vertical interlayer spacing beween the first and second layers, etc., expressed in terms of percentage changes from the bulk value. A notation of (*) for this entry indicates that the bulk value was assumed. Error in parentheses where given.

*Bond lengths:*

Values of bond lengths in angstroms with the identity of the atoms in the bond. Error in parentheses where given.

# 4.2. Clean Surfaces of Metals and Alloys

## 4.2.a. Summary Table A

TABLE 3. (Summary Table A) Clean surfaces of metals and alloys

| Sub-trate | Surf-ace | Struc-ture | Ref. | S | Crys. | Anal. method | Contamn. level | Data coll. | Angs. | Normal | Off norm. | Range | Calc. | Mods. | R-factor | R-Vor | Rating | Bulk d | δd1% | Comments |
|---|---|---|---|---|---|---|---|---|---|---|---|---|---|---|---|---|---|---|---|---|
| Ag | 100 | (1×1) | 1 | 1 | — | AES(S) | 1–2% O | SP/FC | 5 | 2 (1) | 7 (3) | 9 | KKR | 1 | — | −5 | B− | 2.043 | 0.0 | Assumed bulk structure; data from [2]. |
| Ag | 110 | (1×1) | 3 | 1 | L | AES | — | SP | 2 | 4 (1) | 1 (0) | 5 | CT | — | — | −7 | B− | 1.445 | −7.0 | Data from [4] |
| Ag | 110 | (1×1) | 4 | 1 | L | AES | — | SP | 3 | 3 (0) | 12 (1) | 15 | KKR | 5 | — | −8 | B | 1.445 | −7.0 | Poor visual fit, possibly due to surface roughness |
| Ag | 110 | (1×1) | 5 | 1 | H | AES | — | SP | 3 | 3 (0) | 12 (4) | 15 | KKR | 1 | 0.20 (ZJ) | −8.8 | A | 1.445 | −10.0 (1.0) | Repeat of [4] using new data, better agreement attributed to less surface roughness |
| Ag | 110 | (1×1) | 6 | 1 | H | AES | Low | FC | 1 | 7 (>2) | 0 | >4 | KKR | 1 | 0.1 (ZJ) | −10.5 | B | 1.445 | −6.6 (1.5) | |
| Ag | 111 | (1×1) | 7 | 1 | H | None | — | SP | 3 | 0 | 3 (0) | 3 | RFS | 1 | — | −8.5 | C | 2.359 | 0.0 | Assumed bulk structure; tested several scattering potentials |
| Al | 100 | (1×1) | 8 | 1 | H | None | — | SP | 6 | 5 (0) | 2 (0) | 7 | IS | 1 | — | −17 | B− | 2.021 | 0.0 | Experimental data mainly from [9]. |
| Al | 100 | (1×1) | 10 | 1 | H | AES | 5% O | SP | 3 | 2 (0) | 3 (0) | 5 | KKR | 1 | — | −11 | B− | 2.021 | 0.0 | Data at 110 K. |
| Al | 100 | (1×1) | 11 | 1 | H | AES | <5% O | SP | 3 | 2 (0) | 3 (0) | 5 | RFS | 1 | — | −7.5 | B− | 2.021 | 0.0 | Data from [10]. |
| Al | 100 | (1×1) | 12 | 1 | H | AES | Low | SP | Many | — | 0 | — | NIS | 1 | — | −12 | B− | 2.021 | 0.0 | Iso-intensity maps of (00) beam. |
| Al | 110 | (1×1) | 8 | 1 | M | None | — | SP | 4 | 3 (0) | 9 (0) | 12 | IS | 1 | — | −17 | B | 1.432 | −10.0 | Data from [9]. |
| Al | 110 | (1×1) | 13 | 1 | M | None | — | SP | 1 | 0 | 5 (0) | 5 | KKR | 1 | — | −5 | B− | 1.432 | −10.0 | |
| Al | 110 | (1×1) | 14 | 1 | M | None | — | SP | 2 | 1 (0) | 3 (0) | 4 | IS | 1 | — | — | C | 1.432 | −12.5 (2.5) | Data from [9]. |
| Al | 110 | (1×1) | 12 | 1 | H | AES | Low | SP | Many | — | 0 | — | NIS | 1 | — | −12 | B− | 1.432 | −10.0 | Iso-intensity maps of (00) beam. |
| Al | 110 | (1×1) | 3 | 1 | L | AES | Low | SP | 3 | 2 (0) | 4 (0) | 6 | CT | — | — | −8 | B− | 1.432 | −4.0 | Data from [9,13]. |
| Al | 110 | (1×1) | 15 | 1 | H | — | — | SP | 1 | 9 (6) | 0 | 9 | LD | 1 | 0.05 (A) | E-dep | B+ | 1.432 | −8.4 | Data at 100 K. |
| Al | 110 | (1×1) | 16 | 1 | H | AES | Low | FC | 1 | 8 (6) | 0 | 8 | RFS | 1 | 0.034 (ZJ) | −9.6 | B+ | 1.432 | −8.5 | Room temperature data. |
| Al | 110 | (1×1) | 17 | 1 | H | AES | <2% C,O | SP | 1 | 9 (6) | 0 | 9 | LD | 4 | 0.042 (A) | E-dep | B+ | 1.432 | −8.6 (0.8) | Also optimized Debye temp and imaginary part of electron self energy. Same data as [15]. |
| Al | 111 | (1×1) | 13 | 1 | H | None | — | SP | 2 | 0 | 7 (0) | 7 | KKR | 1 | — | −7 | B | 2.334 | <5 | |
| Al | 111 | (1×1) | 8 | 1 | H | None | — | SP | 3 | 1 (0) | 4 (0) | 5 | IS | 1 | — | −17 | B | 2.334 | 0.0 | Data mainly from [9]. |
| Al | 111 | (1×1) | 12 | 1 | H | None | — | SP | 1 | 0 | 3 (0) | 3 | IS | 1 | — | — | C | 2.334 | 0 (5) | Data of [9]. |
| Al | 111 | (1×1) | 18 | 1 | H | None | — | SP | 3 | 2 (0) | 11 (2) | 13 | CHANGE | 1 | 0.21 (ZJ) | −8.7 | A | 2.334 | 2.2 (1.3) | Re-examination of data from [9]. |
| Al | 111 | (1×1) | 19 | 1 | H | AES | <0.1% | SP | 1 | 5 (2) | 0 | 5 | RFS | 1 | 0.063 (A) | −11.6 | B+ | 2.334 | 0.9 (0.5) | Data taken at 90 K. |
| Al | 311 | (1×1) | 20 | 1 | H(P) | AES | <0.5% Si | FC | 1 | 21 | 0 | — | RSP | 2 | 0.07 (ZJ) | −10.9 | A− | 1.227 | −13.3 (1.0) | |
| Au | 100 | (1×1) | 21 | — | — | — | — | TV | 1 | — | — | — | QSD | — | 0.15 (ZJ) | — | ? | 2.039 | — | |
| Au | 110 | (1×2) | 22 | 1 | H | AES | — | FC | 1 | 6 (4) | 0 | 6 | KKR/RFS | 1 | 0.68 (ZJ) | −13 | B | 1.442 | — | Poor agreement with missing row model. |
| Au | 110 | (1×2) | 23 | 1 | * | AES | Low | FC | 1 | 19 (>6) | 0 | >8 | RFS | 3 | 0.28 (ZJ) | −9 | A | 1.442 | −15.0 | *Spots broadened along ⟨001⟩. Missing row model best fit; no 2nd layer displacements; (1×2) structure produced irreversibly from (1×3) at 350 K. |
| Au | 110 | (1×2) | 24 | 1 | * | AES | Low | FC | 1 | 18 (16) | 0 | 18 | RFS | 3 | 0.25 (ZJ) | — | A | 1.442 | −20.0 | Update of [23]. Modified missing-row model best fit with distortions 0.35 (P) down to 3rd layer. See notes. |
| Co | 0001 | (1×1) | 25 | 1 | H | AES(S) | <1% C | SP | 2 | 1 (0) | 6 (1) | 7 | RFS | 2 | — | −16 | B | 2.046 | 0.0 (2.0) | HCP termination; reversible phase change to FCC at 450 °C. |
| Co | 0001 | (1×1) | 26 | 1 | — | AES | — | — | 2 | 1 (0) | 1 (0) | 2 | RFS | 1 | — | — | C | 2.046 | 0.0 | |

TABLE 3. (Summary of Table A) continued

| Sub-trate | Surf-ace | Struc-ture | Ref. | S | Crys. | Anal. method | Contamn. level | Data coll. | Angs. | Normal | Off norm. | Range | Calc. | Mods. | R-factor | Vor | Rating | Bulk d | δd1% | Comments |
|---|---|---|---|---|---|---|---|---|---|---|---|---|---|---|---|---|---|---|---|---|
| Co | 100 | (1×1) | 27 | 1 | — | AES | 10%C,3%O | SP | 3 | 2 (0) | 10 (2) | ⩾6 | KKR | 1 | 0.19 (ZJ) | − 16.5 | A | 1.775 | − 4.0 | Rapid cooling avoided phase change to HCP; cleaning difficult. |
| Co | 11-20 | (1×1) | 28 | — | H | AES | Low | FC | 1 | 6 (5) | 0 | 6 | LD | 2 | 0.088 (ZJ)<br>0.22 (P) | − 16 | A − | 2.507 | − 8.5 (3.0) | No change of interatomic distances within the plane. |
| Co | 111 | (1×1) | 25 | 2 | — | AES(S) | < 1% C | SP | 2 | 1 (0) | 6 (1) | 7 | RFS | 4 | — | − 16 | B | 2.046 | 0.0 | FCC termination; high-temperature allotrope; crystallinity and damage dependent on rate of temperature change. |
| Cu | 100 | (1×1) | 29 | 1 | — | AES | < 1% | FC | Many | — | — | — | MA | 1 | — | — | C | 1.807 | 0.0 | |
| Cu | 100 | (1×1) | 30 | 1 | H | None | — | SP | 8 | 3 (0) | 14 (0) | 14 | IS | 1 | — | − 13 | B | 1.807 | 0.0 (2.0) | Data from [31]–[33]. |
| Cu | 100 | (1×1) | 34 | 1 | — | AES | < 1% | FC | Many | — | — | — | MA | 1 | — | — | C | 1.807 | 0.0 (1.0) | Surface registry vector increased by 8%. |
| Cu | 100 | (1×1) | 35 | 1 | — | AES | Low | FC | 1 | 4 (2) | 0 | 4 | RFS | 1 | — | − 9.5 | B − | 1.807 | − 1.1<br>(0.4) | Data from [36]. |
| Cu | 110 | (1×1) | 37 | 1 | — | AES | Low | FC | 1 | 6 (3) | 0 | 6 | RFS | 1 | 0.12 (ZJ) | − 8.5 | B + | 1.278 | − 10.0 (2.5) | |
| Cu | 110 | (1×1) | 38 | 1 | H | AES | Low | SP | 1 | 9 (6) | 0 | 9 | LD | 1 | 0.066 (A) | − 8.9 | B + | 1.278 | − 8.5 (0.6) | |
| Cu | 111 | (1×1) | 39 | 1 | H | AES | < 3% | P-TV | 2 | 4 (2) | 12 (4) | ⩾12 | RFS | 1 | 0.13 (ZJ) | − 9.5 | A | 2.087 | − 4.0 | Different Cu potentials had little effect. |
| Cu | 111 | (1×1) | 40 | 1 | H | AES | 5% | SP | 2 | 8 (4) | 13 (4) | ⩾6 | RFS | 1 | 0.05 (ZJ)<br>0.41 (P) | − 9 | A | 2.087 | 0.0 (1.0) | |
| Cu | 111 | (1×1) | 41 | — | — | — | — | SP | 1 | 3 (0) | 0 | 3 | KKR | 1 | 0.011 (M) | E-dep | B | 2.087 | − 0.6 (0.1) | Tested several potentials; Hedin- Lundquist local density approximation gave best results. Used unpublished experimental data. |
| Cu | 111 | (1×1) | 42 | 1 | — | — | — | SP | 2 | 2 (0) | 1 (0) | 3 | LD | 1 | 0.39 (M) | E-dep | B | 2.087 | − 0.7 (0.5) | Measured energy-dependent Vor. |
| Cu | 311 | (1×1) | 43 | 1 | H | AES | Low | P-TV | 1 | 8 (6) | 0 | 8 | LD | 1 | 0.09 (ZJ) | − 7.7 | B + | 1.097 | − 5.0 (1.5) | Data from [44]. |
| Fe | 100 | (1×1) | 45 | 1 | H | AES | 2-4%C,O | SP | 3 | 4 (2) | 12 (3) | 15 | KKR | 1 | 0.15 (ZJ ) | − 11.5 | A | 1.433 | − 1.4 (3.0) | Did not test for reconstructions. |
| Fe | 110 | (1×1) | 46 | 2 | — | AES | — | — | 5 | 7 (3) | 16 (5) | 22 | KKR | 2 | 0.10 (ZJ) | − 11.5 | A | 2.026 | 0.0 (0.5) | A reconstruction in which top layer atoms fill quasi 3-fold sites discounted. |
| Fe | 111 | (1×1) | 47 | 1 | — | AES | — | SP | 2 | 5 (2) | 9 (5) | 14 | THIN | 1 | 0.15 (ZJ) | − 11.1 | A | 0.827 | − 15.4 (3.0) | |
| Fe | 210 | (1×1) | 48 | 1 | — | AES | — | SP | 3 | 13 (9) | 18 (10) | 28 | KKR | 8 | 0.103 (ZJ) | − 11.5 | A | 0.641 | − 22.0 (4.7) | Substantial relaxations both parallel and perpendicular down to 5th layer (see notes). |
| Fe | 211 | (1×1) | 49 | 1 | H | AES | Low | SP | 3 | 7 (2) | 12 (4) | 19 | KKR | 3 | 0.111 (ZJ) | − 11.3 | A | 1.170 | − 10.5 | Perpendicular and parallel relaxations. See notes. |
| Fe | 310 | (1×1) | 50 | 1 | — | AES | — | SP | 3 | 9 (5) | 12 (4) | 21 | CHANGE | 3 | 0.116 (ZJ) | − 10.1 | A | 0.906 | − 16.0 (3.0) | Perpendicular and parallel relaxations. See notes. |
| Ir | 100 | (1×1) | 51 | — | — | — | — | TV | 1 | 6 | 0 | — | QSD | 1 | 0.09 (ZJ) | — | B + | 1.910 | − 3.5 (0.5) | |
| Ir | 100 | (1×5) | 52 | 1 | H | AES | Low | P | 3 | 6,4 | 27,⩾14 | 33 | RSP/RFS | 19 | — | − 15 | A − | 1.910 | 10 | Prefer hexagonal reconstruction (see notes). |
| Ir | 100 | (1×5) | 53 | 1 | H | AES | Low | TV | 1 | 11,9 | 0 | 11 | CSM | 9 | 0.34 (ZJ) | − 15 | A − | 1.910 | 10 | Quasi-hexagonal reconstruction. Update of [52]. |
| Ir | 110 | (1×1) | 54 | 1 | — | AES | — | FC | 1 | 8 (5) | 0 | 8 | LD | 1 | — | − 8 | B + | 1.352 | − 7.5 (3.0) | Structure stabilised by 0.25 monolayer of randomly distributed O |
| Ir | 110 | (1×2) | 55 | 1 | — | AES | < 2%C | FC | 1 | 18,10 (12) | 0 | 17 | LD/RSP | 4 | 0.24 (ZJ) | − 13 | A − | 1.352 | − 15.0 (4.0) | Missing-row model favoured. See notes. |
| Ir | 111 | (1×1) | 56 | 1 | H | AES | < 5% | SP | 3 | 1 (0) | 0 | 3 | RFS | 1 | — | − 11 | C | 2.207 | − 2.5 (5.0) | Also used convolution-transform method. |
| Mo | 100 | (1×1) | 57 | 1 | — | AES(S) | Low | SP | 2 | 0 | 10 (0) | 10 | KKR | 1 | — | − 16 | B + | 1.57 | − 11.5 | |
| Mo | 100 | (1×1) | 58 | 1 | — | AES | Low | SP | 2 | 0 | 16 (7) | 13 | LD | 1 | 0.16 (ZJ) | E-Dep | A | 1.57 | − 9.5 (2.0) | |
| Mo | 110 | (1×1) | 59 | 1 | H | AES | Low | SP | 1 | 5 (2) | 0 | 5 | RFS | 2 | 0.09 (ZJ) | E-dep | B | 2.22 | 1.6 (2.0) | Kohn-Sham exchange preferred. |

TABLE 3. (Summary of Table A) continued

| Sub-trate | Surf-ace | Struc-ture | Ref. | S | Crys. | Anal. method | Contamn. level | Data coll. | Angs. | Normal | Off norm. | Range | Calc. | Mods. | R-factor | Vor | Rating | Bulk d | δd1% | Comments |
|---|---|---|---|---|---|---|---|---|---|---|---|---|---|---|---|---|---|---|---|---|
| Na | 110 | (1×1) | 60 | — | M | EELS | — | SP | 1 | 3 (0) | 0 | 3 | RFS | 1 | — | −2.7 | C | 3.040 | 0.0 | Examined role of potential. |
| Na | 111 | (1×1) | 61 | — | — | UPS | — | SP | 2 | 2 (0) | 0 | 2 | KKR | 2 | — | — | C | 1.241 | — | HCP structure favoured. Na evaporated onto Cu(111) at 77 K; little difference between different model intensities. |
| Ni | 100 | (1×1) | 62 | * | * | * | * | * | Many | 5 (0) | 0 | 5 | IC | 1 | — | −18.4 | B− | 1.762 | 0.0 | * Data from Refs. 5 to 9 in this paper. |
| Ni | 100 | (1×1) | 63 | 1 | H | AES | Low | SP | 4 | 3 (0) | 2 (0) | 5 | KKR | 1 | — | −11 | B− | 1.762 | 0.0 (2.5) | Data of [64]. |
| Ni | 100 | (1×1) | 65 | 2 | H | AES | — | FC | Many | — | — | — | CMA | — | — | — | C | 1.762 | 0.0 (4.0) | |
| Ni | 110 | (1×1) | 63 | 1 | H | AES | Low | SP | 6 | 3 (0) | 1 (0) | 4 | KKR | 1 | — | −11 | B− | 1.246 | −5.0 | Data from [64]. |
| Ni | 110 | (1×1) | 56 | 1 | H | AES(S) | Low | SP | 6 | 3 (1) | 5 (0) | 8 | CT | — | — | −20 | B | 1.246 | −5.0 | Data from [64]. |
| Ni | 110 | (1×1) | 66 | 1 | H | AES | Low | SP | Many | — | — | — | RFS | 1 | — | E-dep | B | 1.246 | −7.0 | Used I(g) method. Data from [67]. |
| Ni | 110 | (1×1) | 67 | 1 | H | AES | Low | SP | 7 | 6 (3) | 18 (6) | 24 | RFS | 1 | 0.16 (ZJ) | E-dep | A | 1.246 | −7.0 | Isointensity maps; same structural conclusion from analysis of I(E) and I(g) data. |
| Ni | 110 | (1×1) | 68 | 2 | H | AES | <2% | SP | 7 | 6 (3) | 29 (>6) | >24 | LD | 1 | 0.02 (R2) | −8.4 | A | 1.246 | −8.7 | |
| Ni | 110 | (1×1) | 69 | 1 | H | AES | Low | SP | 7 | 3 | 6 | 9 | RFS/LD | 2 | 0.20 (VHT) | −12.2 | A− | 1.246 | −9.8 (1.8) | Data from [64]. |
| Ni | 110 | (1×1) | 70 | 2 | H | AES | <2% | SP | 1 | 9 (6) | 0 | 9 | LD | 1 | 0.02 (R2) | −8.4 | A− | 1.246 | −8.7 (0.5) | |
| Ni | 111 | (1×1) | 62 | 3 | * | * | * | * | 1 | 6 (0) | 0 | 6 | IC | 1 | — | −14 | B− | 2.035 | 0.0 | See [59]. Experimental data from referneces 8,9 in this paper. |
| Ni | 111 | (1×1) | 63 | 1 | H | AES | Low | FC | 3 | 1 (0) | 2 (0) | 3 | KKR | 1 | — | −11 | C | 2.035 | 0.0 | Data [64]. |
| Ni | 311 | (1×1) | 71 | 2 | H | AES | <2% S | P-TV | 1 | 11 (8) | 0 | 11 | LD | 1 | 0.13 (ZJ)<br>0.34 (P) | −10.5 | B+ | 1.063 | −14.0 | |
| Ni | 311 | (1×1) | 72 | 1 | H | AES | <2% S | F-TV | 1 | 11 (8) | 0 | 11 | LD | 6 | 0.048 (R2) | −11.4 | A− | 1.063 | −15.9 (1.5) | No interlayer registry changes. Data from [71]. |
| Pd | 100 | (1×1) | 73 | 1 | H | AES | Low | FC | 2 | 5(3) | 0 | — | RFS | 1 | — | −10 | B− | 1.929 | 0.0(2.5) | Data not reproduced |
| Pd | 100 | (1×1) | 74 | 1 | H | AES(S) | Low | SP | 1 | 2 (0) | 0 | 2 | LD | 1 | — | −9.0 | C | 1.929 | 0 | |
| Pd | 110 | (1×1) | 75 | 1 | H | AES | — | TV | 1 | 7 (4) | 0 | 7 | CAVLEED | 1 | 0.15 (P)<br>0.11 (R2) | −5.2 | B+ | 1.372 | −5.7 (2) | |
| Pd | 110 | (1×1) | 76 | 1 | M | AES | — | TV | 1 | 7 (4) | 0 | 7 | CAVLEED | 2 | 0.11 (P)<br>0.11 (A) | −5 | B+ | 1.372 | −6.0 (2.0) | No lateral reconstructions. |
| Pd | 110 | (1×2) | 76 | 1 | H | AES | — | TV | 1 | 13,7 (>5) | 0 | >6 | CAVLEED | 4 | 0.37 (P)<br>0.27 (R2) | −6.8 | A− | 1.372 | −5.0 (2.0) | Reconstruction induced by small coverages of Na,Cs. Could not distinguish between missing-row and sawtooth models. |
| Pd | 111 | (1×1) | 77 | 1 | H | AES | Low | SP | 2 | 3 | 4 (0) | >4 | RFS | 1 | — | −11 | B− | 2.228 | 0.0 | |
| Pt | 100 | (14 1<br>−15 | 52 | 1 | H | AES | Low | P | 3 | >5,4 | — | >5 | MI/RFS | 8 | — | −14.3 | B− | 2.176 | — | Subset of experimental data from P.C. Stair Ph.D Thesis University of California, Berkeley. Hexagonal reconstruction (see notes). |
| Pt | 110 | (1×2) | 78 | 2 | H | AES | Low | SP | 1 | 10 (7) | — | 10 | CS | 3 | 0.42 (A) | — | B+ | 1.387 | 23 | Moderate agreement with missing-row model. See notes. |
| Pt | 111 | (1×1) | 79 | 1 | H | AES | Low | P | 4 | 2 (0) | 6 (0) | >8 | TM | 1 | — | −14.3 | B | 2.265 | 0.0 (5.0) | |
| Pt | 111 | (1×1) | 80 | 1 | H | AES | Low | P | 3 | — | >3 | >3 | LD | 1 | — | −14.3 | C | 2.265 | 0.0 (2.5) | More extensive calculations than [79]. |
| Pt | 111 | (1×1) | 81 | 1 | H | AES | <1% | SP | 7 | 5 (3) | 43 (14) | 48 | RFS | 1 | 0.16 (R2) | −5.4 | A | 2.265 | 1.0 (0.5) | Investigated effect of non-structural parameters on fit. |

TABLE 3. (Summary of Table A) continued

| Substrate | Surface | Structure | Ref. | S | Crys. | Anal. method | Contamn. level | Data coll. | Angs. | Normal | Off norm. | Range | Calc. | Mods. | R-factor | Vor | Rating | Bulk d | δd1% | Comments |
|---|---|---|---|---|---|---|---|---|---|---|---|---|---|---|---|---|---|---|---|---|
| Re | 10–10 | (1×1) | 82 | 1 | H | None | — | FC | 1 | 2 (0) | 0 | 2 | — | 2 | 0.15 (ZJ) | −14 | B− | 0.80 | −17.0 | Data from [83]. Distinguished between two possible terminations |
| Rh | 100 | (1×1) | 39 | 1 | H | AES | <2% | P-TV | 2 | 4 (3) | 12 (8) | 15 | RFS | 3 | 0.21 (ZJ) | −11.5 | A | 1.902 | 0.0 (3.0) | Data from [84]. |
| Rh | 110 | (1×1) | 85 | 1 | H | AES | <2% | P-TV | 2 | 5 (2) | 8 (3) | 13 | RFS/LD | 1 | 0.15 (ZJ) | −11 | A | 1.345 | −3.0 (2.0) | |
| Rh | 111 | (1×1) | 86 | 1 | H | AES | <2% | P-TV | 2 | 5 (2) | 9 (3) | 14 | RFS | 2 | 0.18 (ZJ) | −9.5 | A | 2.195 | 0.0 (2.0) | |
| Rh | 111 | (1×1) | 87 | 1 | — | AES(S) | Low B | FC | 1 | 5 (2) | — | 5 | RFS | 2 | — | −10 | B | 2.195 | 0.0 (5.0) | |
| Ru | 0001 | (1×1) | 88 | 1 | — | AES | — | FC | 1 | 5 (3) | 0 | 5 | RFS/LD | 1 | 0.04 (ZJ) | −12.0 | B+ | 2.140 | −2.0 (2.0) | |
| Sc | 0001 | (1×1) | 89 | 1 | — | AES | 5% O | SP | 2 | 2 (0) | 5 (0) | >3 | RFS | 4 | 0.23 (ZJ) | −9.5 | B+ | 2.630 | −2.0 (1.0) | |
| Ta | 100 | (1×1) | 90 | 1 | H(P) | AES | Low | FC | 2 | 5 (3) | 1 (0) | 6 | LD | 1 | 0.21 (ZJ) | — | B+ | 1.652 | −11.0 | Small H exposure affected I(E) curves. |
| Ti | 0001 | (1×1) | 91 | 1 | H | AES(S) | <2% O | SP | 4 | 2 (1) | 22 (10) | 24 | KKR | 2 | — | −10 | A− | 2.340 | −2.0 (2.0) | |
| V | 100 | (1×1) | 92 | 1 | H | AES(S) | V. low O | SP | 1 | 5 (3) | 0 | 5 | RFS | 1 | 0.08 (R2) | −9.2 | B+ | 1.514 | −7.0 (1.0) | (1×5) structure found if O present; Data taken in Ar to avoid CO contamination. |
| V | 110 | (1×1) | 93 | 1 | H(P) | AES(S) | <2% O | SP | 1 | 6 (3) | 0 | 6 | RFS/LD | 1 | 0.03 (R2) | −9.2 | B+ | 2.150 | 1.0 (1.0) | Correction of [94]. |
| W | 100 | (1×1) | 95 | 1 | — | None | — | SP | 1 | 4 (2) | 16 (0) | 20 | LD | 1 | — | −10 | A− | 1.578 | −6.0 (1.0) | Data from [96]. |
| W | 100 | (1×1) | 97 | 1 | H | AES | <1.5% C | FC | 5 | 4 (3) | 8 (1) | 12 | LD | 1 | — | −12 | A− | 1.578 | −4.4 (2.5) | Data at 470 K. |
| W | 100 | (1×1) | 98 | 1 | — | AES(S) | Low C | — | 1 | 4 (1) | 0 | 4 | LD | 1 | — | −10 | B− | 1.578 | −11.0 (2.0) | Care taken to avoid H contamination. |
| W | 100 | (1×1) | 99 | 1 | — | AES | Low | FC | Many | — | — | — | RELEED | 1 | — | −10 | B+ | 1.578 | −5.5 (1.5) | Used rotation diagrams at several energies; relativistic calculations |
| W | 100 | (1×1) | 100 | 1 | — | AES | — | TV | 1 | 4 (2) | 0 | 4 | RFS | 1 | 0.20 (ZJ) | −13 | B | 1.578 | −10.0 (2.0) | |
| W | 100 | (1×1) | 101 | 1 | — | AES | Low | SP | 2 | 4 (2) | 0 | 4 | CAVLEED | 1 | 0.24 (ZJ) | −10.5 | B | 1.578 | −6.7 (1.0) | Used I(E) and I(G) data and relativistic phase shifts. |
| W | 100 | (1×1) | 102 | 1 | — | AES | Low | FC | 2 | 4 (2) | 2 (0) | 6 | LD | 1 | 0.30 (ZJ) | −11 | B+ | 1.578 | −8.0 (1.5) | Pseudo-relativistic phase shift; data from [106]. |
| W | 100 | (1×1) | 103 | 1 | H | AES | Low | Mott | 6 | 3 (1) | 7 (0) | 10 | SPLEED | 1 | — | — | B+ | 1.578 | −7.0 (1.5) | Spin-polarized LEED measurements. |
| W | 100 | c(2×2) | 104 | — | — | — | — | — | 2 | 4,2 (1) | 1 (0) | 5 | KKR | 2 | — | −10 | B | 1.578 | −6.0 | Zig-zag reconstruction (see notes). |
| W | 100 | c(2×2) | 105 | 1 | H(P) | AES | <1.5% C | FC | 1 | 7,5 (4) | 0 | 7 | RFS/LD | 3 | 0.27 (ZJ) | −12 | B+ | 1.578 | −6.0 | See notes. |
| W | 110 | (1×1) | 95 | 1 | H | — | — | FC | 2 | 3 (2) | 2 (1) | 5 | LD | 2 | — | −10 | B | 2.231 | 0.0 (2.0) | Data from [106]. |
| Zn | 0001 | (1×1) | 107 | — | — | None | — | SP | 1 | Many | — | — | CMTA | — | — | −14 | C | 2.120 | 0.0 (2.0) | Averaged experimental data of [108] at 70 K. |
| Zr | 0001 | (1×1) | 109 | 1 | H | AES(S) | Low | P-TV | 2 | 4 | 8 | 13 | RFS | 2 | 0.12 (ZJ) | −9.6 | A | 2.570 | −1.0 (2.0) | Data taken quickly to avoid CO contamination. |

TABLE 3. (Summary of Table A) continued

| Sub-trate | Surf-ace | Struc-ture | Ref. | S | Crys. | Anal. method | Contamn. level | Data coll. | Angs. | Normal | Off norm. | Range | Calc. | Mods. | R-factor | Vor | Rating | Bulk d | δd1% | Comments |
|---|---|---|---|---|---|---|---|---|---|---|---|---|---|---|---|---|---|---|---|---|
| Ni3Al | 100 | (1×1) | 110 | 1 | H | AES | Low | TV | 3 | 5 (>1) | 24 (>1) | >6 | CHANGE | 2 | — | — | A − | 1.78 | 0.0 | Found that surface layer is mixed Ni-Al (see notes). |
| NiAl | 110 | (1×1) | 111 | 1 | H | AES | Low | FC | 1 | 5 (2) | 0 | — | RFS | 2 | 0.05 (ZJ) | — | B + | 2.04 | − 6.0 | Surface is rippled (see notes). |
| Pt50 Ni50 | 111 | (1×1) | 112 | 1 | H | AES | Low | — | 3 | >3 (0) | >3 (0) | 9 | KKR | 2 | 0.11 (R1) | — | A − | 2.16 | − 2.0 (1.0) | Found unusual compositions (see notes). |
| Pt78 Ni22 | 111 | (1×1) | 112 | 1 | H | AES | Low | — | — | — | — | — | KKR | 2 | — | — | B | 2.22 | − 2.0 (1.0) | Found unusual compositions (see notes). |

### 4.2.b. References to Table 3—Clean metals


[1]D. W. Jepsen, P. M Marcus, and F. Jona, Phys. Rev. B **8**, 5523 (1973).
[2]E. W. Hu, R. M. Goodman, and F. Jona, *ibid.*, 5519 (1973).
[3]C. M. Chan, S. L. Cunningham, M. A. Van Hove, and W. H. Weinberg, Surf. Sci. **67**, 1 (1977).
[4]E. Zanazzi, F. Jona, D. W. Jepsen, and P. M. Marcus, J. Phys. C **10**, 375 (1977).
[5]M. Maglietta, E. Zanazzi, F. Jona, D. W. Jepsen, and P. M. Marcus, J. Phys. C **10**, 3287 (1977).
[6]J. R. Noonan and H. L. Davis, Vacuum **32**, 107 (1982).
[7]F. Soria, J. L. Sacedon, P. M. Echenique, and D. Tetterington, Surf. Sci. **68**, 448 (1977).
[8]G. E. Laramore and C. B. Duke, Phys. Rev. B **5**, 267 (1972).
[9]F. Jona, IBM J. Res. Dev. **14**, 4 (1970).
[10]B. A. Hutchins, T. N. Rhodin, and J. E. Demuth, Surf. Sci. **54**, 419 (1976).
[11]M. A. Van Hove and S. Y. Tong, Surf. Sci. **54**, 91 (1976).
[12]Groupe D'Etude Des Surfaces, Surf. Sci. **62**, 567 (1977).
[13]D. W. Jepsen, P. M. Marcus, and F. Jona, Phys. Rev. B **6**, 3684 (1972).
[14]M. R. Martin and G. A. Somorjai, Phys. Rev. B **7**, 3607 (1973).
[15]H. B. Nielsen, J. N. Andersen, and D. L. Adams, J. Phys. C **15**, L111 (1982).
[16]J. R. Noonan and H. L. Davis, Phys. Rev. B **29**, 4349 (1984).
[17]J. N. Andersen, H. B. Nielsen, L. Petersen, and D. B. Adams, J. Phys. C **17**, 173 (1984).
[18]F. Jona, D. Sondericker, and P. M. Marcus, J. Phys. C **13**, L155 (1980).
[19]H. B. Nielsen and D. L. Adams, J. Phys. C **15**, 615 (1982).
[20]J. R. Noonan, H. L. Davis, and W. Erley, Surf. Sci. **152**, 142 (1985).
[21]E. Lang, W. Grimm, and K. Heinz, Surf. Sci. **117**, 169 (1982).
[22]J. R. Noonan and H. L. Davis, J. Vac. Sci. Technol. **16**, 587 (1979).
[23]W. Moritz and D. Wolf, Surf. Sci. **88**, L29 (1979).
[24]W. Moritz and D. Wolf, Surf. Sci. **163**, L655 (1985).
[25]B. W. Lee, R. Alsenz, A. Ingatiev, and M. A. Van Hove, Phys. Rev. B **17**, 1510 (1978).
[26]G. L. P. Berning, G. P. Alldredge, and P. E. Viljoen, Surf. Sci. **104**, L225 (1981).
[27]M. Maglietta, E. Zanazzi, F. Jona, D. W. Jepsen, and P. M. Marcus, Appl. Phys. **15**, 409 (1978).
[28]M. Welz, W. Moritz, and D. Wolf, Surf. Sci. **125**, 473 (1983).
[29]J. M. Burkstrand, G. G. Kleiman, and F. A. Arlinghaus, Surf. Sci. **46**, 43 (1974).
[30]G. E. Laramore, Phys. Rev. B **9**, 1204 (1974).
[31]S. Andersson, Surf. Sci. **18**, 325 (1969).
[32]L. R. Bedell and H. E. Farnsworth, Surf. Sci. **41**, 165 (1974).
[33]R. J. Reid, Surf. Sci. **29**, 603 (1972).
[34]G. C. Kleiman and J. M. Burkstrand, Surf. Sci. **50**, 493 (1975).
[35]H. L. Davis and J. R. Noonan, J. Vac. Sci. Technol. **20**, 842 (1982).
[36]H. L. Davis and J. R. Noonan, J. Vac. Sci. Technol. **17**, 194 (1980).
[37]H. L. Davis, J. R. Noonan, and L. H. Jenkins, Surf. Sci. **126**, 246 (1983).
[38]D. L. Adams, H. B. Nielsen, and J. N. Andersen, Surf. Sci. **128**, 294 (1983).
[39]P. R. Watson, F. R. Shepherd, D. C. Frost, and K. A. R. Mitchell, Surf. Sci. **72**, 562 (1978).
[40]S. P. Tear, K. Roll, and M. Prutton, J. Phys. C **14**, 3297 (1981).
[41]J. Neve, P. Westrin, and J. Rundgren, J. Phys. C **16**, 1291 (1983).
[42]S. A. Lindgren, L. Wallden, J. Rundgren, and P. Westrin, Phys. Rev. B **29**, 576 (1984).
[43]R. W. Streater, W. T. Moore, P. R. Watson, D. C. Frost, and K. A. R. Mitchell, Surf. Sci. **72**, 744 (1978).
[44]W. T. Moore, R. W. Streater, D. C. Frost, and K. A. R. Mitchell, Solid State Commun. **42**, 139 (1977).
[45]K. O. Legg, F. Jona, D. W. Jepsen, and P. M. Marcus, J. Phys. C **10**, 937 (1977).
[46]H. D. Shih, F. Jona, and P. M. Marcus, J. Phys. C **13**, 3801 (1980).
[47]H. D. Shih, F. Jona, D. W. Jepsen, and P. M. Marcus, Surf. Sci. **104**, 39 (1981).
[48]J. Sokolov, F. Jona, and P. M. Marcus, Phys. Rev. B **31**, 1929 (1985).
[49]J. Sokolov, H. D. Shih, U. Bardi, F. Jona, and P. M. Marcus, J. Phys. C **17**, 371 (1984).
[50]J. Sokolov, F. Jona, and P. M. Marcus, Phys. Rev. B **29**, 5402 (1984).
[51]P. Heilmann, K. Heinz, and K. Müller, Surf. Sci. **83**, 487 (1979).
[52]M. A. Van Hove, R. J. Koestner, P. C. Stair, J. P. Biberian, L. L. Kesmodel, I. Bartos, and G. A. Somorjai, Surf. Sci. **103**, 189 (1981).
[53]E. Lang, K. Müller, K. Heinz, M. A. Van Hove, R. J. Koestner, and G. A. Somorjai, Surf. Sci. **127**, 347 (1983).
[54]C. M. Chan, S. L. Cunningham, K. L. Luke, W. H. Weinberg, and S. P. Withrow, Surf. Sci. **78**, 15 (1978).
[55]C. M. Chan, M. A. Van Hove, W. H. Weinberg, and E. D. Williams, Surf. Sci. **91**, 440 (1980).
[56]C-M. Chan, S. L. Cunningham, M. A. Van Hove, W. H. Weinberg, and S. P. Withrow, Surf. Sci. **66**, 394 (1977).
[57]A. Ignatiev, F. Jona, H. D. Shih, D. W. Jepsen, and P. M. Marcus, Phys. Rev. B **11**, 4787 (1975).
[58]L. J. Clarke, Surf. Sci. **91**, 131 (1980).
[59]L. Morales de la Garza and L. J. Clarke, J. Phys. C **14**, 5391 (1981).
[60]P. M. Echenique, J. Phys. C **9**, 3193 (1976).
[61]S. A. Lindgren, J. Paul, L. Wallden, and P. Westrin, J. Phys. C **15**, 6285 (1982).
[62]G. E. Laramore, Phys. Rev. B **8**, 515 (1973).
[63]J. E. Demuth, P. M. Marcus, and D. W. Jepsen, Phys. Rev. B **11**, 1460 (1975).
[64]J. E. Demuth and T. N. Rhodin, Surf. Sci. **42**, 261 (1974).
[65]W. N. Unertl and M. B. Webb, Surf. Sci. **59**, 373 (1976).
[66]L. J. Clarke, R. Baudoing, and Y. Gauthier, J. Phys. C **15**, 3249 (1982).
[67]Y. Gauthier, R. Baudoing, C. Gaubert, and L. Clarke, J. Phys. C **15**, 3223 (1982).
[68]Y. Gauthier, R. Baudoing, Y. Joly, C. Gaubert, and J. Rundgren, J. Phys. C **17**, 4547 (1984).
[69]M. L. Xu and S. Y. Tong, Phys. Rev. B **31**, 6332 (1985).
[70]D. L. Adams, L. E. Petersen, and C. S. Sorensen, J. Phys. C **18**, 1753 (1985).
[71]W. T. Moore, S. J. White, D. C. Frost, and K. A. R. Mitchell, Surf. Sci. **116**, 253 (1982).
[72]D. L. Adams, W. T. Moore, and K. A. R. Mitchell, Surf. Sci. **149**, 407 (1985).
[73]R. J. Behm, K. Christmann, G. Ertl, and M. A. Van Hove, J. Chem. Phys. **73**, 2984 (1980).
[74]W. Berndt, R. Hora, and M. Scheffler, Surf. Sci. **117**, 188 (1982).
[75]R. D. Diehl, M. Linroos, A. Kearsley, C. J. Barnes, and D. A. King, J. Phys. C **18**, 4069 (1985).
[76]C. J. Barnes, M. Q. Ding, M. Lindroos, R. D. Diehl, and D. A. King, Surf. Sci. **162**, 59 (1985).
[77]F. Maca, M. Scheffler, and W. Berndt, Surf. Sci. **160**, 467 (1985).
[78]D. L. Adams, H. B. Neilsen, M. A. Van Hove, and A. Ignatiev, Surf. Sci. **104**, 47 (1981).
[79]L. L. Kesmodel and G. A. Somorjai, Phys. Rev. B **11**, 630 (1975).
[80]L. L. Kesmodel, P. C. Stair, and G. A. Somorjai, Surf. Sci. **64**, 342 (1977).
[81]D. L. Adams, H. B. Nielsen, and M. A. Van Hove, Phys. Rev. B **20**, 4789 (1979).
[82]H. L. Davis and D. M. Zehner, J. Vac. Sci. Technol. **17**, 190 (1980).
[83]D. M. Zehner and H. E. Farnsworth, Surf. Sci. **30**, 335 (1972).
[84]K. A. R. Mitchell, F. R. Shepherd, P. R. Watson, and D. C. Frost, Surf. Sci. **64**, 737 (1977).
[85]D. C. Frost, S. Hengrasmee, K. A. R. Mitchell, F. R. Shepherd, and P. R. Watson, Surf. Sci. **76**, L585 (1978).
[86]F. R. Shepherd, P. R. Watson, D. C. Frost, and K. A. R. Mitchell, J. Phys. C **11**, 4591 (1978).
[87]C-M. Chan, P. A. Thiel, J. T. Yates, Jr. , and W. H. Weinberg, Surf. Sci. **76**, 296 (1978).
[88]G. Michalk, W. Moritz, H. Pfnür, and D. Menzel, Surf. Sci. **129**, 92 (1983).
[89]S. Tougaard and A. Ignatiev, Surf. Sci. **115**, 270 (1982).
[90]A. Titov and W. Moritz, Surf. Sci. **122**, L709 (1982).
[91]H. D. Shih, F. Jona, D. W. Jepsen, and P. M. Marcus, J. Phys. C **9**, 1405 (1976).
[92]V. Jensen, J. N. Andersen, H. B. Neilsen, and D. L. Adams, Surf. Sci. **116**, 66 (1982).
[93]D. L. Adams and H. B. Neilsen, Surf. Sci. **116**, 598 (1982).
[94]D. L. Adams and H. B. Neilsen, Surf. Sci. **107**, 305 (1981).
[95]M. A. Van Hove and S. Y. Tong, Surf. Sci. **54**, 91 (1976).
[96]P. S. P. Wei, J. Chem. Phys. **53**, 2939 (1970).
[97]M. K. Debe, D. A. King, and F. S. March, Surf. Sci. **68**, 437 (1977).
[98]B. W. Lee, A. Ignatiev, S. Y. Tong, and M. A. Van Hove, J. Vac. Sci. Technol. **14**, 291 (1977).
[99]J. Kirschner and R. Feder, Surf. Sci. **79**, 176 (1979).
[100]P. Heilmann, K. Heinz, and K. Müller, Surf. Sci. **89**, 84 (1979).
[101]L. J. Clarke and L. Morales de la Garca, Surf. Sci. **99**, 419 (1980).
[102]F. S. Marsh, M. K. Debe, and David A. King, J. Phys. C **13**, 2799 (1980).
[103]R. Feder and J. Kirschner, Surf. Sci. **103**, 75 (1981).

[104]R. A. Barker, P. J. Estrup, F. Jona, and P. M. Marcus, Solid State Commun. **25**, 375 (1978).
[105]J. A. Walker, M. K. Debe, and D. A. King, Surf. Sci. **104**, 405 (1981).
[106]J. C. Buchholz, G-C. Wang, and M. G. Lagally, Surf. Sci. **49**, 508 (1975).
[107]W. N. Unertl and H. V. Thapliyal, J. Vac. Sci. Technol. **12**, 263 (1975).
[108]J. M. Baker and J. M. Blakely, Surf. Sci. **32**, 45 (1972).
[109]W. T. Moore, P. R. Watson, D. C. Frost, and K. A. R. Mitchell, J. Phys. C **12**, L887 (1979).
[110]D. Sondericker, F. Jona, V. L. Moruzzi, and P. M. Marcus, Solid State Commun. **53**, 175 (1985).
[111]H. L. Davis and J. R. Noonan, J. Vac. Sci. Technol. A **3**, 1507 (1985).
[112]Y. Gauthier, Y. Joly, R. Baudoing, and J. Rundgren, Phys. Rev. Lett. **31**, 6216 (1985).

#### 4.2.c. Notes—Clean metal surfaces

Clean metal surfaces were the earliest types of system to be studied by LEED crystallography and interest persists to the present day. Most studies have focused on the low-index faces of the face-centered cubic (FCC) metals. The body-centered cubic (BCC) materials W, Fe, and Mo have also received attention while only a few surfaces, almost exclusively the basal (0001) planes, of the hexagonal close-packed (HCP) metals have been studied.

Figure 2 shows the arrangement of surface atoms for some ideal low-index planes of these three systems. Here the top and bottom parts of each panel show top and side views, respectively. Thin-lined atoms lie behind the plane of thick-lined atoms. Dotted lines represent atoms in bulk positions; displacements are shown by arrows. While many metal surfaces closely resemble a truncated bulk lattice, some surfaces exhibit reconstructions that can involve vertical and lateral displacements of atoms from their bulk positions.

Table 3 (Summary Table A) reveals that sometimes a wide range of results and reliability ratings appear for the same surface. This is largely a result of the various investigations occurring over a time period of up to 15 yr. Some early studies appeared before many of the critical factors affecting the reliability of LEED experiments were understood. Nevertheless, later studies with more data and assisted by R-factors have often shown that the original studies were in essence correct. This is particularly in the case of simple surfaces like Al(100) where later studies refined, but did not alter the sense of, the older results.

In the case of the complex reconstructions of the (100) and (110) surfaces of Au, Ir, and Pt, it is only relatively recently that approximate LEED theory and the collection of large experimental databases have enabled investigators to at least narrow down the range of possible surface structures.

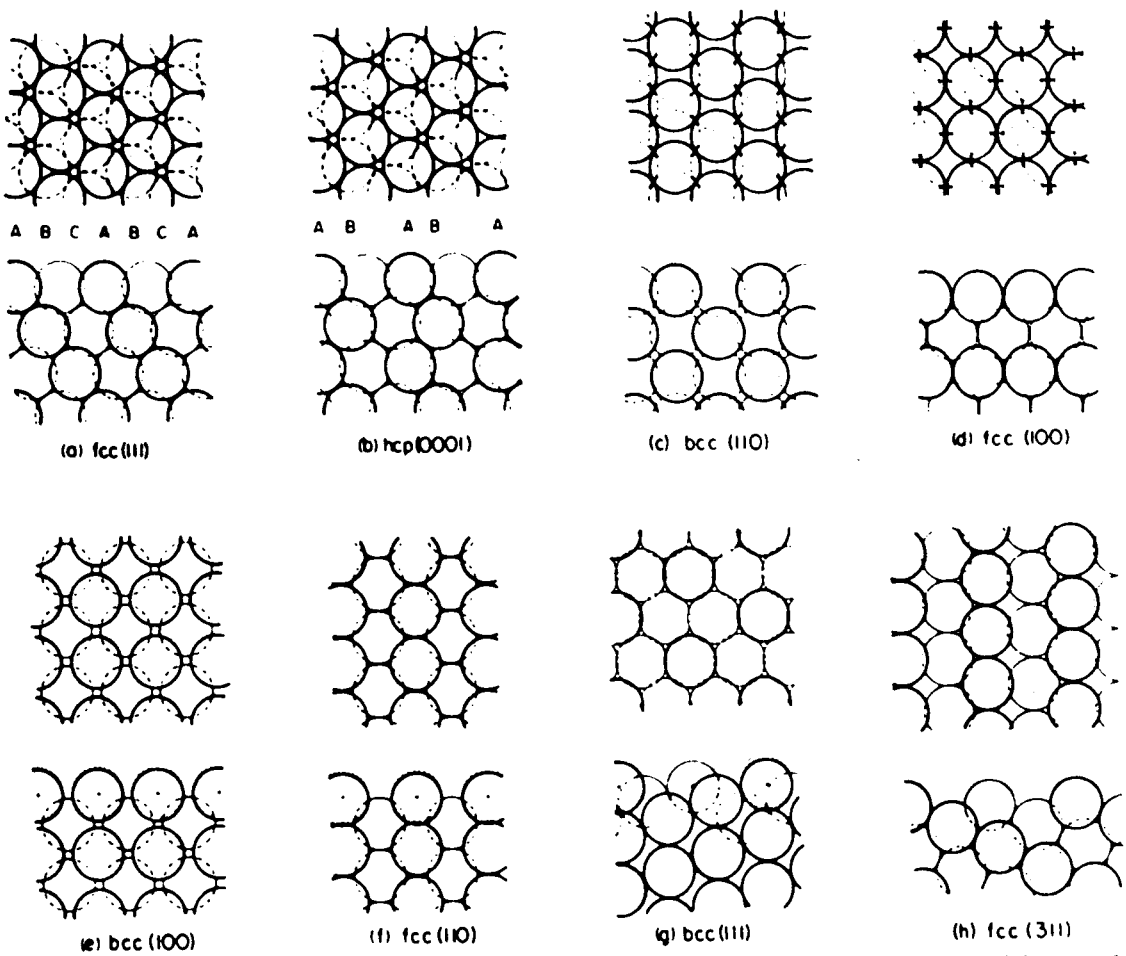


FIG. 2. Schematic diagram of the ideal structures of some simple low-index surfaces of metals. In each panel the top and bottom parts are top and side views, respectively (from Ref. 13). Reprinted with the permission of Springer [G. A. Somorjai and M. A. Van Hove, *Adsorbed Monolayers on Surfaces* (Springer, Berlin, 1981), Figs. 6.1 and 6.2].

TABLE 4. Structural parameters derived for metal surfaces exhibiting multilayer relaxations

| Surface | Bulk d (Å)[a] | $\delta d_{12}$ (%) | $\delta d_{23}$ (%) | $\delta d_{34}$ (%) | $\delta d_{45}$ (%) | Reference |
|---|---|---|---|---|---|---|
| FCC | | | | | | |
| Cu(100) | $d_z = 1.808$ | $-1.1 \pm 0.4$ | $+1.7 \pm 0.6$ | ··· | ··· | A35 |
| Al(110) | $d_z = 1.432$ | $-8.4 \pm 0.8$ | $+5.0 \pm 1.0$ | $-1.6 \pm 1.1$ | $+0.2 \pm 1.1$ | A15,A17 |
| | | $-8.5 \pm 1.0$ | $+5.0 \pm 1.1$ | $+2.2 \pm 1.3$ | $+1.6$ | A16 |
| Cu(110) | $d_z = 1.278$ | $-8.5 \pm 0.6$ | $+2.3 \pm 0.8$ | $-0.9 \pm 0.9$ | $-0.8 \pm 0.9$ | A38 |
| | | $-9.1$ | $+2.3$ | ··· | ··· | A37 |
| Ni(110) | $d_z = 1.246$ | $-8.7 \pm 0.5$ | $+3.0 \pm 0.9$ | $-0.5 \pm 0.7$ | ··· | A71 |
| | | $-8.4 \pm 0.8$ | $+3.1 \pm 1.0$ | ··· | ··· | A68 |
| | | $-9.8 \pm 1.8$ | $+3.8 \pm 1.8$ | ··· | ··· | A69 |
| Al(311) | $d_z = 1.221$ | $-13.3 \pm 1.0$ | $+8.8 \pm 1.5$ | ··· | ··· | A20 |
| | $d_x = 2.158$ | 0 | ··· | ··· | ··· | |
| Ni(311) | $d_z = 1.063$ | $-15.9 \pm 1.0$ | $+4.1 \pm 1.5$ | $-1.6 \pm 1.6$ | ··· | A72 |
| | $d_x = 1.878$ | $-0.8 \pm 1.9$ | $-1.4 \pm 1.9$ | $-0.5 \pm 3.2$ | ··· | |
| BCC | | | | | | |
| Fe(100) | $d_z = 1.433$ | $-5 \pm 2$ | $+5 \pm 2$ | ··· | ··· | A45 |
| Ta(100) | $d_z = 1.652$ | $-11$ | $+1$ | ··· | ··· | A90 |
| V(100) | $d_z = 1.519$ | $-6.7 \pm 1.5$ | $+1.0 \pm 1.3$ | ··· | ··· | A92 |
| Fe(210) | $d_z = 0.641$ | $-22.0 \pm 4.7$ | $-11.1 \pm 4.7$ | $+17.0 \pm 4.7$ | $+4.8 \pm 4.7$ | A48 |
| | $d_x = 1.923$ | $+7.1 \pm 1.6$ | $+1.4 \pm 2.6$ | $0.0 \pm 2.6$ | $+4.0 \pm 2.6$ | |
| Fe(211) | $d_z = 1.170$ | $-10.4 \pm 2.6$ | $+5.4 \pm 2.6$ | $-1.3 \pm 3.4$ | ··· | A49 |
| | $d_x = 1.655$ | $-14.5 \pm 1.8$ | $+2.2 \pm 1.8$ | ··· | ··· | |
| Fe(310) | $d_z = 0.906$ | $-16.1 \pm 3.3$ | $+12.6 \pm 3.3$ | $-4.0 \pm 4.4$ | ··· | A50 |
| | $d_x = 1.813$ | $+7.2 \pm 2.8$ | $+1.6 \pm 2.8$ | ··· | ··· | |

[a] $x$ axes are located along the following directions: FCC(311)-⟨233⟩, BCC(210)-⟨120⟩, BCC(211)-⟨111⟩, BCC(310)-⟨130⟩.

#### 4.2.c.1. Almost Ideal Low-Index Surfaces

The (100) and (111) surfaces of FCC metals and the BCC(110) and HCP(0001) surfaces have high-density close-packed arrays of atoms. With only a few exceptions, such surfaces do not reconstruct, or their topmost interlayer spacing alter by no more than 5% of the bulk value, usually in the form of a contraction. The accuracy of the modern determinations is usually within 1% to 2% of an interlayer spacing. R-factors are in general use, but some authors still use short databases that limit the reliability of their results.

#### 4.2.c.2. Multilayer Relaxed Low-Index Surfaces

The more open FCC(110) and BCC(100) surfaces of several metals have been found to exhibit damped oscillatory variations of their interlayer spacings extending sometimes up to four layers into the interior of the crystal. Such investigations require a careful approach in order to detect such small structural changes. In particular, they require large amount of reproducible data, and careful attention to the details of optimization of nonstructural parameters and scattering potentials. A summary of results for such surfaces can be found in Table 4.

#### 4.2.c.3. Relaxed High-Index Surfaces

High-index surfaces offer more possibilities for the relaxation of atoms away from their bulk positions. In the FCC metals only the (311) surfaces of Al,Ni and Cu have had their structures determined. The studies for Al[A20] and Ni[A72] are high-reliability investigations which showed a strong multilayer relaxation. In the Cu case,[A43] the authors did not explore this possibility.

Jona *et al.*[A48–A50] studied a range of less-symmetrical high-index faces of Fe using R-factors and a large database.

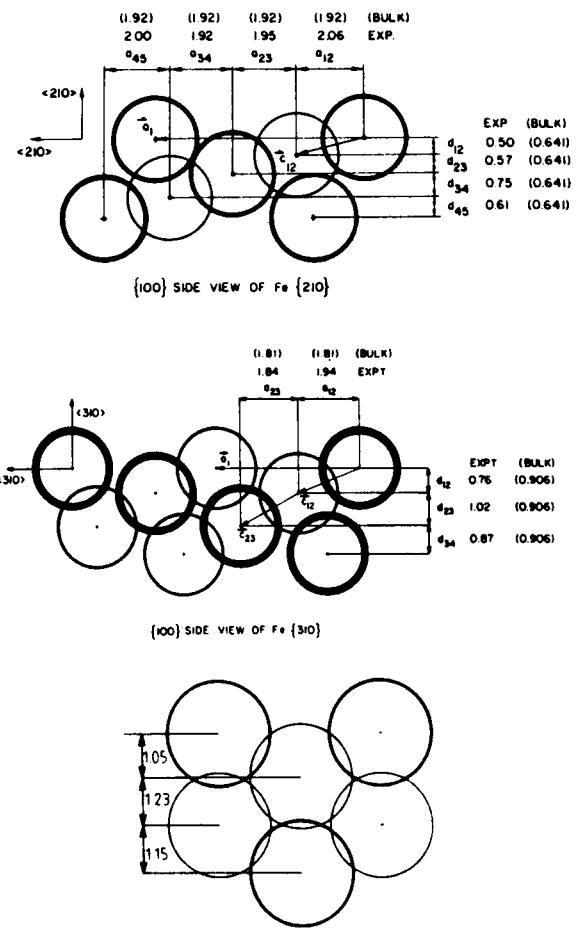


FIG. 3. Schematic diagram of the relaxed structures of (a) Fe(210), (b) Fe(211), and (c) Fe(310). (from Refs. A48–A50). Reprinted with the permission of AIP [Phys. Rev. B **31**, 1929 (1985)—Fig. 5; J. Phys. C **17**, 371 (1984)—Fig. 5; Phys. Rev. B **29**, 5402 (1984)—Fig. 5].

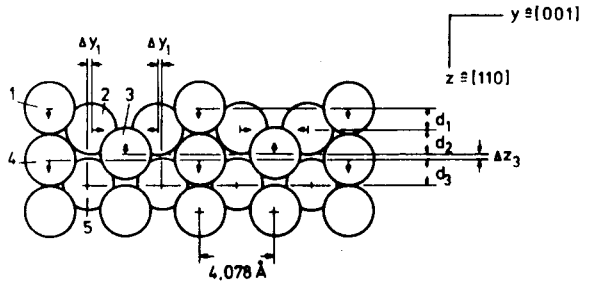


FIG. 4. Schematic diagram of the missing-row model of the (2×1) reconstructed (110) surface of Au, Ir, Pd, and Pt (from Ref. A24). Reprinted with the permission of North-Holland [Surf. Sci. **163**, L655 (1985)—Fig. 1].

They found parallel and perpendicular relaxations, down to the fifth layer, of up to 22% for Fe(210) (although this surface has a small bulk interlayer spacing of 0.641 Å). The structures of Fe(210), (211), and (310) are shown in Fig. 3 and details of the structural parameters in Table 4.

#### 4.2.c.4. Reconstructed Surfaces

A. Au, Ir, Pd, and Pt(110)

All three of these surfaces exhibit a (2×1) reconstruction that is thought to involve a "missing row" of atoms in the [ − 110] direction in the surface leading to a doubling of the unit cell in the [001] direction as shown in Fig. 4. The Au surface structure seems to be the best established[A24] with a large contraction of the first layer, a lateral pairing displacement of the second layer and a buckling of the third layer (see Table 5). The Ir study[A55] found the missing row model with a similarly large contraction of the first layer spacing to produce a slightly better fit than a row-pairing or buckled surface model. The Pd[A76] and Pt[A78] investigations could not resolve conflicting model structures satisfactorily, but tended to favor missing-row arrangements. In some cases, e.g., Pd(110) these types of reconstructions only occur in the presence of small amount of alkali adsorbate.

B. Ir and Pt(100)

There have been two studies of the (5×1) reconstruc-

TABLE 5. Structural parameters for the (2×1) reconstructed (110) surfaces of Au, Ir, and Pt. (Parameters are defined in Fig. 4. Distances are in Å with percentage changes relative to bulk values in parentheses.)

| | $d_1$ | $d_2$ | $d_3$ | $\delta z_3$ | $\delta y_1$ | Reference |
|---|---|---|---|---|---|---|
| Au(110) | 1.15 (−20%) | 1.35 (+2%) | 1.35 (+2%) | 0.23 | 0.07 | A24 |
| Ir(110) | 1.16 (−15%) | ... | ... | ... | ... | A55 |
| Pt(110) | 1.7 (+23) | 1.38 | ... | ... | 0.05 | A78 |

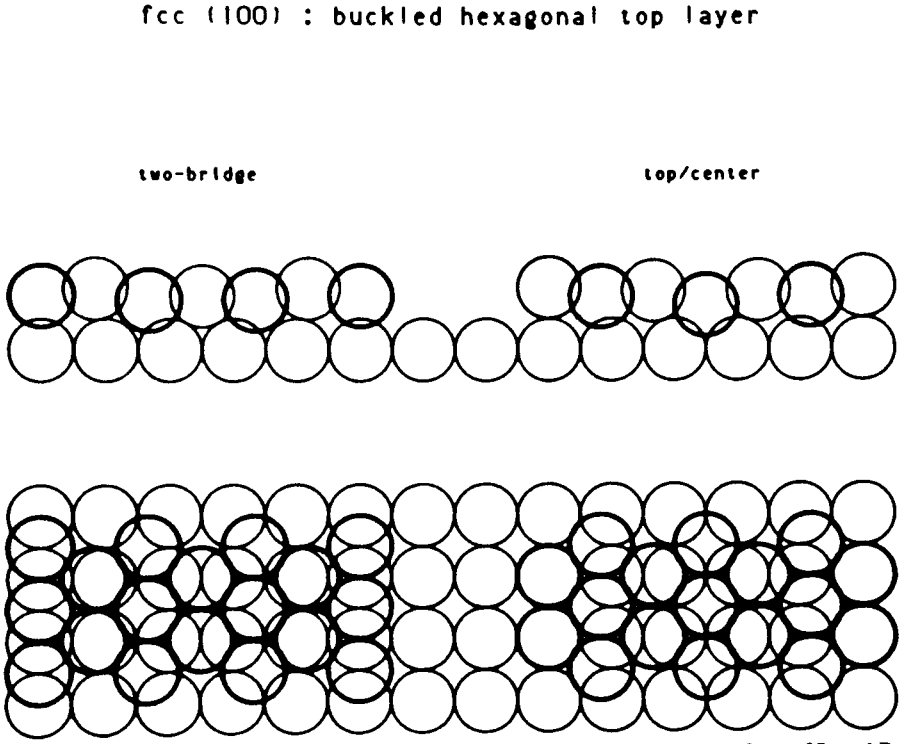


FIG. 5. Schematic diagram of the hexagonal model for the reconstructed (100) surfaces of Ir and Pt (from Ref. A53). Reprinted with the permission of North-Holland [Surf. Sci. **127**, 347 (1983)—Fig. 9].

TABLE 6. Structural parameters for the hexagonal model of the reconstructed (100) surfaces of Ir and Pt (Parameters are defined in Fig. 5. Distances are in Å with percentage changes relative to bulk values in parentheses.)

| | $d_1$ | $\delta d$ | Reference |
|---|---|---|---|
| Ir(1×5) | 2.0 (+10%) | 0.48 | A53 |
| Pt(14 1/−1 5) | 2.0 (−9%) | 0.5 | A52 |

tion of Ir using large datasets.[A51,A52] The preferred structure has a buckled top layer that is quasihexagonally closepacked and involves bridge sites resting on a bulk lattice, as shown in Fig. 5. The Pt(100) surface shows a complex LEED pattern indexed as (14 1/−1 5). Van Hove *et al.*[A52] carried out a simplified analysis for this complicated system and found reasonable agreement for a similar contracted hexagonal top-layer structure with less buckling, but rotated by about 0.7°. Further details are provided in Table 6.

C. W(100)

The normal (1×1) W(100) surface undergoes a transition to a reconstructed c(2×2) form below 300 K. Two studies using rather small databases[A104,A105] and, in one case R-factors,[A105] have found good agreement with a model in which lateral displacements of atoms in the [110] direction form a zig-zag row structure, together with a contraction of the first layer spacing by 6%. This model, which has p2 mg symmetry, is shown in Fig. 6.

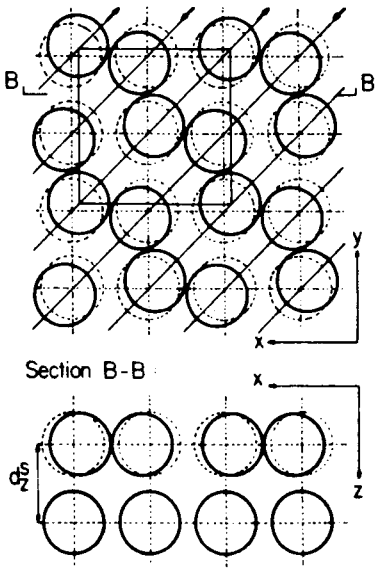


FIG. 6. Schematic diagram of the W(100) c(2×2) reconstructed surface structure (from Ref. A104). Reprinted with the permission of Pergamon [Solid State Commun. **25**, 375 (1978)—Fig. 1].

#### 4.2.c.4. Alloy Surfaces

Only four alloy surfaces involving (Ni,Al) and (Pt,Ni) appear in the LEED crystallographic literature[A110–A112]. An interesting aspect of these studies is the ability of LEED to not only yield structural information but to also allow a direct estimation of the relative composition of *each layer* to which the technique is sensitive (Table 7). We can contrast this to the compositional information produced by, for instance, AES which is averaged over the sampling depth of the electrons and must be subjected to deconvolution procedures in order to extract layer-by-layer compositions.

TABLE 7. Composition of the surface layers of some alloys determined by LEED

| Alloy $A_xB_y$ | Layer | | Theoretical composition A (%) | Theoretical composition B (%) | Experimental composition A (%) | Experimental composition B (%) | Reference |
|---|---|---|---|---|---|---|---|
| NiAl(100) | 1,2 | | 50 | 50 | 50 | 50 | A110 |
| $Ni_3Al$(110) | 1 | | 50 | 50 | 50 | 50 | A111 |
| | | or | 100 | 0 | | | |
| | 2 | | 50 | 50 | 100 | 0 | |
| | | or | 100 | 0 | | | |
| PtNi(111) | 1 | | 50 | 50 | 88 | 12 | A112 |
| | 2 | | 50 | 50 | 9 | 91 | |
| | 3 | | 50 | 50 | 65 | 35 | |
| $Pt_xNi_y$(111) | 1 | | 78 | 22 | 99 | 1 | A112 |
| ($x=0.78$, | 2 | | 78 | 22 | 30 | 70 | |
| $y=0.22$) | 3 | | 78 | 22 | 87 | 13 | |

# 4.3. Adsorbate-Covered Metal Surfaces

## 4.3.a. Summary Table B

TABLE 8. (Summary Table B) Adsorbate-covered metal surfaces

| Substrate | Surface | Ads. | Structure | Ref. | S | Crys. | Anal. meth. | Cont. level | Data coll. | Angs. | Normal | Off-norm. | Range | Calc. | Mod. | R-factor | Vor | Rating | Ads. site | $d0$ | Bond length | $\delta d1\%$ | Com. |
|---|---|---|---|---|---|---|---|---|---|---|---|---|---|---|---|---|---|---|---|---|---|---|---|
| Ag | 100 | Cl | (1×1) | 1 | 1 | H | AES | Low | SP | 3 | 4.2(0) | 17.8(4) | 21 | KKR | 4 | — | −8 | A− | 4−F | 1.57–1.78 | 2.67 | 0* | a |
| Ag | 100 | Se | c(2×2) | 2 | 1 | H | AES | — | SP | 1 | 0 | 3,1(0) | 3 | KKR | 3 | — | — | B− | 4−F | — | — | — | b |
| Ag | 110 | O | (1×2) | 3 | 1 | H | AES | Low | SP | 3 | 5,2(1) | 10,4(2) | 15 | KKR | 13 | >0.4 (ZJ) | −8 | A | 2−F(L) | — | — | — | c |
| Ag | 111 | Au | (1×1) | 4 | 1 | H | AES | Low | SP | 1 | 0 | 1(0) | 1 | RFS | 4 | — | −8 | C | 3−F(1) | — | — | — | d |
| Ag | 111 | I | (√3×√3)R30 | 5 | 1 | M(P) | AES | — | SP | 1 | 2 | 0 | 2 | RFS | 3 | — | −11 | C | 3−F(1) | 2.25(5%) | 2.8 | 0* | e |
| Ag | 111 | I | (√3×√3)R30 | 7 | 1 | H | AES | Low | SP | 3 | 3.1(0) | 11.5(1) | 14 | KKR | 4 | 0.22(ZJ) | −11 | A | 3−F(1,2) | — | — | — | f |
| Ag | 111 | Xe | Incomm. | 8 | 1 | — | None | — | FC | 2 | >2 | ? | 2 | Incomm. | 1 | — | −10 | B | — | 3.55(0.1) | — | — | g |
| Al | 100 | Na | c(2×2) | 10 | 1 | H | AES | <5%O | SP | 3 | 3,1(0) | 1,0(0) | 4 | KKR | 3 | — | −12 | B− | 4−F | 2.05(0.1) | 2.86 | 0* | h |
| Al | 100 | Na | c(2×2) | 11 | 1 | H | AES | <5%O | SP | 3 | 3,1(0) | 1,0(0) | 4 | RFS | 3 | — | −7.5 | B− | 4−F | 2.08(0.12) | 2.90 | 0* | i |
| Al | 111 | O | (1×1) | 12 | 1 | H | AES | <1%O | SP | 2 | 2(0) | 0 | 2 | RFS | 4 | — | −7.7 | C | 3−F(1) | 1.33(0.08) | 2.12 | 0* | j |
| Al | 111 | O | (1×1) | 13 | 1 | — | AES | — | SP | 3 | 2(0) | 4(0) | >3 | RFS | 2 | — | −8.5 | B− | 3−F(1) | 1.46(0.05) | 2.21 | 0* | k |
| Al | 111 | O | (1×1) | 14 | 1 | H | AES | <1%O | SP | 1 | 2(0) | 0 | 2 | KKR | 1 | — | E−dep | C | 3−F(1) | 0.7 | — | 0* | l |
| Al | 111 | O | (1×1) | 15 | 1 | H | AES | <1% | — | 3 | 1(0) | 6(0) | >5 | CAVLEED | 1 | 0.16(ZJ) | −9.0 | B | 3−F(1)* | −0.3(1.0) | — | −15(5) | m |
| | | | | | | | | | | | | | | | | | | | 3−F(1)* | 0.7(0.1) | 1.79(0.05) | — | |
| Au | 111 | Ag | (1×1) | 4 | 1 | H | AES | Low | SP | 1 | 0 | 1(0) | 1 | RFS | 3 | — | −8 | C | 3−F(1) | — | — | — | n |
| Co | 100 | O | c(2×2) | 17 | 1 | M | AES | 10%C | SP | 3 | 3,1(0) | 10,5(1) | 13 | KKR | 3 | 0.21(ZJ) | −16 | A | 4−F | 0.80 | 1.94 | 0.0(5.0) | o |
| Co | 100 | S | c(2×2) | 18 | 1 | — | — | — | — | 1 | 3,1(0) | 0 | 3 | None | — | — | — | B− | 4−F | 1.3 | — | — | p |
| Cu | 100 | Cl | c(2×2) | 19 | 1 | H | AES XPS | Low | SP | 2 | 5,2(2) | 7,2(2) | 12 | CHANGE | 2 | 0.12(ZJ) | −9 | A | 4−F | 1.60(0.03) | 2.37(0.02) | 2.5(1.5) | q |
| Cu | 100 | CO | c(2×2) | 20 | 1 | H | — | — | SP | 2 | 4,2(0) | 1,0(0) | 5 | LD | 1 | 0.39(P) | −12.5 | B+ | 1−F | 1.90(Cu−C) | 1.13(C−O) | 0* | r |
| Cu | 100 | N | c(2×2) | 21 | 1 | — | AES | — | SP | Many | — | — | 4 | CMTA | 1 | — | — | B− | 4−F | 1.45 | — | — | s |

Comments

(a) Results dependent on choice of Cl potential.
(b) Agreement not good enough to fix $d0$.
(c) No model gives satifactory agreement though O atoms in bridge sites of troughs best. Substrate may reconstruct.
(d) Used Ag spheres electrocrystallized to expose (111), Au grown by deposition. Pyramidal growth with wide terraces.
(e) Experimental data from [6].
(f) Could not reproduce a stable structure using method of [6]. Possibly different structure from [5]. I atoms in both kinds of 3-F sites.
(g) Experimental data from [9]; Xe layer assumed planar; Vor not refined.
(h) Data at 110 K; Na from liquid source.
(i) Expt. data of [10].
(j) O orders up to 1 monolayer (150 L).
(k) Al(111) grown epitaxially on mica.
(l) Used cluster-DVM potential; data from [11].
(m) For <30L $O_2$ (0.30 ML), O atoms in under layer 3-F sites in islands with contracted surface.
(m) For >90L (>0.7ML), O atoms mainly in overlayer sites with some oxide. Experimental data from [16].
(n) For 1–4 monolayers.
(o) O adsorption to remove 4% contraction in clean surface d1%.
(p) Compared with clean Ni(100) and c(2×2) Ni(100)-S.
(q) Cl from electro chemical cell; tested several Cl potentials that showed only small effect on structural result.
(r) CO vertical; data at 80 K.
(s) Atomic N used, made by e-dissociation.

TABLE 8. (Summary Table B) continued

| Substrate | Surface | Ads. | Structure | Ref. | S | Crys. | Anal. meth. | Cont. level | Data coll. | Angs. | Normal | Off-norm. | Range | Calc. | Mod. | R-factor | Vor | Rating | Ads. site | $d0$ | Bond length | $\delta d$ 1% | Com. |
|---|---|---|---|---|---|---|---|---|---|---|---|---|---|---|---|---|---|---|---|---|---|---|---|
| Cu | 100 | O | c(2×2) | 22 | 1 | — | — | — | FC | Many | — | — | 3 | CMTA | — | — | — | C | — | 1.95(0.05) | — | — | a |
| Cu | 100 | O | c(2×2) | 23 | 2 | L | AES | <2%S | FC | 2 | 3,1(0) | 3,1(0) | 6 | RSP | 4 | — | −14 | B | 2–F? | 1.4 | — | — | b |
| Cu | 100 | Pb | (√2×√2)/R45 | 24 | 1 | H(P) | AES | Low | FC | 1 | 7,3(5) | 0 | 7 | LD | 3 | 0.17(ZJ) | −8 | B+ | 4–F | 2.40(0.05) | 3.0 | 0* | c |
| Cu | 100 | Pb | c(5√2×√2)R45 | 24 | 1 | H(P) | AES | Low | FC | 1 | >12,11(6) | 0 | >12 | LD | 5 | 0.4(ZJ) | −8 | A− | 4–F | 2.40* | 3.0* | 0* | c |
| Cu | 100 | Te | p(2×2) | 25 | 1 | M(P) | None | — | — | 1 | 3,0(0) | 0 | 3 | RFS | 3 | — | −6 | C | 4–F | 1.70(0.15) | 2.48(0.10) | 0* | d |
| Cu | 111 | Cs | p(2×2) | 27 | — | — | — | — | SP | 2 | 4,2(0) | 1,0(0) | 5 | LD | 3 | — | E-dep | B | 1–F | 3.01(0.05) | 3.01(0.05) | 0* | e |
| Cu | 111 | Ni | (1×1) | 28 | — | H | AES(S) | 6%C | — | 2 | 12(6) | 15(4) | >7 | CAVLEED | 1 | 0.05(ZJ)<br>0.43(P) | — | A | 3–F | 2.04(0.02) | — | 0* | f |
| Fe | 100 | CO | c(2×2) | 29 | — | — | AES | — | SP | 3 | 5,>1(>1) | 18 | >3 | KKR | 5 | — | — | A− | 4–F | 0.48 | — | — | g |
| Fe | 100 | N | c(2×2) | 30 | 1 | H | AES | Low | FC | 3 | >4,3(2) | >6,3(2) | >10 | LD | 4 | 0.20(ZJ) | −9.5 | A | 4–F | 0.27 | 1.83 | 10 | h |
| Fe | 100 | O | (1×1) | 31 | 1 | H | AES(S | <4%C,O | SP | 3 | 4(2) | 12(4) | 16 | KKR | 2 | — | −12 | A− | 4–F | 0.48(0.06) | — | 7.5 | |
| Fe | 100 | S | c(2×2) | 32 | 1 | H | AES(S | 2%–4% C,O | SP | 3 | 6,2(3) | 18,8(8) | 24 | KKR | 3 | — | −11 | A− | 4–F | 1.09(0.05) | 2.30 | 0.0 | i |
| Fe | 110 | H | (2×1) | 33 | 1 | H | AES | <5%C,O | FC/TV | 5 | >3,2(0) | >9,6(0) | >12 | LD/RFS | 4 | 0.23(ZJ)<br>0.46(P) | −11 | A | 3–F | 0.9(0.1) | 1.75(0.05) | 0.0(1.0) | j |
| Fe | 110 | H | (3×1) | 33 | 1 | H | AES | <5%C,O | FC/TV | 2 | >4,3(1) | >5,3(0) | >9 | LD/RFS | 4 | 0.40(ZJ)<br>0.58(P) | −11 | A | 3–F | 0.9(0.1) | 1.75(0.05) | 0.0(1.0) | k |
| Fe | 110 | S | p(2×2) | 34 | 1 | H | AES | — | SP | 2 | 8,>1 | 7 | >2 | KKR | 3+ | — | −11.5 | A− | 4–F* | 1.43 | 2.16,2.36 | 0 | l |
| Ir | 110 | O | c(2×2) | 35 | 1 | — | AES | — | FC | 1 | 8,4(5) | 0 | 8 | LD | 4 | — | −15 | B | 2–F(S) | 1.37(0.05) | 1.93(0.07) | 2(5) | m |
| Ir | 111 | O | (2×2) | 36 | 1 | H | AES | Low | FC | 1 | 10,7(4) | 0 | 10 | RFS | 3 | 0.22(ZJ) | −12 | A− | 3–F(1) | 1.30 | 2.04 | 0* | n |
| Ir | 111 | S | (√3×√3)R30 | 37 | 1 | — | AES | Low | FC | 1 | 11,6(6) | 0 | 11 | RFS | 3 | 0.19(ZJ) | −10 | A− | 3–F(1) | 1.65 | 2.28 | 0* | o |
| Mo | 100 | N | c(2×2) | 38 | 1 | — | AES | — | SP | 1 | 0 | 11,5(>2) | >7 | KKR | 3 | — | −15 | A− | 4–F | 1.02 | 2.45 | — | p |
| Mo | 100 | S | c(2×2) | 39 | 1 | H(P) | AES | Low | SP | 2 | 9 | 7,3(1) | — | LD | 3 | — | — | A− | 4–F | — | — | −2.5(2.5) | q |
| Mo | 100 | Si | (1×1) | 40 | 1 | — | AES | — | SP | 2 | 0 | 10(0) | 10 | KKR | 3 | — | −16 | A− | 4–F | 1.16(0.1) | 2.51(0.05) | <5.0 | r |

Comments

(a) Reconstruction involving nearly coplanar Cu and O top layer.
(b) LEED structure dependent on adsorption temperature.
(c) Pb atoms do not form hexagonal layer but maintain nearly 4-F coordination in groups separated by antiphase boundaries.
(d) Experimental data from [26].
(e) Used $Cu_7Cs$ cluster potential.
(f) Epitaxial Ni deposition at 180 °C.
(g) C,O randomly occupy 4–F sites.
(h) No evidence for underlayer; N from decomposition of $NH_3$.
(i) Allowing d1 to vary did not improve fit.
(j) No H-induced reconstruction. Good long-range order. H atoms in dense-packed rows in ⟨001⟩ direction, separated by an unoccupied row.
(k) H atoms on alternate sites, no domains. Only moderate agreement.
(l) *0.25 ML S induces surface reconstruction that leads to most favourable bondlengths, but retains rectangular symmetry.
(m) Ir(110) (1×1) first stabilized by addition of 0.25 ML. O randomly adsorbed; clean Ir(110)(1×1) has d1 contracted by 7.5%.
(n) Cannot distinguish p(2×2) from 3 domains of p(1×2).
(o) From decomposition of $H_2S$.
(p) Level of agreement only moderate.
(q) S from $H_2S$ dissociation forms c(2×2) islands for <0.5 ML; d1 is relaxed from clean value of −10%. Could not determined dO.
(r) Si deposited by sublimation. Surface relaxes from clean state where d1% = -11%.

TABLE 8. (Summary of Table B) continued

| Substrate | Surface | Ads. | Structure | Ref. | S | Crys. | Anal. meth. | Cont. level | Data coll. | Angs. | Normal | Off-norm. | Range | Calc. | Mod. | R-factor | Vor | Rating | Ads. site | $d0$ | Bond length | $\delta d$ 1% | Com. |
|---|---|---|---|---|---|---|---|---|---|---|---|---|---|---|---|---|---|---|---|---|---|---|---|
| Ni | 100 | C | p(2×2) | 41 | — | — | — | — | SP | 1 | >2,1 | — | >1 | LD | 2 | — | — | C | 4-F | 1.2 | — | 8.5 | a |
| Ni | 100 | C | c(2×2)(p4g) | 43 | 1 | M(P) | AES | <5%C,O | FC | 2 | 4,2(0) | 4,1(0) | 8 | RS | 5 | — | — | B | 4-F | 0.1 | 1.80(0.15) | 10 | b |
| Ni | 100 | $C_2H_2$ | c(2×2) | 44 | 1 | H | AES | — | P-MD | 1 | 2,1(0) | 0 | 3 | RFS | Many | — | −11 | C+ | 4-F | 2.02 | 2.2(Ni–C) | 0* | c |
| Ni | 100 | CO | c(2×2) | 46 | 1 | H | AES | — | SP | 2 | 3,1(0) | 7,2(0) | 10 | CHANGE | 3 | — | — | A− | 1-F | 1.72 | 1.72(Ni–C)<br>1.15(C–C) | 0* | d |
| Ni | 100 | CO | c(2×2) | 47 | 1 | H | AES | Low | TV | 2 | 3,1(0) | 1,0(0) | 4 | LD | 1 | — | −12.5 | B− | 1-F | 1.80 | 1.80(0.1) (Ni–C)<br>1.15(0.1)(C–O) | 0* | e |
| Ni | 100 | CO | c(2×2) | 48 | 1 | — | AES | Low | SP | 2 | 4,2(0) | 1,0(0) | 5 | LD | 1 | 0.55(P) | −12.5 | B | 1-F | 1.72 | 1.72(Ni–C)<br>1.15(C–O) | 0.0(1.0) | f |
| Ni | 100 | CO | c(2×2) | 49 | 1 | H | AES | — | SP | 2 | 3,1(0) | 7,2(0) | 10 | — | 1 | — | −11.8 | A− | 1-F | 1.7 | 1.7(Ni–C)<br>1.13(C–O) | 0* | g |
| Ni | 100 | Cu | (1×1) | 50 | 1 | H | AES | — | SP | 1 | 4(2) | 1(0) | 5 | RFS | 1 | — | −14 | B | 4-F* | 1.80 | — | 0* | h |
| Ni | 100 | Na | c(2×2) | 51 | 1 | H | AES | Low | SP | 1 | 3,1(0) | 0 | 3 | RFS/LD | 1 | — | −12 | C | 4-F | 2.2(0.1) | — | 0* | i |
| Ni | 100 | Na | c(2×2) | 53 | 1 | H | AES | Low | SP | 1 | 3,1(0) | 0 | 3 | KKR | 1 | — | −11 | C | 4-F | 2.23(0.1) | — | 0* | j |
| Ni | 100 | Na,S | c,p(2×2) bilayers | 54 | 1 | H(P) | AES | Low | SP | 1 | 4,2(0) | 0 | 4 | RFS/LD | 6 | — | −7 | B− | 4-F | 1.3(S) | — | 0* | k |
| Ni | 100 | NO | c(2×2) | 55 | 1 | — | — | Low | SP | 2 | 3,1(0) | 7,2(0) | >2 | RFS/LD | 6 | 0.25(ZJ) | −10 | A | 4-F | 0.93 | — | 0* | m |
| Ni | 100 | O | c(2×2) | 56 | — | H | — | Low | — | 1 | 4,1(0) | 0 | 4 | RFS | 4 | — | — | B− | 4-F | 1.5(0.1) | 2.3(0.1) | 0* | |
| Ni | 100 | O | c(2×2) | 57 | 1 | H | AES | Low | — | 2 | 3,1(0) | 1 | 4 | KKR | 1 | — | −11 | B− | 4-F | 0.90(0.1) | 1.97(0.05) | 0* | n |
| Ni | 100 | O | c(2×2) | 59 | 1 | H | AES | Low | SP | 5 | 3,1(0) | 4,0(0) | 4 | CSM | 1 | 0.28(ZJ) | −13.2 | B+ | 4-F | 0.90 | — | 0* | o |
| Ni | 100 | O | c(2×2) | 60 | — | — | AES | Low | TV | 3 | 4,2(1) | 4,2(0) | >3 | KKR | 3 | 0.17(ZJ) | — | A− | 2-F | 0.80(0.02) | 1.75,2.14 | 0* | p |
| Ni | 100 | O | p(2×2) | 61 | 1 | H | AES | Low | SP | 10 | 4,2(0) | 9,0,(0) | 13 | LD | 3 | — | −11.2 | B | 4-F | 0.90(0.1) | 1.98(0.05) | 0* | q |
| Ni | 100 | S | c(2×2) | 62 | 1 | H | AES | Low | SP | 1 | 5,1(0) | 0 | >3 | KKR | 1 | — | −11 | B− | 4-F | 1.30(0.1) | 2.18(0.06) | 0* | r |
| Ni | 100 | S | c(2×2) | 63 | 1 | H | AES | Low | SP | 4 | 2,1(0) | 6.2(0) | 8 | IS | 1 | — | −14 | B | 4-F | 1.3 | — | 0* | s |
| Ni | 100 | S | c(2×2) | 65 | 1 | — | AES | Low C | SP | 6+ | >2 | >4 | >6 | RFS | 1 | — | E-dep | B | 4-F | 1.30 | — | 0* | t |
| Ni | 100 | S | p(2×2) | 61 | 1 | H | AES | Low | SP | 10 | 2,2(0) | 9,0(0) | 11 | LD | 3 | — | −11.2 | B+ | 4-F | 1.30(0.1) | 2.19(0.06) | 0* | u |
| Ni | 100 | Se | c(2×2) | 66 | 1 | H | AES | Low | SP | 1 | >3 | — | >3 | KKR | 1 | — | −10.9 | C | 4-F | 1.45(0.1) | 2.27(0.06) | 0* | v |
| Ni | 100 | Se | p(2×2) | 61 | 1 | H | AES | Low | SP | 10 | 4,2(0) | 9,0(0) | 13 | LD | 3 | — | −11.2 | B+ | 4-F | 1.55(0.1) | 2.34(0.07) | 0* | w |
| Ni | 100 | Te | c(2×2) | 66 | 1 | H | AES | Low | SP | 1 | >3 | — | >3 | KKR | 1 | — | −10.6 | C | 4-F | 1.90(0.1) | 2.58(0.08) | 0* | x |
| Ni | 100 | Te | p(2×2) | 61 | 1 | H | AES | Low | SP | 10 | 3,1(0) | 9,0(0) | 12 | LD | 3 | — | −11.2 | B+ | 4-F | 1.80(0.01) | 2.52(0.07) | 0* | y |

Comments

(a) Data from [42]; C from dissociation of CO.
(b) C from cracking of $C_2H_4$ at 300 °C. Pattern has missing spots that implies glide symmetry. Surface Ni atoms distort about 0.35 Å parallel and 0.20 Å perpendicular to surface. See notes.
(c) Adsorption at room temperature. See notes.
(d) Specimen translated to avoid damage at 100 K. Data from [45].
(e) Fast LEED measurements at 100 K reduced damage. Used calculations of [47].
(f) Avoided e-beam damage.
(g) Used Scott potential consistent with structure; data from [46].
(h) Epitaxial layer. Ni-Cu layer expanded 1.7% relative to Ni(100).
(i) Mattheis potential. New data that refutes older work [52].
(j) Data from [51].
(k) S from $H_2S$ decomposition, Na metal vapor. S always 1.3 Å in 4-F hollows; Na bonds to S so that it is 2.5 Å from surface.
(m) NO dissociates and randomly occupies 4-F sites.
(n) Experimental data of [58].
(o) Experimental data of [58]. Overlayer spacing of 0.9 Å only slightly favoured over coplanar Ni and O.
(p) Oxygen absorbed at 250 °C; data at 160 K. O displaced 0.3 Å along ⟨110⟩ in psuedo-bridge bonding arrangement.
(q) Data of [58].
(r) Data of [58].
(s) Reworking of [64].
(t) Used iso-intensity maps; S from diffusion.
(u) Data from [58].
(v) Data from [58].
(w) Data from [58].
(x) Data from [58].
(y) Data from [58].

TABLE 8. (Summary of Table B) continued

| Substrate | Surface | Ads. | Structure | Ref. | S | Crys. | Anal. meth. | Cont. level | Data coll. | Angs. | Normal | Off-norm. | Range | Calc. | Mod. | R-factor | Vor | Rating | Ads. site | $d0$ | Bond length | $\delta d$ 1% | Com. |
|---|---|---|---|---|---|---|---|---|---|---|---|---|---|---|---|---|---|---|---|---|---|---|---|
| Ni | 110 | H | (1×2) | 67 | 1 | H | AES | Low | FC | 3 | 7,3(3) | 3,0(2) | 10 | RS | 3 | 0.63(P) | — | A– | — | — | — | | a |
| Ni | 110 | O | (2×1) | 68 | 1 | H | AES | Low | SP | 2 | 5,2(0) | 1,0(0) | 6 | KKR/LD | 7 | — | −11 | B | 2-F(S) | 1.46(0.05) | 1.92 | 0* | b |
| Ni | 110 | S | c(2×2) | 62 | 1 | H | AES | Low | SP | 1 | 5,1(0) | 0 | >3 | KKR | 1 | — | −11 | B– | 4-F | 1.40(0.1) | 2.02(0.06) | 0* | c |
| Ni | 110 | S | c(2×2) | 69 | 1 | — | AES | Low | SP | 1 | 11,6(2) | 0 | 11 | CSM | 4 | — | — | B+ | 4-F | 0.84(0.03) | — | 10.0 | d |
| Ni | 111 | $C_2H_2$ | (2×2) | 70 | 5 | — | AES | Low | P-MD | 1 | 5,3(0) | 0 | * | LD | 9 | 0.18(avg) | −11 | B | 2-F | — | 2.1(Ni–C) | 0* | e |
| | | | | | | | | | | | | | | | | | | | | | 1.5(C–C) | | f |
| Ni | 111 | H | (2×2) | 71 | 1 | — | AES | Low | FC | 2 | 5,3(0) | 1,0(0) | 6 | RFS/LD/ | Many | — | −11 | B | 3-F(1,2) | 1.15(0.1) | 1.84 | 0* | g |
| Ni | 111 | S | p(2×2) | 62 | 1 | H | AES | Low | SP | 1 | 5,1(0) | 0 | >3 | KKR | 1 | — | −11 | B– | 3-F(1) | 1.40(0.1) | 2.02(0.06) | 0* | h |
| Pd | 100 | CO | c(2√2×√2)R45 | 72 | 1 | H | AES | Low | FC | 2 | 3,2(1) | 1,0(0) | 4 | RFS | 2 | — | −10 | B | 2-F | — | 1.93(0.07)(Pd–C) | 0* | i |
| | | | | | | | | | | | | | | | | | | | | | 1.15(0.1)(C–O) | | |
| Pd | 100 | S | c(2×2) | 73 | 1 | H | AES | Low | SP | 2 | 2,1(0) | 2,1(0) | 4 | LD | 3 | 0.3(P) | −9 | B | 4-F | 1.30(0.05) | 2.35(0.03) | 0* | j |
| Pd | 111 | S | (√3×√3)R30 | 74 | 1 | — | AES | Low | SP | 2 | >4 | >10,2 | >8 | RFS | 3 | 0.24(P) | −11 | A | 3-F(1) | 1.53(0.05) | 2.22(0.03) | 0* | |
| Pt | 100 | Cs | c(4×2) | 75 | 1 | M | — | — | TV | 1 | 3,2(1) | 0 | 3 | RFS | 3 | — | −12.5 | C | 4-F | 4.25(0.1) | — | 0* | k |
| Pt | 111 | $C_2H_2$ | (2×2) | 76 | 1 | H | AES | <20%H | P-MD | 3 | >6 | — | — | LD | Many | — | — | B | 3-F(1) | — | 2.00(0.05)(Pt–C) | 0* | l |
| | | $C_2H_4$ | | | | | | | | | | | | | | | | | | | 1.50(0.05)(C–C) | | |
| Pt | 111 | S | (√3×√3)R30 | 77 | 1 | — | AES | Low | TV | 2 | 9 | 4,2(1) | 8 | CAVLEED | 3 | 0.48(P) | −9.3 | A | 3-F(1) | 1.62(0.05) | 2.28(0.03) | 0.0 | m |
| Rh | 100 | S | p(2×2) | 78 | 1 | H | AES | Low | P-TV | 1 | 9,5(5) | 0 | 9 | LD | 3 | 0.33(ZJ) | −13.6 | B+ | 4-F | 1.29(0.1) | 2.30 | 0* | n |
| Rh | 110 | S | c(2×2) | 79 | 1 | H | AES(S | Low | P-TV | 1 | 14,5(8) | 0 | 14 | LD | 4 | 0.17(ZJ) | −12.2 | B+ | 4-F | 0.77(0.05) | 2.12,2.45 | 0* | o |
| Rh | 111 | $C_2H_4$ | (2×2) | 80 | 1 | — | AES | <5%CO | P-D | 4 | ? | ? | 48? | RFS | 4 | 0.49(ZJ) | — | A | 3-F(1) | — | 2.03(0.07)(Rh–C) | 0* | p |
| | | | | | | | | | | | | | | | | 0.53(P) | | | | | 1.45(0.1)(C–C) | | |
| Rh | 111 | $C_6H_6$ | (31) | 81 | — | — | — | — | — | 1 | ? | ? | 13? | BSN | Many | 0.29(ZJ) | — | A | 3-F(2) | — | 2.35(0.05)(Rh–C) | 0* | q |
| | | | (13) | | | | | | | | | | | | | 0.55(P) | | | | | | | |

Comments

(a) Data at 150 K. Missing-row favoured over row-pairing model.
(b) Data from [58].
(c) Data from [58].
(d) Multilayer relaxation of Ni(110) changes in sign and increases d2% = −3.5%.
(e) * Measured at 150 K; short data set. See notes.
(f) Along ⟨11 − 2⟩ direction.
(g) 0.5ML H in both types of 3-F site in graphitic structure.
(h) Data from [58].
(i) 0.5ML structure with CO vertical.
(j) Decomposed $H_2S$ at 500 °C.
(k) Small energy range. Bridge sites also gave reasonable agreement.
(l) Ethylidyne forms with C–C axis near normal. 3 equivalent Pt–C bonds. Used HREELS to assist identification.
(m) S from electrochemical source.
(n) S from $H_2S$ at 300 °C.
(o) S from $H_2S$ at 300 °C.
(p) Ethylidyne forms perpendicularly above 3-F site.
(q) Benzene molecules lie flat on 3-F (2) sites, with possible planar ring distortion. See notes.

TABLE 8. (Summary Table B) continued

| Substrate | Surface | Ads. | Structure | Ref. | S | Crys. | Anal. meth. | Cont. level | Data coll. | Angs. | Normal | Off-norm. | Range | Calc. | Mod. | R-factor | Vor | Rating | Ads. site | $d0$ | Bond length | $\delta d$ 1% | Com. |
|---|---|---|---|---|---|---|---|---|---|---|---|---|---|---|---|---|---|---|---|---|---|---|---|
| Rh | 111 | CO | $(\sqrt{3}\times\sqrt{3})R30$ | 82 | 1 | H | AES(S) | <2%O | P-MD | 3 | 4,2(0) | 18,8(4) | 22 | RFS | 3 | 0.40(ZJ)<br>0.50(P) | −8 | A | 1-F | — | 1.94(0.1)(Rh–C)<br>1.15(0.1)(C–O) | 0* | a |
| Rh | 111 | CO | (2×2)-3CO | 83 | 1 | — | AES | Low | P-MD | 3 | 5 | 16 | — | QSD/RFS | Many | 0.25(ZJ)<br>0.47(P) | — | A | 1-F,2-F | — | 2.03(0.1)(Rh–C)<br>1.15(0.1)(C–O) | 0* | b |
| Rh | 111 | O | (2×2) | 84 | 1 | H | AES | — | TV | 1 | 10,5 | 0 | 10 | RFS | 3 | 0.39(P) | −12.6 | B+ | 3-F(1) | 1.23(0.09) | 1.98 | 0* | c |
| Rh | 111 | S | $(\sqrt{3}\times\sqrt{3})R30$ | 85 | 1 | H | AES | — | TV | 1 | 9,4(4) | 0 | 8 | RFS | 4 | 0.27(P) | −10 | B+ | 3-F | 1.53 | 2.18 | 0* | d |
| Ru | 0001 | CO | $(\sqrt{3}\times\sqrt{3})R30$ | 86 | 1 | — | AES | — | FC | 1 | 7,4(3) | 0 | 7 | RFS/LD | 4 | 0.12(ZJ)<br>0.51(P) | −12.0 | B | 1-F | — | 2.00(0.1)(Ru–C)<br>1.10(0.1)(C–O) | 0* | |
| Ta | 100 | O | (1×3) | 87 | 1 | M(P) | AES | — | FC | 1 | 10,6(6) | 0 | 10 | — | 13 | 0.22(ZJ) | −6 | B+ | * | −0.4 | 2.0(0.1)(Ta–O)<br>3.05(Ta–Ta) | −5 | e |
| Ti | 0001 | Cd | (1×1) | 88 | 2 | — | AES(S) | Low | SP | 2 | 3(1) | 7(4) | 10 | KKR | 3 | — | −6 | B+ | 3-F(1) | 2.57 | 3.08 | 0* | f |
| Ti | 0001 | CO | p(2×2) | 89 | 2 | H | AES(S) | Low | SP | 2 | 4,2(0) | 6,2(1) | >4 | KKR | 5 | — | — | B+ | 3-F(1,2) | — | — | 0* | g |
| Ti | 0001 | N | (1×1) | 90 | 2 | H | AES(S) | Low | SP | 3 | 3(0) | 6(2) | 9 | KKR | 7 | — | −11.5 | B | * | −1.223 | 2.095 | 4.6 | h |
| W | 100 | CO | c(2×2) | 91 | — | H | AES | Low | FC | 1 | 8,5(5) | 0 | 8 | — | 1 | — | −12.5 | B | 4-F | — | — | 0.0 | i |
| W | 100 | H | p(1×1)-2H | 92 | 1 | — | AES | Low C | SP | 2 | 4(2) | 6(1) | >4 | RSP/RFS | 1 | 0.21(ZJ) | — | A | 2-F | 1.17(0.04) | 1.97 | <−2.0 | j |
| W | 100 | N2 | c(2×2) | 91 | — | H | AES | Low | FC | 2 | 10,5(7) | 21,10(16) | 31 | CAVLEED | 1 | 0.55(P) | −12.5 | A | 4-F | 0.49(0.06) | — | 0.0(1.0) | k |
| W | 100 | O | Disordered | 93 | — | — | — | — | TV | 1 | — | — | — | DLEED | 1 | 0.16(P) | — | B | 4-F | 0.55(0.1) | — | 0* | l |
| W | 110 | O | p(2×1) | 95 | — | — | — | — | — | 1 | 5,2(1) | — | >3 | LD | 5 | 0.17(VHT) | −10 | B | 3-F | 1.25(0.03) | 2.08 | 0* | m |
| Zr | 0001 | O | (2×2) | 96 | 1 | H | AES | Low | P-TV | 1 | 6,4(1) | — | >1 | — | 16 | 0.32(P) | −11.6 | B | — | −1.37 | 2.31 | 6.6 | n |

Comments

(a) CO perpendicular.
(b) 0.75ML coverage with constant background of CO to maintain pattern. Used different levels of approximation. See notes.
(c) O layer disorders in 2 min in electron beam.
(d) S from $H_2S$ at 200 °C.
(e) *Surface reconstructs from −11% contraction in clean Ta(100). See notes.
(f) Cd not in expected HCP 3-F (2) site.
(g) CO probably dissociated. Could not distinguish between two 3-F sites, may involve underlayer. Fit only moderate.
(h) *N atoms in O holes under Ti surface.
(i) By comparison with N data, suggest C and O randomly occupy 4-F sites with surface relaxed from clean contraction of 6%.
(j) Surface relaxed from clean contraction of 6%.
(k) Coverage determined by molecular beam dosing system. W surface relaxed from clean contraction of −8%.
(l) "Considerable" O coverage to remove reconstruction. Measured diffuse LEED intensity over 1/4 screen for 2 energies.
(m) O atoms. Repeat of [94] using R-factors.
(n) O atoms in O holes in FCC Zr surface with expanded 1st layer.

### 4.3.b. References to Summary Table 8—Metal/adsorbate systems


[1]E. Zanazzi, F. Jona, D. W. Jepsen, and P. M. Marcus, Phys. Rev. B **14**, 432 (1976).
[2]A. Ignatiev, F. Jona, D. W. Jepsen, and P. M. Marcus, Surf. Sci. **40**, 439 (1973).
[3]E. Zanazzi, M. Maglietta, U. Bardi, F. Jona, and P. M. Marcus, J. Vac. Sci. Technol. A **1**, 7 (1983).
[4]C. Ammer, M. Klaua, and H. Bethge, Phys. Status Solidi. **71**, 415 (1982).
[5]F. Forstmann, Jpn. J. Appl. Phys. Suppl. **2**, 675 (1974).
[6]W. Berndt, Jpn. J. Appl. Phys. Suppl. **2**, 653 (1974).
[7]M. Maglietta, E. Zanazzi, U. Bardi, D. Sondericker, F. Jona, and P. M. Marcus, Surf. Sci. **123**, 141 (1982).
[8]N. Stoner, M. A. Van Hove, S. Y. Tong, and M. B. Webb, Phys. Rev. Lett. **40**, 243 (1978).
[9]P. I. Cohen, J. Unguris, and M. B. Webb, Surf. Sci. **58**, 429 (1976).
[10]B. A. Hutchins, T. N. Rhodin, and J. E. Demuth, Surf. Sci. **54**, 419 (1976).
[11]M. Van Hove, S. Y. Tong, and N. Stoner, Surf. Sci. **54**, 259 (1976).
[12]C. W. B. Martinson, S. A. Flodstrom, J. Rundgren, and P. Westrin, Surf. Sci. **89**, 102 (1979).
[13]H. L. Yu, M. C. Munoz, and F. Soria, Surf. Sci. **94**, L184 (1980).
[14]J. Neve, J. Rundgren, and P. Westrin, J. Phys. C **15**, 4391 (1982).
[15]V. Martinez, F. Soria, M. C. Munoz, and J. L. Sacedon, Surf. Sci. **128**, 424 (1983).
[16]F. Soria, V. Martinez, M. C. Munoz, and J. L. Sacedon, Phys. Rev. B **24**, 6926 (1980).
[17]M. Maglietta, E. Zanazzi, U. Bardi, F. Jona, D. W. Jepsen, and P. M. Marcus, Surf. Sci. **77**, 101 (1978).
[18]M. Maglietta, Solid State Commun. **43**, 395 (1982).
[19]F. Jona, D. Westphal, A. Goldman, and P. M. Marcus, J. Phys. C **16**, 3001 (1983).
[20]S. Andersson and J. B. Pendry, J. Phys. C **13**, 3547 (1980).
[21]J. M. Burkstrand, G. G. Kleiman, G. G. Tibbetts, and J. C. Tracy, J. Vac. Sci. Technol. **13**, 291 (1976).
[22]L. McDonnell, D. P. Woodruff, and K. A. R. Mitchell, Surf. Sci. **45**, 1 (1975).
[23]J. H. Onuferko and D. P. Woodruff, Surf. Sci. **95**, 555 (1980).
[24]W. Hoesler and W. Moritz, Surf. Sci. **117**, 196 (1982).
[25]A. Salwen and J. Rundgren, Surf. Sci. **53**, 523 (1975).
[26]D. E. Andersson and S. Andersson, Surf. Sci. **23**, 311 (1970).
[27]S. A. Lindgren, L. Wallden, J. Rundgren, P. Westrin, and J. Neve, Phys. Rev. **28**, 6707 (1983).
[28]S. P. Tear and K. Roll, J. Phys. C **15**, 5521 (1982).
[29]F. Jona, K. O. Legg, H. D. Shih, D. W. Jepsen, and P. M. Marcus, Phys. Rev. Lett. **40**, 1466 (1978).
[30]R. Imbihl, R. J. Behm, G. Ertl, and W. Moritz, Surf. Sci. **123**, 129 (1982).
[31]K. O. Legg, F. Jona, D. W. Jepsen, and P. M. Marcus, Phys. Rev. B **16**, 5271 (1977).
[32]K. O. Legg, F. Jona, D. W. Jepsen, and P. M. Marcus, Surf. Sci. **66**, 25 (1975).
[33]W. Moritz, R. Imbihl, R. J. Behm, G. Ertl, and T. Matsushima, J. Chem. Phys. **83**, 1959 (1985).
[34]H. D. Shih, F. Jona, J. W. Jepsen, and P. M. Marcus, Phys. Rev. Lett. **46**, 731 (1981).
[35]C.-M. Chan, K. L. Luke, M. A. Van Hove, W. H. Weinberg, and S. P. Withrow, Surf. Sci. **78**, 386 (1978).
[36]C. M. Chan and W. H. Weinberg, J. Chem. Phys. **71**, 2788 (1979).
[37]C. M. Chan and W. H. Weinberg, J. Chem. Phys. **71**, 3988 (1979).
[38]A. Ignatiev, F. Jona, D. W. Jepsen, and P. M. Marcus, Surf. Sci. **49**, 189 (1975).
[39]L. J. Clarke, Surf. Sci. **102**, 331 (1981).
[40]A. Ignatiev, F. Jona, D. W. Jepsen, and P. M. Marcus, Phys. Rev. B **11**, 4780 (1975).
[41]M. A. Van Hove and S. Y. Tong, Surf. Sci. **52**, 673 (1975).
[42]J. E. Demuth, Ph.D. thesis, Cornell University, 1973.
[43]J. H. Onuferko, D. P. Woodruff, and B. W. Holland, Surf. Sci. **87**, 357 (1979).
[44]G. Casalone, M. G. Cattania, and M. Simonetta, Surf. Sci. **103**, L121 (1981).
[45]G. Casalone, M. G. Cattania, M. Simonetta, and M. Tescati, Surf. Sci. **62**, 321 (1977).
[46]M. Passler, A. Ignatiev, F. Jona, P. M. Marcus, and D. W. Jepsen, Phys. Rev. Lett. **43**, 360 (1979).
[47]K. Heinz, E. Lang, and K. Müller, Surf. Sci. **87**, 595 (1979).
[48]S. Andersson and J. B. Pendry, J. Phys. C **13**, 3547 (1980).
[49]S. Y. Tong, A. Maldonado, C. H. Li, and M. A. Van Hove, Surf. Sci. **94**, 73 (1980).
[50]M. Abu-Joudeh, P. P Vaishnava, and P. A. Montano, J. Phys. C **17**, 6899 (1984).
[51]S. Andersson and J. B. Pendry, Solid State Commun. **16**, 563 (1975).
[52]S. Andersson and J. B. Pendry, J. Phys. C **6**, 601 (1973).
[53]J. E. Demuth, D. W. Jepsen, and P. M. Marcus, J. Phys. C **8**, L25 (1975).
[54]S. Andersson and J. B. Pendry, J. Phys. C **9**, 2721 (1976).
[55]M. A. Passler, T. H. Lin, and A. Ignatiev, J. Vac. Sci. Technol. **18**, 481 (1981).
[56]S. Andersson, B. Kasemo, J. B. Pendry, and M. A. Van Hove, Phys. Rev. Lett. **31**, 595 (1973).
[57]P. M. Marcus, J. E. Demuth, and D. W. Jepsen, Surf. Sci. **53**, 501 (1975).
[58]J. E. Demuth and T. N. Rhodin, Surf. Sci. **45**, 249 (1974).
[59]S. Y. Tong and K. H. Lau, Phys. Rev. **25**, 7382 (1982).
[60]J. E. Demuth, N. J. DiNardo, and G. S. Cargill III, Phys. Rev. Lett. **50**, 1373 (1983).
[61]M. A. Van Hove and S. Y. Tong, J. Vac. Sci. Technol. **12**, 230 (1975).
[62]J. E. Demuth, D. W. Jepsen, and P. M Marcus, Phys. Rev. Lett. **32**, 1182 (1974).
[63]C. B. Duke, N. O. Lipari, and G. E. Laramore, J. Vac. Sci. Technol. **12**, 222 (1975).
[64]C. B. Duke, N. O. Lipari, and G. E. Laramore, Solid State Commun. **13**, 579 (1973).
[65]Y. Gauthier, D. Aberdam, and R. Baudoing, Surf. Sci. **78**, 339 (1978).
[66]J. E. Demuth, D. W. Jepsen, and P. M. Marcus, Phys. Rev. Lett. **31**, 540 (1973).
[67]G. J. R. Jones, Julia H. Onuferko, D. P. Woodruff, and B. W. Holland, Surf. Sci. **147**, 1 (1984).
[68]J. E. Demuth, J. Colloid Interface Sci. **58**, 184 (1977).
[69]R. Baudoing, Y. Gauthier, and Y. Joly, J. Phys. C **18**, 4061 (1985).
[70]G. Casalone, M. G. Cattania, F. Merati, and M. Simonetta, Surf. Sci. **120**, 171 (1982).
[71]K. Christmann, R. J. Behm, G. Ertl, M. A. Van Hove, and W. H. Weinberg, J. Chem. Phys. **70**, 4168 (1979).
[72]R. J. Behm, K. Christmann, G. Ertl, and M. A. Van Hove, J. Chem. Phys. **73**, 2984 (1980).
[73]W. Berndt, R. Hora, and M. Scheffler, Surf. Sci. **117**, 188 (1982).
[74]F. Maca, M. Scheffler, and W. Berndt, Surf. Sci. **160**, 467 (1985).
[75]T. Grandke and K. Heintz, Z. Naturforsch **32**, 1049 (1977).
[76]L. L. Kesmodel, L. H. Dubois, and G. A. Somorjai, J. Chem. Phys. **70**, 2180 (1979).
[77]K. Hayek, H. Glassl, A. Gutmann, H. Leonhard, M. Prutton, S. P. Tear, and M. R. Welton-Cook, Surf. Sci. **152**, 419 (1985).
[78]S. Hengrasmee, P. R. Watson, D. C. Frost, and K. A. R. Mitchell, Surf. Sci. **87**, L249 (1979).
[79]S. Hengrasmee, P. R. Watson, D. C. Frost, and K. A. R. Mitchell, Surf. Sci. **92**, 71 (1980).
[80]R. J. Koestner, M. A. Van Hove, and G. A. Somorjai, Surf. Sci. **121**, 321 (1982).
[81]M. A. Van Hove, Rongfu Lin, and G. A. Somorjai, Phys. Rev. Letts. **51**, 778 (1983).
[82]R. J. Koestner, M. A. Van Hove, and G. A. Somorjai, Surf. Sci. **107**, 439 (1981).
[83]M. A. Van Hove, R. J. Koestner, J. C. Frost, and G. A. Somorjai, Surf. Sci. **129**, 482 (1983).
[84]P. C. Wong, K. C. Hui, M. Y. Zhou, and K. A. R. Mitchell, Surf. Sci. **165**, L21 (1986).
[85]P. C. Wong, M. Y. Zhou, K. C. Hui, and K. A. R. Mitchell, Surf. Sci. **163**, 172 (1985).
[86]G. Michalk, W. Moritz, H. Pfnur, and D. Menzel, Surf. Sci. **129**, 92 (1983).
[87]A. V. Titov and H. Jagodzinski, Surf. Sci. **152**, 409 (1985).
[88]H. D. Shih, F. Jona, D. W. Jepsen, and P. M. Marcus, Phys. Rev. B **15**, 5561 (1977).
[89]H. D. Shih, F. Jona, D. W. Jepsen, and P. M. Marcus, J. Vac. Sci. Technol. **15**, 596 (1978).
[90]H. D. Shih, F. Jona, D. W. Jepsen, and P. M. Marcus, Surf. Sci. **60**, 445 (1976).
[91]K. Griffiths, D. A. King, G. C. Aers, and J. B. Pendry, J. Phys. C **15**, 4921 (1982).
[92]M. A. Passler, B. W. Lee, and A. Ignatiev, Surf. Sci. **150**, 263 (1985).
[93]K. Heinz, D. K. Saldin, and J. B. Pendry, Phys. Rev. Letts. **55**, 2312 (1985).

[94]J. C. Buchholz, Ph.D. thesis, University of Wisconsin, 1974.
[95]M. A. Van Hove, S. Y. Tong, and M. H. Elconin, Surf. Sci. **64**, 85 (1977).
[96]K. C. Hui, R. H. Milne, K. A. R. Mitchell, W. T. Moore, and M. Y. Zhou, Solid State Commun. **56**, 83 (1985).

#### 4.3.c. Notes for Adsorbate-Covered Metal Surfaces

There have been a wide variety of LEED studies of species adsorbed on clean metal surfaces. The reliability of investigations varies quite widely, from modern R-factor assisted studies with a large database to older work relying on visually fitting only a few diffraction beams. Most adsorbates studied adsorb as atomic species in high-symmetry coordination sites on the surface, sometimes resulting in reconstruction of the metal surface itself, or incorporation as an underlayer. Molecular adsorbate studies are less numerous, being confined to CO and simple hydrocarbons adsorbed primarily on Group VIII metals.

##### 4.3.c.1. Atomic Adsorption on High-Symmetry Sites

In the main, atomic species adsorbed on low-index surfaces have been found to occupy the high-symmetry sites shown in Fig. 7. In this figure adsorbate atoms are drawn shaded, while dotted lines represent clean surface atomic positions and arrows show atomic displacements due to adsorption. These adsorption sites are expressed in Table 8 (Summary Table B) as *x-F*, meaning *x*-fold coordinate, considering only the first shell of nearest neighbors. In some cases, alternate sites of the same coordination are distinguished by the presence or absence of an atom directly below in the next atomic layer, e.g., 3-F(1) and 3-F(2) sites on an FCC(111) surface, or by the arrangement of metal atoms making up the site, e.g., 2-F(S) and 2-F(L)—short and long 2-F bridge sites on an FCC(110) surface.

##### 4.3.c.2. Adsorption-Induced Surface Reconstruction

Changes in the geometry of substrate atoms due to adsorption fall into three classes: alteration, usually removal, of a reconstruction or relaxation pre-existing on the clean surface, underlayer formation, or the formation of a new reconstruction of the metal atoms.

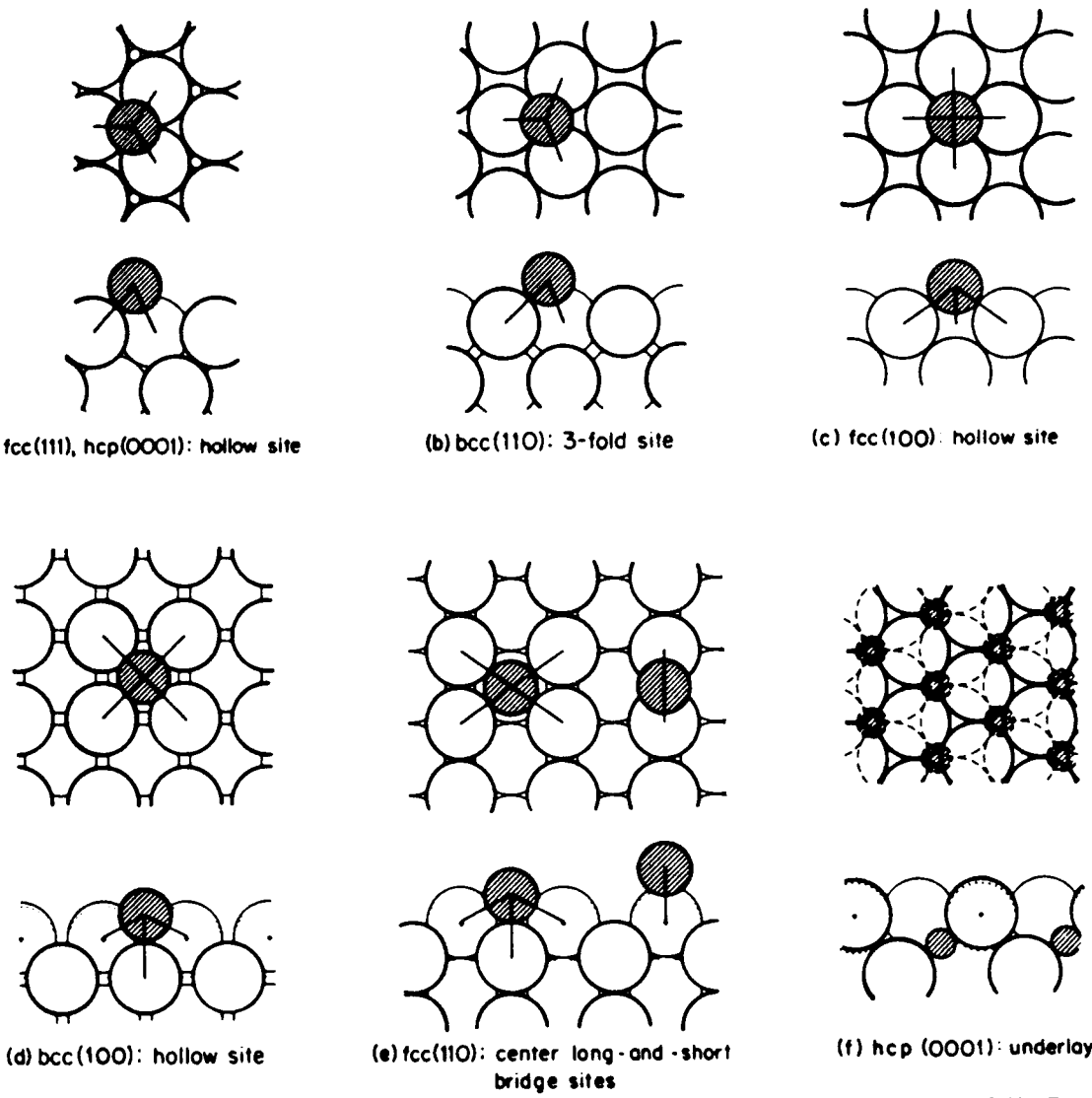


FIG. 7. Schematic diagram (top and side views) of high-symmetry adsorption sites on low-index surfaces of metals (from Ref. 13). Reprinted with the permission of Springer [G. A. Somorjai and M. A. Van Hove, *Adsorbed Monolayers on Surfaces* (Springer, Berlin, 1981), Figs. 6.1 and 6.2].

TABLE 9. Relaxations of metal first interlayer spacings upon adsorption [Expressed as percentage changes ($\delta d_1$) from the bulk value.]

| Metal | $\delta d_1$ (%) clean surface | Adsorbate | $\delta d_1$ (%) after adsorption | Reference |
|---|---|---|---|---|
| Co(100) | −4 | c(2×2) − O | 0 | B17 |
| Cu(100) | 0 | c(2×2) − Cl | +2.5 | B19 |
| Fe(100) | −1 | (1×1) − O | +7.5 | B31 |
| Mo(100) | −10 | c(2×2) − S | 0 to −5 | B39 |
| | −11 | (1×1) − Si | 0 to −5 | B30 |
| Ni(100) | 0 | p(2×2) − C | +8.5 | B41 |
| Ni(110) | −8.4 | c(2×2) − S | +10 | B69 |
| W(100) | −6 | c(2×2) − CO,N | 0 | B91 |
| | −5 to −7 | p(1×1) − 2H | −2 | B92 |

A. Alteration of a reconstruction or relaxation

The removal of a clean surface reconstruction upon adsorption is quite common. Typical examples include the removal of the (1×5) reconstructions (see Table 3) of Ir(100) and Pt(100) by the adsorption of O,[B36] and Cs,[B75] respectively, and the (2×2) W(100) reconstruction by O.[B93]

Those metals that show significant relaxations of their surface layers (see Table 3) also often have those relaxations changed by adsorption. They are summarized in Table 9. Most often the substrate atoms tend to revert to a structure more closely resembling that of the bulk, although in at least one case, that of Ni(110) c(2×2)-S,[B69] the multilayer relaxation observed on the clean surface appears to change sign and increases in magnitude upon adsorption.

B. Formation of a new reconstruction

There are a few well-documented cases of structural determinations which reveal that adsorbates can induce a reconstruction of a metallic substrate. In the cases of Fe(110) p(2×2)-S[B34] and Ni(100) (2×2)-C (p4g),[B43] although the adsorbate atoms reside in the expected fourfold hollow sites, they induce a 2×2 reconstruction which enlarges that hollow by contracting other hollows.

In the Fe case, adsorption of a 1/4 monolayer of S atoms leads to a lengthening of the two shorter bonds and a decrease in the two longer bonds to its surrounding atoms until the displaced atoms jam (as fixed by bulk hard-sphere radii) as shown in Fig. 8. The (2×2) structure on the Ni(100) surface is produced by a 1/2 monolayer of C and here parallel displacements of Ni atoms stop short of jamming (Fig. 9), but do lower the symmetry from p4m to p4g as is observed experimentally.

Another high-quality LEED study showed that the (1×2) LEED pattern seen after hydrogen adsorption on Ni(110)[B67] could not be solved satisfactorily, but that a missing-row construction of the type seen for Ir(110) (see Table 3) with H atoms adsorbed in the missing row gave an encouraging fit. A study of O on Cu(100)[B23] that used a small dataset and did not use R-factors suggested that the O atoms are incorporated in a coplanar Cu–O surface layer.

C. Underlayer formation

The LEED literature contains four quite reliable studies that provide instances of adsorbate species on metals that penetrate below the topmost layer of metal atoms to form an underlayer. The derived structural parameters are given in Table 10. In the Al/O,[B15] Ti/N,[B90] and Zr/O[B96] systems, adsorbate atoms occupy octahedral interstitial holes in the

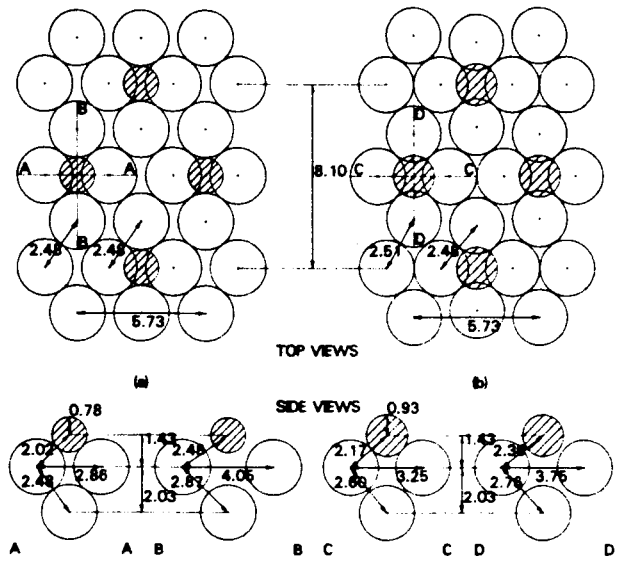


FIG. 8. Model of the Fe(110) (2×2)-S structure: (a) the unreconstructed surface and (b) the reconstructed surface (from Ref. B34). Reprinted with the permission of AIP [Phys. Rev. Lett. **46**, 731 (1981)—Fig. 1].

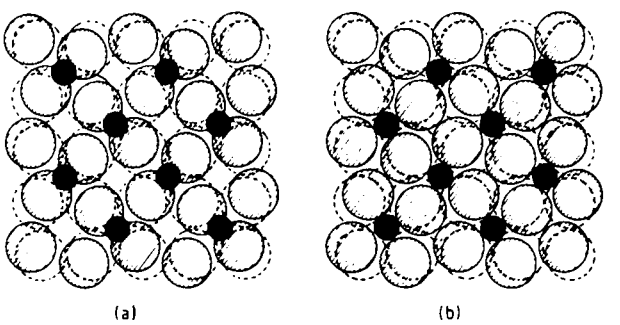


FIG. 9. Model of the reconstructed surface of the Ni(100) (2×2)-C system (from Ref. B43). Reprinted with the permission of North-Holland [Surf. Sci. **87**, 357 (1979)—Fig. 4].

TABLE 10. Structural parameters for metal-adsorbate systems showing underlayer formation [The distance of the adsorbate atom from the topmost metal layer ($d_0$), the metal surface interlayer separation ($d_1$) and the metal-adsorbate bond-length are given in Å. The change of the metal interlayer spacing ($\delta d_1$) is expressed in % of the bulk value.]

| System | Underlayer site | $d_0$ (Å) | $d_1$ (Å) | $\delta d_1$ (%) | $d(M-X)$ (Å) | Reference |
|---|---|---|---|---|---|---|
| Al(111) (1×1) – O | $O_h$ | – 0.3 | 1.99 | – 15 | ··· | B15 |
| Ta(100) (1×3) – O | $T_d$[a] | – 1.55 | 3.05 | – 5 | 2.0 | B87 |
| Ti(0001) (1×1) – N | $O_h$ | – 1.22 | 2.44 | 4.6 | 2.09 | B90 |
| Zr(0001) (2×2) – O | $O_h$[b] | – 1.37 | 2.74 | 6.6 | 2.31 | B96 |

[a] Reconstructed Ta surface.
[b] Zr surface layers FCC rather than HCP.

lattice, illustrated for Ti/N in Fig. 10. However, in the Zr/O case, a structure in which the uppermost layers of Zr had rearranged to an FCC structure produced a better fit with experiment. The structure derived for Ta(100) (1×3)-O[B87] featured O atoms in underlayer quasitetrahedral holes with a reconstructed surface layer of buckled chains of Ta atoms with a lateral contraction of the Ta-Ta distance (Fig. 11).

#### 4.3.c.3. Molecular Adsorbates

A. CO

Reliable LEED structure determinations have been carried out for CO adsorption on a few surfaces of mainly Group VIII metals. After some debate in the Ni(100) case, it now seems to be generally accepted that CO bonds perpendicularly to the surface through the C atom, usually in a 1-F configuration. Structural details are given in Table 11.

The most complex system is that studied by Van Hove *et al.*[B83] in which 3/4 monolayer coverage of CO on the Rh(111) surface involves one bridge and two near-top sites, Fig. 12. In this figure the large circles represent Rh atoms with dotted ones being outside the plane of the paper. Small dotted circles represent C and O atoms satisfying an hexagonal overlayer of 3/4 coverage, while small full circles represent optimum positions. In this structure the near-top site is asymmetrical, yielding a bent Rh–C–O species. The near-top molecules are forced sideways by about 0.53 Å due to the bridge-bonded molecules 2.85 Å away.

B. Hydrocarbons

A few structures of hydrocarbons adsorbed on Group VIII metals have been performed. The most reliable of these extremely difficult and time-consuming studies are probably the recent work on Pt(111) and Rh(111) from Van Hove *et al.*[B76,B80,B81] The $C_2$–$C_4$ olefins and acetylene all appear to bond to these two surfaces similarly,[56] in that the olefin dehydrogenates to form an alkyne species bonded perpendicularly above a 3-F(2) site on the FCC surface with strong metal-carbon bonding as evidenced by the short bond lengths (see Table 12). The best characterized is ethylidyne shown in Fig. 13.

On Ni(111) acetylene is thought to bond parallel to the surface over a bridge site,[B70] while on Ni(100) it is thought to be bonded at a tilt angle of 50° over the same site.[B44] However, these latter studies are of lower reliability.

A single study of benzene adsorption on Rh(111),[B81]

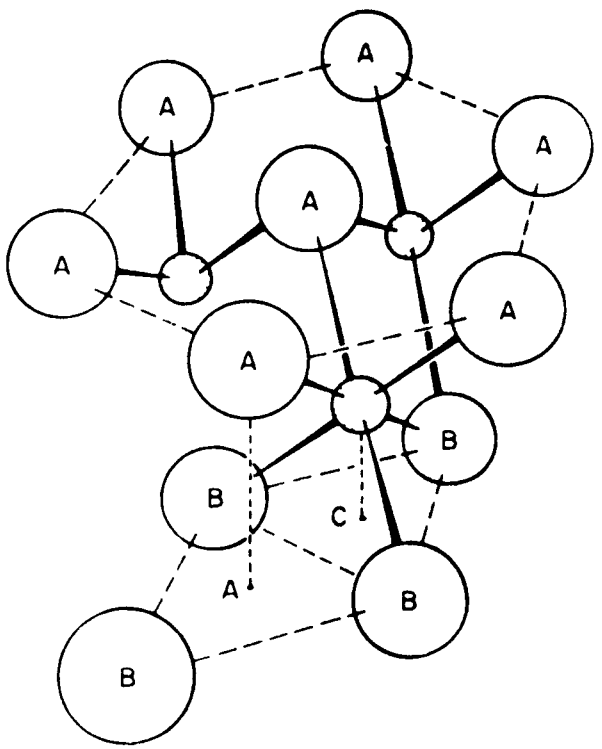


FIG. 10. Model of the Ti(0001) (1×1)-N structure (from Ref. B90). Reprinted with the permission of North-Holland [Surf. Sci. 60, 445 (1976)—Fig. 12].

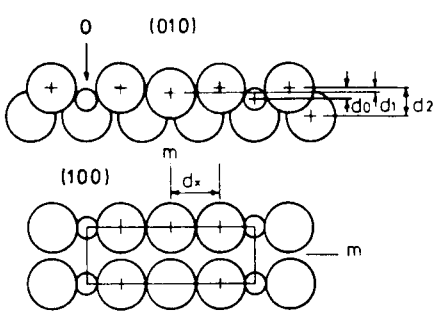


FIG. 11. Model of the (1×3)-O structure on Ta(100) (from Ref. B87). Reprinted with the permission of North-Holland [Surf. Sci. 152, 409 (1985)—Fig. 7].

TABLE 11. Structural parameters for CO molecularly adsorbed on various metal surfaces [In all cases the CO is thought to be bonded perpendicularly through the C atom. The separation of the overlayer C atom from the topmost metal layer ($d_0$), and the metal-carbon and carbon-oxygen bond length are in (Å). In all cases the substrate was assumed to be unaffected.]

| Metal surface | Structure | Adsorption site | $d_0$ (Å) | d(M–C) (Å) | d(C-O) (Å) | Ref. |
|---|---|---|---|---|---|---|
| Cu(100) | c(2×2) | 1 – F | 1.90 | 1.90 | 1.13 | B20 |
| Ni(100) | c(2×2) | 1 – F | 1.72 | 1.72 | 1.13 | B46–49 |
| Pd(100) | c(2√2×√2)R45 | 2 – F | 1.36 | 1.93 | 1.15 | B72 |
| Rh(111) | (√3×√3))R30 | 1 – F | 1.95 | 1.95 | 1.07 | B82 |
| | (2×2)-3CO | 1 – F | 1.94 | 1.94 | 1.15 | B83 |
| | | 2 – F | 1.52 | 2.03 | 1.15 | |
| Ru(0001) | (√3×√3)R30 | 1 – F | 2.00 | 2.00 | 1.10 | B86 |

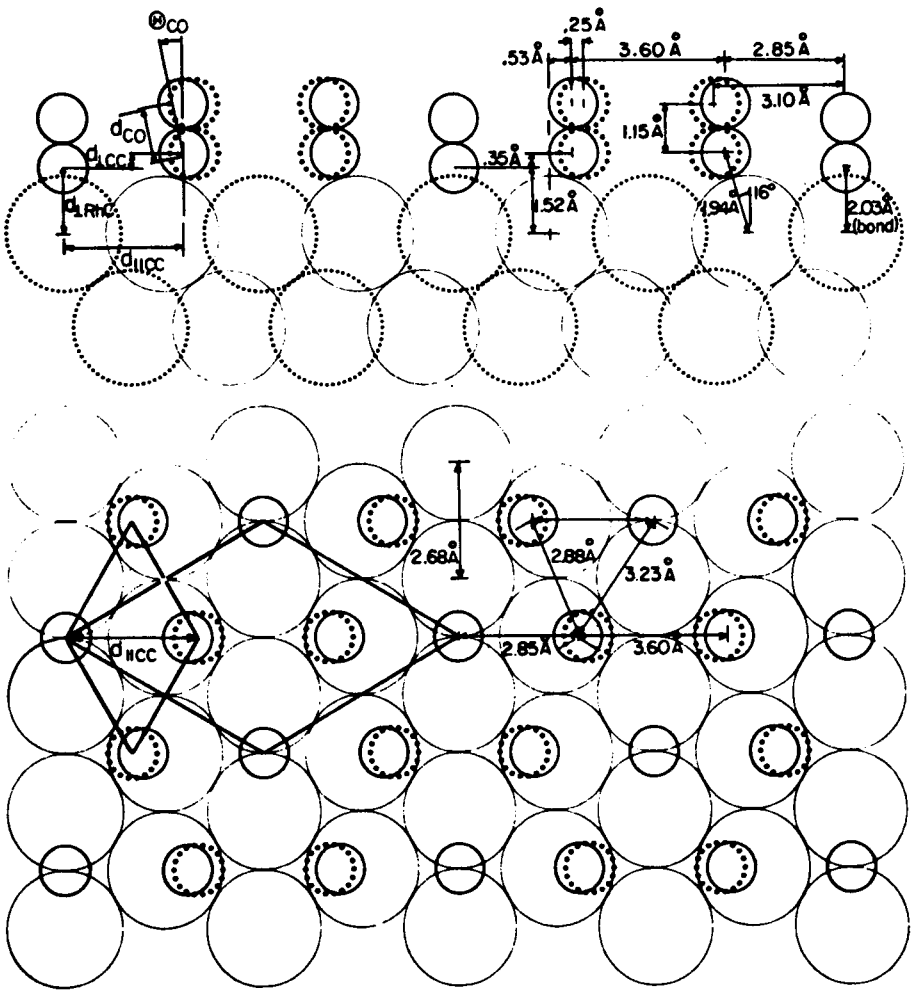


FIG. 12. Schematic diagram of the Rh(111) (2×2)-3CO surface structure showing projections onto the surface plane (bottom) and onto a mirror plane of the structure (top) (from Ref. B83). Reprinted with the permission of North-Holland [Surf. Sci. **129**, 482 (1983)—Fig. 1].

TABLE 12. Structural parameters for hydrocarbons adsorbed on various metal surfaces [The metal-carbon and carbon-carbon bond lengths are in (Å) and the angle of tilt of the C-C axis ($\theta$) in degrees. Figures in square parentheses indicate direction of molecule or tilt. In all cases the substrate was assumed to be unaffected.]

| System | Adsorption site | d(M–C) (Å) | d(C–C) (Å) | $\theta$ (deg) | Reference |
|---|---|---|---|---|---|
| Ni(100)c(2×2)$C_2H_2$ | 4-F | 2.20 | 1.20 | 50 [011] | B44 |
| Ni(111)p(2×2)$C_2H_2$ | 2-F [11-2] | 2.10 | 1.50 | 0 | B70 |
| Pt(111)(2×2)$C_2H_2$ (ethylidyne) $C_2H_4$ | 3-F(2) | 2.00 | 1.50 | 90 | B77 |
| Rh(111)(2×2)$C_2H_4$ (ethylidyne) | 3-F(2) | 2.03 | 1.45 | 90 | B80 |
| Rh(111)(3 1/3 1)$C_6H_6$ | 3-F(2) | 2.35 | 1.25<br>1.60 | 0 | B81 |

yielded a structure in which the benzene molecules lie flat over the 3-F(2) site with a possible planar ring distortion and alternating C–C bond lengths (see Table 12 and Fig. 14). The large size of the unit cell necessitated an approach using approximate LEED theory which nevertheless seems to give impressive results.

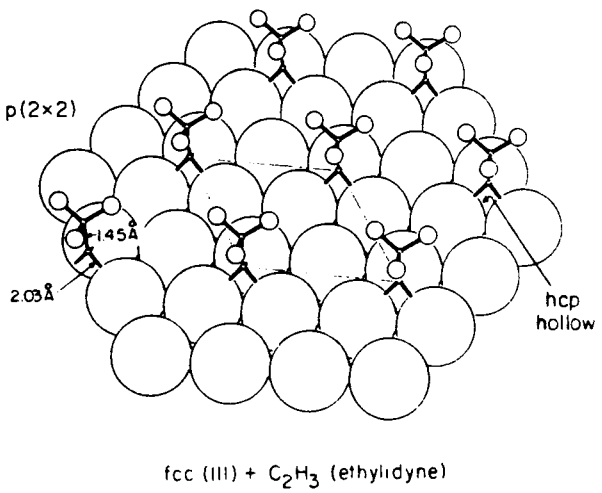


FIG. 13. Proposed structure for the (2×2) ethylidyne structure on Rh(111) (Ref. B80). Reprinted with the permission of North-Holland [Surf. Sci. **121**, 321 (1982)—Fig. 6].

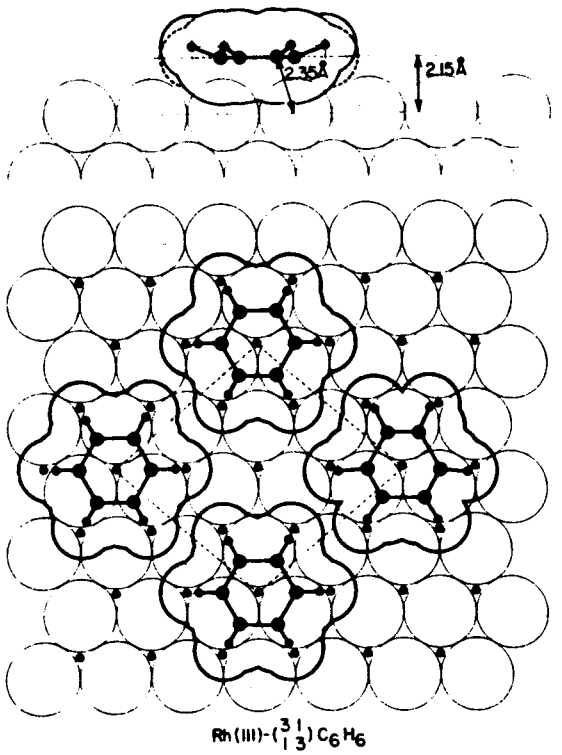


FIG. 14. Proposed structure for benzene adsorbed on Rh(111) showing in-plane distortion (from Ref. B81). Reprinted with the permission of AIP [Phys. Rev. Lett. **51**, 778 (1983)—Fig. 1].

# 4.4. Nonmetallic Clean Surfaces

## 4.4.a. Summary Table C

TABLE 13. (Summary Table C) Clean surfaces of nonmetals

| Substrate | Surface | Struct. | Ref. | S | Anal. Crys. | Cont. meth. | level | Data | Angs. | Off-Normal | Norm. | Range | Calc. | R-Mods. | factor | Vor | Rating | δd1% | Comments |
|---|---|---|---|---|---|---|---|---|---|---|---|---|---|---|---|---|---|---|---|
| AlP | 110 | (1×1) | 1 | 1 | H | AES(S) | Low | SP | 1 | 14(7) | 0 | >7 | MI | Many | 0.19(Rx) | −15 | A− | — | High coverage of Al to form AlP by Ga replacement from GaAs(110). Modified GaAs structure (see notes). |
| AlAs | 110 | (1×1) | 2 | 2 | — | AES | — | SP | 1 | 9,4 | 0 | 9 | MI | 5 | 0.25(Rx)<br>0.30(ZJ) | — | A− | — | Replacement of Ga by Al at 450 °C. Modified GaAs structure (see notes). |
| C(d) | 111 | (1×1) | 3 | 2 | H | — | — | — | 2 | 2(0) | 2(1) | 4 | CHANGE | 1 | — | −10 | C | 0.0 | No difference between insulating and semi-conducting samples. |
| C(g) | 0001 | (1×1) | 4 | — | — | AES | — | SP | 1 | 3(0) | 0 | 3 | RSP/RFS | 2 | 0.19(ZJ) | −8 | B− | −1.5 | Cleaved natural graphite; no cleaning to avoid damage. Bulk stacking ABABA. |
| CaO | 100 | (1×1) | 5 | 2 | — | AES(S) | Low | SP | 7 | 4(2) | 35 | ≥9 | CAVLEED | 2 | 0.156(ZJ) | −11.2 | A | −1.0 | Simple termination with no rumpling. |
| CdTe | 110 | (1×1) | 6 | 5 | H | AES | Low | SP | 1 | 12(7) | 0 | >9 | MI | 4 | 0.41(ZJ) | −5 | A− | — | Data at 110 K on cleaved surface. GaAs-type structure (see note). |
| CoO | 100 | (1×1) | 7 | 1 | — | AES | — | P-MO | 1 | 7(5) | 0 | >3 | CAVLEED | 1 | 0.10(ZJ) | −11 | B+ | 0.0(3.0) | Simple termination with no rumpling. |
| GaAs | 110 | (1×1) | 8 | 1 | — | AES | — | SP | 1 | 5(0) | 0 | 5 | LD | 2 | — | −8 | B− | 0.0 | Rippled geometry with As rotated out, Ga rotated in. Ga-As-Ga nearly parallel to ⟨1–10⟩, no changes in bond-lengths. |
| GaAs | 110 | (1×1) | 9 | — | H | AES | <1% C | SP | 1 | 16(>5) | 0 | >8 | CSM | 12 | — | −10 | A− | * | As [8] but As back-bond contracted 5%, Ga to 2nd layer 1.45 Å. Data at 95 K. |
| GaAs | 110 | (1×1) | 10 | 2 | H | AES | Low | SP | 1 | 10(5) | 0 | 10 | MI | Many | — | −10 | B+ | — | As [9] with 2nd layer distortion in opposite sense to 1st layer. Data at 150 K and 300 K. |
| GaAs | 110 | (1×1) | 11 | 2 | H | AES | Low | SP | 1 | 14(9) | 0 | >10 | MI | Many | 0.21(Rx) | −10 | A− | — | Experimental data of [9]. Alternative structure with lower angle of rotation and reversed relaxations almost as good fit. |
| GaAs | 110 | (1×1) | 12 | 2 | H | AES | Low | SP | 1 | 14((9) | 0 | >10 | MI | Many | 0.12(Rx) | −10 | A− | — | Re-examination of [11] showed that parallel relaxation and a large rotation can be reduced to <1% without effecting fit. |
| GaAs | 110 | (1×1) | 13 | * | H | AES | Low | SP | 1 | * | * | * | CSM | Many | 0.27(VHT)<br>0.31(ZJ)<br>0.29(Rx) | — | A− | — | Experimental data of [8, 9]. 2 layer, large rotation structure. Laterial shifts must be >0.1 Å. See reply [14] and notes. |
| GaAs | 111 | (2×2) | 15 | 1 | H | — | — | — | 1 | 10.5 | 0 | ≥3 | CSM | 6 | 0.13(?) | — | A− | — | Vacancy buckling model with 1/4 ML of surface Ga missing, similar to GaAs(110). See notes. |
| GaP | 110 | (1×1) | 16 | 2 | H | AES | Low | SP | 1 | 14(9) | 0 | >9 | MI | Many | 0.30(ZJ)<br>0.17(Rx) | −13 | A− | — | P out, Ga in, no evidence for 2nd layer reconstructions. Similar to GaAs(110) (see notes). Data at 300 K. |
| GaP | 110 | (1×1) | 17 | 1 | H | AES | Low | SP | 1 | 14(9) | 0 | — | MI | Many | 0.22(Rx) | −13 | A− | — | Re-examination of [16] using new data at 125 K. Ruled out any small angle rotations. |
| GaP | 110 | (1×1) | 18 | — | H(P) | AES | Low | SP | 1 | 16 | 0 | ≥3 | RFS | 17 | — | — | B+ | — | Data taken at room temperature and 90 K. |
| GaP | 111 | (2×2) | 19 | 1 | H | AES | <1% C | — | 1 | 10,5(4) | 0 | 10 | CSM | — | 0.21(VHT) | −9 | A− | — | 1/4 of surface Ga missing; surface Ga-P bilayer almost coplanar surface and deeper atoms show vertical and lateral displacements. |

TABLE 13. (Summary Table C) continued

| Substrate | Surface | Struct. | Ref. | S | Anal. Crys. | Cont. meth. | level | Data | Angs. | Off-Normal | Norm. | Range | Calc. | R-Mods. | R-factor | Vor | Rating | δd1% | Comments |
|---|---|---|---|---|---|---|---|---|---|---|---|---|---|---|---|---|---|---|---|
| GaSb | 110 | (1×1) | 20 | 1 | H | AES | Low | SP | 1 | 14(9) | 0 | 10 | MI | 5 | 0.25(Rx) | −10 | A− | — | Similar to GaAs(110). Ga in, Sb out, no 2nd layer effects. Data taken at 125 K. See notes. |
| Ge | 100 | (2×1) | 21 | — | — | — | — | SP | 3 | 7 | 20 | — | CHANGE | Many | 0.38(ZJ) | — | A | — | At least 3 layers involved. Buckled asymmetric dimers preferred over symmetric dimes, but structure uncertain. Experimental data of H. P. Shih and F. Jona (unpublished). |
| InAs | 110 | (1×1) | 22 | 2 | H | AES | — | SP | 1 | 14(9) | 0 | >10 | MI | 4 | 0.29(Rx) | −12 | A− | — | Similar to GaAs(110). Ga out, In in, top layer, opposite in 2nd layer. Data taken at 110 K. See notes. |
| InP | 110 | (1×1) | 23 | 1 | H | AES | <2% | SP | 5 | 9.6 | 0 | 9 | RFS | 7 | — | — | B | — | Unknown reconstruction. |
| InP | 110 | (1×1) | 24 | 2 | H | AES | Low | SP | 1 | 14(9) | 0 | >12 | MI | 4 | 0.16(Rx) | −11 | A− | — | Similar to GaAs(110). P out, In in and relaxed towards substrate. Some evidence for 2nd layer distortion. Measured at 150 K. See notes. |
| InSb | 110 | (1×1) | 25 | 1 | H | AES | Low | SP | 1 | 14(9) | 0 | >11 | MI | 5 | — | −8 | B+ | — | Similar to GaAs(110). Sb out, In in and relaxed towards substrate. Some evidence for 2nd layer distortion. Measured at 150 K. See notes. |
| LiF | 100 | (1×1) | 26 | — | — | None | — | — | 1 | 0 | 3,0 | 3 | IS | 2 | — | −11.6 | C | — | Rumpled surface with Li underlayer 0.25 Å below F layer. Data from [27]; LiF surface now known to become Li-rich on e-bombardment [28]. |
| MgO | 100 | (1×1) | 29 | 1 | H | AES(S) | <10% | SP | 1 | 4(2) | 0 | 4 | RFS | 1 | — | −10 | B− | 0.0 | Cleaved *in situ*; used ionic and atomic potentials. Data from [30]. |
| MgO | 100 | (1×1) | 31 | 1 | H | AES(S) | <10% | SP | 8 | 0 | 52(20) | >20 | RFS | 1 | — | −10 | B+ | 0.0(2.0) | Cleaved *in situ*; used ionic and atomic potentials. Data from [30]. |
| MgO | 100 | (1×1) | 32 | 1 | H | AES(S) | Low | SP | 7 | 2(0) | 25(11) | >10 | CAVLEED | 2 | 0.25(P) | −13 | A | 0.0(0.75) | Measured data to lower energy by suppressing charging. Slight rumple anions out, cations in by 0.02 Å. |
| MgO | 100 | (1×1) | 33 | 3 | — | AES | Low | SP | 1 | 3(1) | 0 | 3 | RFS | 2 | — | — | C | 0.0(2.5) | Same results for 3 different heat treatments. No rumpling. |
| $MoS_2$ | 111 | (1×1) | 34 | — | — | AES | <3%C | SP | 1 | 5(3) | 0 | >2 | RFS | 4 | — | −5 | B− | < −5.0 | Data taken at 95 K. No reconstruction. |
| $MoS_2$ | 111 | (1×1) | 35 | — | — | AES | <3% C | SP | 1 | 5(3) | 0 | >2 | RFS | 3 | 0.08(VHT) | −5 | B | −4.7(0.3) | Update of [34] using R-factors. No. reconstruction; 1st Van der Waals gap contracted by 3%. |
| Na2O | 111 | (1×1) | 36 | — | M(P) | EELS | — | SP | 1 | 3(0) | 0 | 3 | RFS | 3 | — | −4 | C | 0.0 | Assumed neutral termination with no dilation. Oxidized Na on Ni. |
| $NbSe_2$ | 111 | (1×1) | 34 | — | — | AES | <3%C | SP | 1 | 5(3) | 0 | >2 | RFS | 3 | — | −2 | B− | 0.0 | Data taken at 95 K. No reconstruction. |
| $NbSe_2$ | 111 | (1×1) | 35 | — | — | AES | <3%C | SP | 1 | 5(3) | 0 | >2 | RFS | 3 | 0.15(VHT) | −2 | B | −1.4(1.4) | Update of [34] using R-factors. No reconstruction; 1st Van der Waals gap contracted by 0.6%. |
| NiO | 100 | (1×1) | 37 | 1 | H | AES(S) | Low | SP | 2 | 4(2) | 4(2) | 8 | CAVLEED | 2 | — | −9 | B | 0.0(5.0) | Rumpling unlikely. Data from [38]. |
| NiO | 100 | (1×1) | 39 | 1 | H | AES | ~1% Cl | SP | 3 | 2(0) | 5(1) | 7 | CAVLEED | 1 | 0.22(ZJ) | −12 | B+ | −2.0(2.0) | No rumpling. New data at 120 °C: update of [37]. |

TABLE 13. (Summary Table C) continued

| Substrate | Surface | Struct. | Ref. | S | Anal. Crys. | Cont. meth. | level | Data | Angs. | Off-Normal | Norm. | Range | Calc. | Mods. | R-factor | Vor | Rating | δd1% | Comments |
|---|---|---|---|---|---|---|---|---|---|---|---|---|---|---|---|---|---|---|---|
| $NiSi_2$ | 111 | (1×1) | 40 | 1 | H | AES | — | — | 2 | 2(0) | 2(0) | 4 | KKR | 2 | — | — | B− | −25 | 1st layer all Si, 2nd layer Ni. Epitaxial growth on Si(111). |
| Si | 100 | (1×1) | 41 | 1 | — | AES | Low | FC | 11 | 2(0) | 11(0) | 13 | RSP | 1 | — | −4 | B+ | 0.0 | Surface from (2×1) with adsorbed H. |
| Si | 100 | (2×1) | 42 | 3 | H | AES | Low | FC/SP | 1 | 7,3(4) | 0 | 7 | QSD | 3 | — | — | B | — | Reasonable agreement for a model [43] with dimers and disturbances down to 5 layers. Data from [44]. |
| Si | 100 | (2×1) | 45 | 1 | H | AES | Low | SP | 1 | 6 | 0 | 6 | KKR | 3 | — | — | B | — | Best fit for conjugated surface chains with 1st and 2nd layer distortions [46]. Data from [44]. |
| Si | 100 | (2×1) | 46 | 1 | H | AES | Low | FC/SP | 1 | 6,3(3) | 0 | 6 | QSD | 2 | — | — | B | — | Preferred dimer model [43] or puckered HCP overlayer. Data from [44]. |
| Si | 100 | (2×1) | 47 | 1 | H | AES | Low | FC/SP | 1 | 5 | 0 | 5 | QSD | 4 | — | — | B | — | Best fit for buckled asymmetric dimers [40] incorrect. Data from [44]. |
| Si | 100 | (2×1) | 49 | 1 | H | AES | Low | FC/SP | 1 | 5,2(4) | 0 | 5 | RSP | 5 | — | −4 | B | — | Concluded that asymmetric dimer model [48] incorrect. Data from [44]. |
| Si | 100 | (2×1) | 50 | 2+ | H | AES | <5% Ni,Pt | TV | 2 | 7,3(4) | 7.0(3) | 14 | QSD/ CHANGE | 4 | 0.16(ZJ) | −9 | A | −8.0 | Best fit has asymmetric and buckled dimers and strains extending 4 layers. New set of data; surface impurity established. |
| Si | 100 | (2×1) | 51 | 1 | H | AES | Low | FC/SP | 2 | 8,4(4) | 7.0(3) | 15 | MI | 3 | 0.13(Rx) | — | A | | New asymmetric dimer model with top-layer buckling and strains 4 layers deep; no twisting as in [50]. Data from [44]. |
| Si | 111 | (1×1) | 52 | 1 | H | AES | 1–5% Te | SP | 2 | 5(2) | 6(2) | 11 | KKR | 1 | — | −9.0 | B+ | −15.0 | Bulk-like, stabilized by Te. |
| Si | 111 | (1×1) | 53 | 1 | H | AES | 1–5% Te | SP | 2 | 5(2) | 6(2) | 11 | CHANGE | 1 | 0.25(ZJ) | −11.7 | A | −21.0 | Update of data from [52]. Spacing between 2nd and 3rd layers unchanged within 1.5%. |
| Si | 111 | (1×1) | 54 | 1 | — | AES | — | FC | 1 | 6(3) | 0 | 6 | ? | — | 0.11(ZJ) | — | B | −25.5(2.5) | Spacing between 2nd and 3rd layers expanded 3.2%(1.5). Laser annealed surface. |
| Si | 111 | (1×1) | 55 | 1 | *(P) | — | — | — | ? | >2 | >1 | ? | — | — | — | | B | — | Quenched structure not same as Te-stabilized, has (2×1) domains. |
| Si | 111 | (1×1) | 56 | 1 | — | AES | — | FC | 1 | 6.3 | 0 | 6 | RSP | 4+ | 0.38(P) | −13.2 | B | — | Model with graphite-like top double layer 2.95 Å from a second double layer with large displacements normal to surface. Data from [54]. |
| Si | 111 | (2×1) | 57 | >2 | — | — | — | SP | 1 | >3 | ? | 11 | RFS | 1 | — | −9 | B | −10.0 | Top layer buckled by 0.3 Å, 2nd layer shows slight pairing between adjacent rows. 2nd-3rd layer spacing contracted by 3.5%. Sample cleaved *in situ*. |
| Si | 111 | (2×1) | 58 | >2 | — | — | — | SP | 1 | >3 | ? | 11 | RFS | 2 | — | −9 | B | — | Pi-bonded chain model [59] not favoured relative to buckling model. Data from [57]. |
| Si | 111 | (2×1) | 60 | 1 | — | — | — | TV | 1 | 11(5) | 0 | 11 | CHANGE | 4 | — | — | B | — | Buckling [61], chain [59] and molecular [62] pi-bonded, and conjugated chain models not compatible with new dataset. |
| Si | 111 | (2×1) | 63 | — | — | — | — | TV | 1 | 12,1(6) | 0 | 12 | CHANGE | Many | 0.42(ZJ) | — | A | — | Moderate agreement for pi-bonded chain model [59] with buckling in outer chain and an overall compression. |
| Si | 111 | (7×7) | 64 | 1 | H(P) | AES | Low | P | 1 | — | — | — | KIN | 5 | — | −10 | B | — | Surface nearly ideally terminated, no vacancies or adatoms; small ripple of 1st two double layers. Fitted intensity of some peaks, I(E) curves kinematically. |
| Si | 111 | (7×7) | 65 | 1 | H(P) | AES | Low | P | 1 | — | — | — | KIN | 7 | — | — | B | — | Surface vacancies or adatoms ruled out; data favor an hexagon-based distortion over several layers. Used energy-averaged data from [64]. |

TABLE 13. (Summary Table C) continued

| Substrate | Surface | Struct. | Ref. | S | Anal. Crys. | Cont. meth. | level | Data | Angs. | Off-Normal | Norm. | Range | Calc. | Mods. | R-factor | Vor | Rating | δd1% | Comments |
|---|---|---|---|---|---|---|---|---|---|---|---|---|---|---|---|---|---|---|---|
| Si | 111 | (7×7) | 66 | — | H(P) | — | — | P | — | — | — | — | KIN | — | — | — | B | 0.0(5.0) | Data consistent with triangular islands with ⟨ − 1–10⟩ step edges with area 1/2 of (7×7) mesh. |
| Si | 111 | (7×7) | 67 | — | — | — | — | FC | Many | — | — | 3 | CMTA | — | — | — | B | — | Unit cell has 2 equal triangular features separated by a stacking fault; agrees with ion-channeling data. |
| Si | 111 | (7×7) | 68 | — | — | — | — | TV | 2 | — | — | — | — | — | — | — | B | — | By comparison with (2×1) data, surface contains 3 domains of (2×1) subunits, each with a mirror plane. Energy averaged non-integral beam data. |
| Si | 111 | (7×7) | 69 | — | H(P) | — | — | P | — | — | — | — | KIN | — | — | — | A | — | Comparison of patterns, not I(E) data), fits triangular checkerboard structure in which AaBbA and AaCcA stacking sequences alternate in neighbouring units. Surface has deep hole (6.3 Å) at apex. Substantially in accord with data from other techniques. |
| Te | 10–10 | (1×1) | 70 | >2 | H | AES/ EELS | Low | P-MO | 1 | 12(4) | 0 | >9 | MI | Many | — | −13 | B | — | Structure similar to GaAs(110), top layer Te in by 0.21 Å and 2nd layer out by 0.46 Å. See notes. Data taken at 55 K. |
| ZnO | 0001 | (1×1) | 71 | 1 | M(P) | AES | Low | SP | 1 | 1 | 0 | 1 | IC | 1 | — | — | C− | — | Data from [72]. Possible contraction but poor agreement. Possible domain structure. |
| ZnO | 10–10 | (1×1) | 73 | 1 | M(P) | AES | Low | SP | 3 | 6(0) | 12(0) | >15 | MI/LO | 4 | — | −10 | B | — | Oxygen in by 0.1Å, Zn by 0.3Å; may be some lateral changes. Data from [74]. |
| ZnO | 11–20 | (1×1) | 75 | 1 | M(P) | AES | Low | SP | ? | ? | ? | ? | LD | 1 | — | −8 | ? | — | No reconstruction. Data from [74]. |
| ZnS | 110 | (1×1) | 76 | 1 | — | AES | Low | SP | 1 | 14(8) | 0 | >2 | MI | 3 | 0.22(Rx) 0.23(ZJ) | −14 | A | — | Several structures gave similar fits; GaAs structure likely (see notes). |
| ZnSe | 110 | (1×1) | 77 | — | — | AES(S) | Low C | SP | 1 | 4(0) | 0 | >2 | LD | 3 | — | −8 | B− | — | Appeared unreconstructed. |
| ZnSe | 110 | (1×1) | 78 | 2 | 4 | AES | Low | SP | 1 | 14(8) | 0 | 14 | MI | 1 | 0.22(Rx) | — | A− | — | Small and large (GaAs-type) rotation structures indistinguishable Se out, Zn in. Data at 200 K; ZnSe grown epitaxially on GaAs (110). |
| ZnTe | 110 | (1×1) | 79 | 1 | — | AES | Low | SP | 1 | 14(9) | 0 | >7 | MI | 7 | — | −4 | B | — | 1st layer Te out by 0.20 Å, Zn in by 0.55 Å; no changes in 2nd layer; different from GaAs(110). Data at 125 K. |
| ZnTe | 110 | (1×1) | 80 | 1 | — | AES | Low | SP | 1 | 14(9) | 0 | >7 | MI | 1 | 0.26(Rx) | −8 | A | — | Re-evaluation of [79]. Similar to GaAs(110). 1st layer Te out by 0.16 Å, Zn in by 0.55 Å. 2nd layer Te in, Zn in by 0.22 Å. See notes. |

#### 4.4.b. References to Table 13—Clean Nonmetals


[1]C. B. Duke. A. Paton, A. Kahn, and C. R. Bonapace, Phys. Rev. B **28**, 852 (1983).
[2]A. Kahn, J. Carelli, D. Kanani, C. B. Duke, A. Paton, and L. Brillson, J. Vac. Sci. Technol. **19**, 331 (1981).
[3]W. S. Wang, J. Sokolov, F. Jona, and P. M. Marcus, Solid State Commun. **41**, 191 (1982).
[4]N. J. Wu and A. Ignatiev, Phys. Rev. B **25**, 2983 (1982).
[5]M. Prutton, J. A. Ramsey, J. A. Walker, and M. R. Welton-Cook, J. Phys. C **12**, 5271 (1979).
[6]C. B. Duke, A. Paton, W. K. Ford, A. Kahn, and G. Scott, Phys. Rev. B **24**, 3310 (1981).
[7]R. C. Felton, M. Prutton, S. P. Tear, and M. R. Welton-Cook, Surf. Sci. **88**, 474 (1979).
[8]C. B. Duke, A. R. Lubinsky, B. W. Lee, and P. Mark, J. Vac. Sci. Technol. **13**, 761 (1976).
[9]S. Y. Tong, A. R. Lubinsky, B. J. Mrstik, and M. A. Van Hove, Phys. Rev. B **17**, 3303 (1978).
[10]R. J. Meyer, C. B. Duke, A. Paton, A. Kahn, E. So, J. L. Yeh, and P. Mark, Phys. Rev. B **19**, 5194 (1979).
[11]C. B Duke, S. L. Richardson, A. Paton, and A. Kahn, Surf. Sci. **127**, L135 (1983).
[12]C. B. Duke and A. Paton, J. Vac. Sci. Technol. B **2**, 327 (1984).
[13]M. W. Puga, G. Xu, and S. Y. Tong, Surf. Sci. **164**, L789 (1985).
[14]C. B. Duke and A. Paton, Surf. Sci. **164**, L797 (1985).
[15]S. Y. Tong, G. Xu, and W. N. Mei, Phys. Rev. Lett. **52**, 1693 (1984).
[16]C. B. Duke, A. Paton, W. K. Ford, A. Kahn, and J. Carelli, Phys. Rev. **24**, 562 (1981).
[17]A. Kahn, J. Vac. Sci. Technol. **19**, 515 (1984).
[18]B. W. Lee, R. K. Ni, N. Masud, S. R. Wang, D. C. Wang, and M. Rowe, J. Vac. Sci. Technol. **19**, 294 (1981).
[19]G. Xu, W. Y. Hu, M. W. Puga, S. Y. Tong, J. L. Yeh, S. R. Wang, and B. W. Lee, Phys. Rev. **32**, 8473 (1985).
[20]C. B. Duke, A. Paton, and A. Kahn, Phys. Rev. B **27**, 3436 (1983).
[21]J. C. Fernandez, W. S. Yang, H. D. Shih, F. Jona, D. W. Jepsen, and P. M. Marcus, J. Phys. C **14**, L55 (1981).
[22]C. B. Duke, A. Paton, A. Kahn, and C. R. Bonapace, Phys. Rev. **27**, 6189 (1983).
[23]S. P. Tear, M. R. Welton-Cook, M. Prutton, and J. A. Walker, Surf. Sci. **99**, 598 (1980).
[24]R. J. Meyer, C. B. Duke, A. Paton, J. C. Tsang, J. L. Yeh, A. Kahn, and P. Mark, Phys. Rev. **22**, 6171 (1980).
[25]R. J. Meyer, C. B. Duke, A. Paton, J. L. Yeh, J. C. Tsang, A. Kahn, and P. Mark, Phys. Rev. **21**, 4740 (1980).
[26]G. E. Laramore and A. C. Switendick, Phys. Rev. B **7**, 3615 (1973).
[27]E. G. McRae and C. W. Caldwell, Surf. Sci. **2**, 509 (1964).
[28]T. E. Gallon, Surf. Sci. **21**, 224 (1970).
[29]C. G. Kinniburgh, J. Phys. C **8**, 2382 (1975).
[30]K. O Legg, M. Prutton, and C. G. Kinniburgh, J. Phys. C **7**, 4236 (1974).
[31]G. C. Kinniburgh, J. Phys. C **9**, 2695 (1976).
[32]M. R. Welton-Cook and W. Berndt, J. Phys. C **15**, 5691 (1982).
[33]T. Urano, T. Kanaji, and M. Kaburagi, Surf. Sci. **134**, 109 (1983).
[34]B. J. Mrstik, R. Kaplan, T. L. Reinecke, M. A. Van Hove, and S. Y. Tong, Phys. Rev. B **15**, 897 (1977).
[35]M. A. Van Hove, S. Y. Tong, and M. H. Elconin, Surf. Sci. **64**, 85 (1977).
[36]S. Andersson, J. B. Pendry, and P. M. Echenique, Surf. Sci. **65**, 539 (1977).
[37]C. G. Kinniburgh and J. A. Walker, Surf. Sci. **63**, 274 (1977).
[38]F. P. Netzer and M. Prutton, J. Phys. C **8**, 2401 (1975).
[39]M. R. Welton-Cook and M. Prutton, J. Phys. C **13**, 3993 (1980).
[40]W. S. Wang, F. Jona, and P. M. Marcus, Phys. Rev. B **28**, 7377 (1983).
[41]S. J. White, D. P. Woodruff, B. W. Holland and R. S. Zimmer, Surf. Sci. **74**, 43 (1978).
[42]S. Y. Tong and A. L. Maldonado, Surf. Sci. **78**, 459 (1978).
[43]J. A. Appelbaum and D. R. Hamann, Surf. Sci. **74**, 21 (1978).
[44]A. Ignatiev, F. Jona, M. Debe, D. E. Johnson, S. J. White, and D. P. Woodruff, J. Phys. C **10**, 1109 (1977).
[45]F. Jona, H. D. Shih, A. Ignatiev, D. W. Jepsen, and P. M. Marcus, J. Phys. C **10**, L67 (1977).
[46]K. A. R. Mitchell and M. A. Van Hove, Surf. Sci. **75**, 147L (1978).
[47]S. J. White, D. C. Frost, and K. A. R. Mitchell, Solid State Comm. **42**, 763 (1982).
[48]D. J. Chadi, Phys. Rev. Lett. **43**, 43 (1979).
[49]. J. R. Jones and B. W. Holland, Solid State Commun. **46**, 651 (1983).
[50]W. S. Yang, F. Jona, and P. M. Marcus, Phys. Rev. **28**, 2049 (1983).
[51]B. W. Holland, C. B. Duke, and A. Paton, Surf. Sci. **140**, L269 (1984).
[52]H. D. Shih, F. Jona, D. W. Jepsen, and P. M. Marcus, Phys. Rev. Lett. **37**, 1622 (1976).
[53]D. W. Jepsen, H. D. Shih, F. Jona, and P. M. Marcus, Phys. Rev. **22**, 814 (1980).
[54]D. M. Zehner, J. R. Noonan, H. L. Davis, and C. W. White, J. Vac. Sci. Technol. **18**, 852 (1981).
[55]W. S. Yang and F. Jona, Phys. Rev. **28**, 1178 (1983).
[56]G. J. R. Jones and B. W. Holland, Solid State Commun. **53**, 45 (1985).
[57]R. Feder, W. Monch, and P. P. Auer, J. Phys. C **12**, L179 (1979).
[58]R. Feder, Solid State Commun. **45**, 51 (1983).
[59]K. C. Pandey, Phys. Rev. Lett. **47**, 1913 (1981).
[60]H. Liu, M. R. Cook, F. Jona, and P. M. Marcus, Phys. Rev. B **28**, 6173 (1983).
[61]D. Haneman, Phys. Rev. **121**, 1093 (1961).
[62]D. J. Chadi, Phys. Rev. B **26**, 4762 (1982).
[63]F. J. Himpsel, P. M. Marcus, F. M. Tromp, I. P. Batra, M. R. Cook, F. Jona, and H. Liu, Phys. Rev. B **30**, 2257 (1984).
[64]J. D. Levine, S. H. McFarlane, and P. Mark, Phys. Rev. B **16**, 5415 (1977).
[65]D. J. Miller and D. Haneman, J. Vac. Sci. Technol. **16**, 1270 (1979).
[66]E. G. McRae and C. H. Caldwell, Phys. Rev. Lett. **46**, 1632 (1981).
[67]P. A. Bennett, L. C. Feldman, Y. Kuk, E. G. McRae, and J. E. Rowe, Phys. Rev. B **28**, 3656 (1983).
[68]W. S. Yang and F. Jona, Solid State Commun. **48**, 377 (1983).
[69]E. G. McRae, Surf. Sci. **147**, 663 (1984).
[70]R. J. Meyer, W. R. Salaneck, C. B. Duke, A. Paton, C. H. Griffiths, L. Kovnat, and L. E. Meyer, Rev. B **21**, 4542 (1980).
[71]C. B. Duke and A. R. Lubinsky, Surf. Sci. **50**, 605 (1975).
[72]S-C. Chang and P. Mark, Surf. Sci. **46**, 293 (1974).
[73]C. B. Duke, A. R. Lubinsky, S. C. Chang, B. W. Lee, and P. Mark, Phys. Rev. B **15**, 4865 (1977).
[74]S. C. Chang and P. Mark, Surf. Sci. **45**, 721 (1974).
[75]A. R. Lubinsky, C. B. Duke, S. C. Chang, B. W. Lee, and P. Mark, J. Vac. Sci. Technol. **13**, 189 (1976).
[76]C. B. Duke, R. J. Meyer, A. Paton, A. Kahn, J. Carelli, and J. L. Yeh, J. Vac. Sci. **18**, 866 (1981).
[77]C. B. Duke, A. R. Lubinsky, M. Bonn, G. Cisneros, and P. Mark, J. Vac. Sci. Technol. **14**, 294 (1977).
[78]C. B. Duke, A. Paton, A. Khan, and D. W. Tu, J. Vac. Sci. Technol. B **2**, 366 (1984).
[79]R. J. Meyer, C. B. Duke, A. Paton, E. So, J. L. Yeh, A. Kahn, and P. Mark, Phys. Rev. **22**, 2875 (1980).
[80]C. B. Duke, A. Paton, and A. Khan, J. Vac. Sci. Technol. A **1**, 672 (1983).


#### 4.4.c. Notes on Clean Nonmetallic Surfaces

LEED studies in this class have concentrated, not suprisingly, upon semiconductor substrates, particularly Si and the III–V and IV–VI compound semiconductors, together with a few studies of binary oxides.

##### 4.4.c.1. Si and Ge(100)

The cleaved Si(100) surface exhibits a $(2\times1)$ LEED pattern indicative of a reconstruction. Adsorption of hydrogen results in a $(1\times1)$ pattern that has been shown to be due to an essentially truncated bulk structure.[C41] The $(2\times1)$ reconstruction has been the subject of a number of studies.[C42–C51] The latest and most reliable studies in terms of the size of the database and the use of R-factors are those of Yang *et al.*[C50] and Holland *et al.*[C51] A schematic of this surface is shown in Fig. 15 and the values of the structural parameters from these two studies listed in Table 14. The two structures share many similarities; both involve asymmetric dimers, where atoms such as $Si_{11}$ and $Si_{12}$ come closer together, with strains extending several layers into the material. The principle difference is that in the model of Holland *et al.*[C51] the dimers lie along the $x$ axis, while the Yang

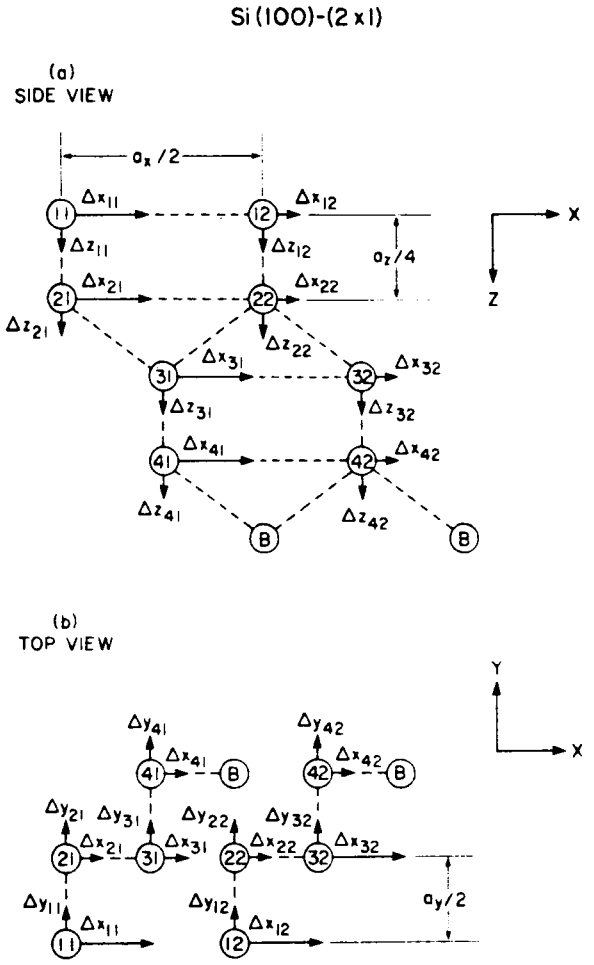


FIG. 15. Schematic diagram of the asymmetric dimer geometry of the (2×1) structure of Si(100). (a) projection of the 2×1 unit cell on {110} plane of bulk Si ($a_x = 7.68$ Å, $a_y = 5.44$ Å) (b) Projection of the 2X1 unit cell on the {001} plane of bulk Si ($a_y = 3.84$ Å) (from Ref. 58). Reprinted with the permission of North-Holland [Surf. Sci. **140**, L269 (1984)—Fig. 1].

*et al.* model[C50] has buckled dimers which have equal and opposite nonzero $y$ displacements. Holland *et al.*[C51] claim that a buckled dimer model does not fit with ion-scattering data.

Ge(100) may have a similar structure.[C21]

TABLE 14. Atomic geometry of the Si(100) (2×1) structure [Parameters are defined in Fig. 15. (From Ref. C51).]

| Atom | Holland *et al.*[a] δx | δy | δz | Yang *et al.*[b] δx | δy | δz |
|---|---|---|---|---|---|---|
| $Si_{11}$ | 0.500 | 0 | 0.250 | 0.650 | −0.300 | 0.045 |
| $Si_{12}$ | −0.900 | 0 | 0.614 | −0.750 | 0.300 | 0.445 |
| $Si_{21}$ | 0.094 | 0 | 0.022 | 0.060 | −0.100 | 0.136 |
| $Si_{22}$ | −0.105 | 0 | −0.055 | −0.102 | 0.100 | 0.136 |
| $Si_{31}$ | −0.016 | 0 | 0.146 | 0 | 0 | 0.208 |
| $Si_{32}$ | −0.002 | 0 | −0.131 | 0 | 0 | −0.152 |
| $Si_{41}$ | 0.026 | 0 | 0.112 | 0 | 0 | 0.100 |
| $Si_{42}$ | −0.032 | 0 | −0.100 | 0 | 0 | −0.100 |

[a] Reference C51.
[b] Reference C50.

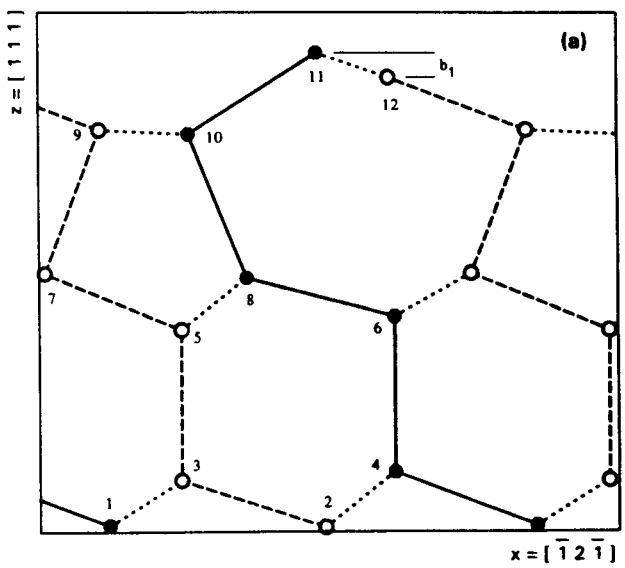


FIG. 16. Schematic diagram of the buckled $\pi$-bonded chain model for the (2×1) structure of Si(111) showing a side view (Ref. C63). Reprinted with the permission of AIP [Phys. Rev. B **30**, 2257 (1984)—Fig. 1].

## A. Si(111)

The Si(111) surface cleaved in vacuum shows a (2×1) LEED pattern that evolves to a (7×7) structure after annealing. The surface relaxes to a (1×1) structure if quenched at high temperatures, stabilized by Te or laser annealed. All these structures have been the subject of intense investigation.

The (1×1) and (7×7) structures show experimental and presumably structural similarities, which have lead some authors[C56] to doubt that the (1×1) structure is simply bulklike as earlier thought.[C52–54]

Many models involving buckling,[C57,C58,C61] molecular[C62] and $\pi$-bonded chains,[C59] and conjugated chains[C63] have been proposed to account for the (2×1) LEED pattern observed from cleaved Si(111). The most recent study using a relatively large normal incidence database and an R-factor analysis by Himpsel *et al.*[C63] favors a modified $\pi$-bonded chain model in which the outer chain is buckled with an

TABLE 15. Atomic geometry for the buckled $\pi$-bonded chain model of (2×1)Si(111) {The x,y,z coordinates (Å) refer to the [−12−1], [−101], and [111] directions shown in Fig. 16 with the origin at a third layer atoms of the truncated bulk lattice (from Ref. C63).}

| Atom | x | y | z |
|---|---|---|---|
| 1 | 1.09 | 1.92 | −3.90 |
| 2 | 4.45 | 0.0 | −3.93 |
| 3 | 2.21 | 0.0 | −3.21 |
| 4 | 5.54 | 1.92 | −3.08 |
| 5 | 2.22 | 0.0 | −0.89 |
| 6 | 5.54 | 1.92 | −0.69 |
| 7 | 0.09 | 0.0 | −0.02 |
| 8 | 3.24 | 1.92 | −0.09 |
| 9 | 0.95 | 0.0 | 2.18 |
| 10 | 2.34 | 1.92 | 2.11 |
| 11 | 4.34 | 1.92 | 3.37 |
| 12 | 5.46 | 0.0 | 2.99 |

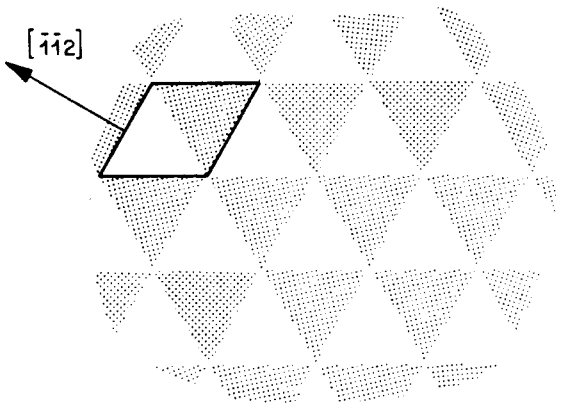


FIG. 17. Triangular checkerboard structure for the Si(111) (7×7) surface (from Ref. C69). Reprinted with the permission of North-Holland [Surf. Sci. **147**, 663 (1984)—Figs. 1 and 2].

overall compression. This structure is detailed in Fig. 16 and Table 15.

The (7×7) reconstruction of Si(111) has such a large unit cell that full-scale multiple scattering LEED calculations are not practicable and investigators have had to rely upon kinematical approximation methods. Much evidence concerning this surface has come from other techniques than LEED and will be the subject of a forthcoming review.[57] The latest study by McRae[C69] favors a triangular checkerboard structure (Fig. 17) of dimers formed by pairing surface Si atoms with stacking faults that produce a roughly 50:50 mixture of AaBb|A and AaCa|A stacking sequences. The topological requirements of joining double layers across the subunit boundaries leads to the prediction of a 6.3 Å deep hole at the apex of the subunit as shown in Fig. 18(a). In addition there are arrays of alternating dimers and deep holes along the subunit sides [Fig. 18(b)].

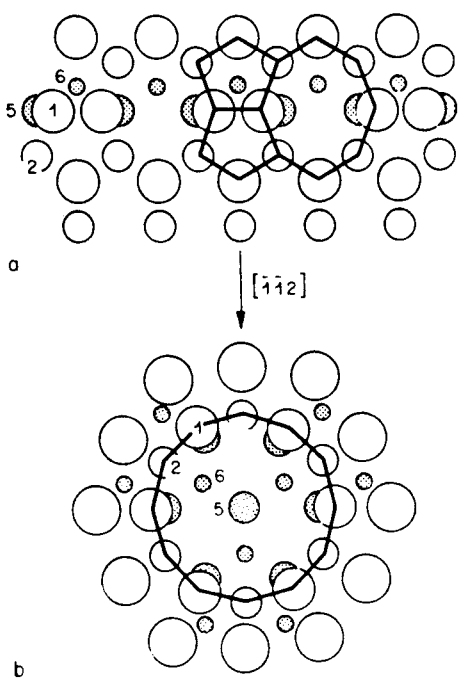


FIG. 18. Schematic diagram of the Si(111) (7×7) structure (from Ref. C69). Numbers index atomic layers. (a) Plan view showing joining of double layers at the edge of a triangular island. Dimers are formed by pairing atoms common to each pair of five-membered rings. (b) Plan view showing the apex structure of a hole in a 12-membered ring. Reprinted with the permission of North-Holland [Surf. Sci. **147**, 663 (1984)—Figs. 1 and 2].

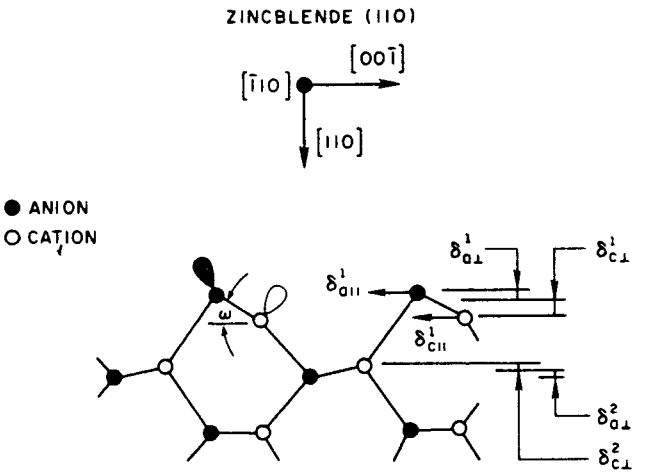


FIG. 19. Schematic diagram of the relaxed zincblende (110) surface (from Ref. 59). Reprinted with the permission of North-Holland [Surf. Sci. **168**, 1 (1986)—Fig. 1].

B. The zincblende structures [GaAs(110)-type]

The structure of the (110) cleavage faces of a large number of zincblende semiconductors have been studied, principally by Duke and co-workers. Nearly all these studies have fulfilled most of the criteria for highly reliable LEED determinations. In all cases, a large amount of normal incidence data was measured, but, given the complexity of the structure of this type of surface, it is probably not reasonable to expect investigators to able to utilize off-normal incidence data.

These surfaces are nonpolar and, unlike the Si surfaces, in all cases the surface unit mesh is the size and symmetry expected for a truncated bulk structure. However, it was soon discovered that GaAs(110), the first member of this series to be investigated, was in fact reconstructed in a subtle manner. Although the details of the GaAs structure took some time to resolve, the major structural elements are now well established.

A schematic diagram of the GaAs(110) structure is reproduced in Fig. 19. The surface is relaxed from its bulk configuration through bond rotations (w) in the first bilayer of about 27°, which induce vertical and horizontal displacements of surface atoms, resulting in a small contraction of the top bilayer towards the bulk. The effect spreads into the second layer where smaller bond rotations occur in the opposite sense. This type of reconstruction actually serves to conserve the bulk bondlengths to within a few percent.

The (110) surfaces of most semiconductors of this type have been found to have GaAs-type structures. Table 16 shows the details of their structures. Bond rotations vary only by 5°. The first layer vertical shear, $(\delta_a + \delta_c)$ in Table 16, and the bond rotation angle increase with the lattice constant of the crystal. Although not listed in Table 16, the $(10\bar{1}0)$ surfaces of ZnO and Te have a similar structure.

TABLE 16. Atomic geometries of zincblende (110) surfaces determined by LEED crystallography [Parameters are defined in Fig. 19 (After Ref. 59).]

| | Lattice constant $a_0$ (Å) | Layer | $\delta_a$ (Å) | $\delta_c$ (Å) | $\delta_a$ (Å) | $\delta_c$ (Å) | $w$ (deg) | Ref. |
|---|---|---|---|---|---|---|---|---|
| AlP | 5.450 | 1 | ↑0.06 | ↓0.57 | −0.21 | −0.24 | | Cl |
| | | 2 | ↓0.04 | ↑0.04 | ... | ... | 25.2 | |
| AlAs | 5.660 | 1 | ↑0.04 | ↓0.61 | −0.33 | −0.49 | | C2 |
| | | 2 | ↓0.06 | ↑0.06 | 0.0 | 0.0 | 27.3 | |
| CdTe | 6.480 | 1 | ↑0.18 | ↓0.64 | −0.39 | −0.61 | | C6 |
| | | 2 | ↓0.09 | ↓0.09 | 0.0 | 0.0 | 30.5 | |
| GaAs | 5.654 | 1 | ↑0.14 | ↓0.51 | −0.33 | −0.49 | | C8–13 |
| | | 2 | ↓0.06 | ↑0.06 | 0.0 | 0.0 | 27.3 | |
| GaP | 5.451 | 1 | ↑0.09 | ↓0.54 | −0.32 | −0.47 | | C16–19 |
| | | 2 | 0.0 | 0.0 | 0.0 | 0.0 | 27.5 | |
| GaSb | 6.095 | 1 | ↑0.22 | ↓0.55 | −0.38 | −0.58 | | C20 |
| | | 2 | 0.0 | 0.0 | 0.0 | 0.0 | 30 | |
| InAs | 6.058 | 1 | ↑0.22 | ↓0.56 | −0.13 | −0.57 | | C22 |
| | | 2 | ↓0.07 | ↑0.07 | 0.0 | 0.0 | 31 | |
| InP | 5.869 | 1 | ↑0.06 | ↓0.63 | −0.34 | −0.54 | | C23–C24 |
| | | 2 | ↓0.07 | ↑0.07 | 0.0 | 0.0 | 28.1 | |
| InSb | 6.478 | 1 | ↑0.18 | ↓0.60 | −0.38 | −0.58 | | C25 |
| | | 2 | ↓0.09 | ↑0.09 | 0.0 | 0.0 | 28.8 | |
| ZnS | 5.409 | 1 | ↑0.07 | ↓0.55 | −0.20 | −0.20 | | C76 |
| | | 2 | 0.0 | 0.0 | 0.0 | 0.0 | 25 | |
| ZnTe | 6.089 | 1 | ↑0.16 | ↓0.55 | −0.36 | −0.54 | | C79-C80 |
| | | 2 | ↓0.03 | ↑0.03 | 0.0 | 0.0 | 28 | |

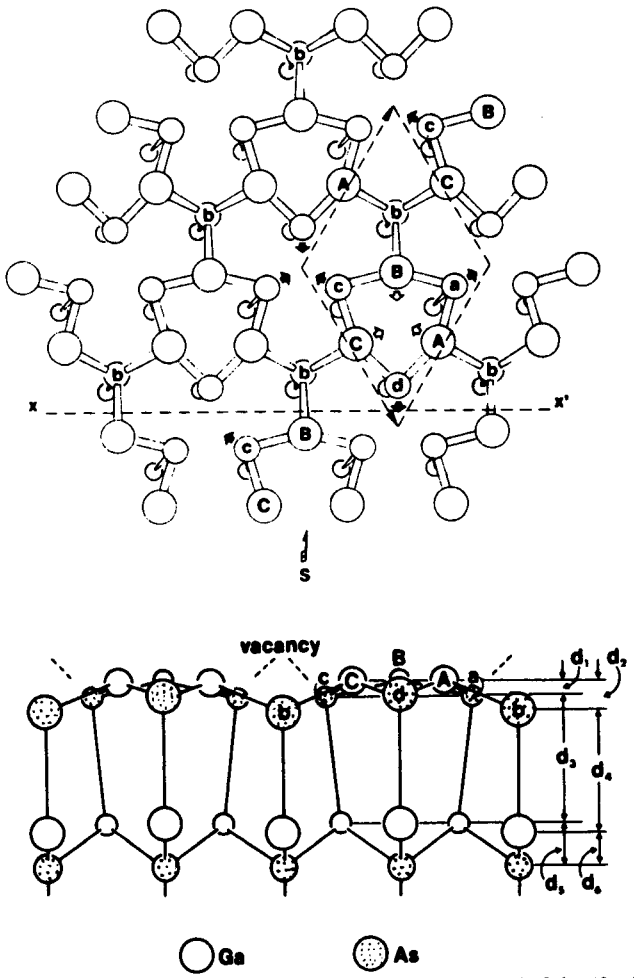


FIG. 20. Schematic diagram of the vacancy buckling model of the (2×2) reconstruction of GaAs and GaP(111) (from Ref. C15): (a) top view and (b) side view. Reprinted with the permission of AIP [Phys. Rev. Lett. **52**, 1693 (1984)—Figs. 1 and 2].

There may however, be exceptions to this rule. The structure of ZnSe may have a structure with large (29°) or a small (4°) bond rotation.

C. The (111) surfaces of GaAs and GaP

These surfaces are monopolar and consist in the bulk of alternating planes of the Group III and V elements. Both surfaces show a (2×2) reconstruction which Tong *et al.*[C15,C19] have ascribed to a vacancy buckling structure in which a quarter of the surface Ga atoms are missing and the surface Ga–*X* bilayer is almost co-planar as shown in Fig. 20.

TABLE 17. Atomic displacements from bulk positions for the vacancy buckling model of the (2×2) reconstructed surfaces of GaAs and GaP(111) [Notation as defined in Fig. 20 (from Refs. C15 and C19).]

| | Atoms | Vertical displacement (Å) up(+), down(−) | Lateral displacement (Å) |
|---|---|---|---|
| GaAs(111) | | | |
| First bilayer | Ga (missing) | | |
| | Ga (A,B,C) | −0.706 | 0.10 |
| | As (a,c,d) | 0.04 | 0.28 |
| | As (d) | −0.08 | 0.0 |
| Second bilayer | Ga (open) | 0.01 | 0.0 |
| | Ga (hatched) | 0.0 | 0.0 |
| | As (not shown) | 0.0 | 0.0 |
| GaP(111) | | | |
| First bilayer | Ga (missing) | | |
| | Ga (A,B,C) | −0.746 | 0.136 |
| | P (a,c,d) | 0.04 | 0.115 |
| | P (d) | −0.05 | 0.0 |
| Second bilayer | Ga (open) | 0.02 | 0.0 |
| | Ga (hatched) | −0.09 | 0.0 |
| | P (not shown) | 0.0 | 0.0 |

TABLE 18. Interlayer distances in the vacancy buckling structure for the (2×2) reconstruction of GaAs and GaP(111) [Distances are in Å and defined in Fig. 20 (from Refs. C15 and C19)].

| | $d_1$ | $d_2$ | $d_3$ | $d_4$ | $d_5$ | $d_6$ |
|---|---|---|---|---|---|---|
| GaAs | 0.07 | 0.20 | 2.48 | 2.44 | 0.83 | 0.74 |
| GaP | 0.0 | 0.09 | 2.49 | 2.38 | 0.62 | 0.61 |

These views show three atomic layers; A,B,C are surface layer Ga atoms while a,b,c, and d are As atoms in the layer below. In the third layer Ga atoms are shown by open and hatched circles.

In this model of the reconstruction vertical and lateral displacements of atoms persist into the second bilayer as detailed in Tables 17 and 18. These studies also relied on normal incidence data.

#### 4.4.c.2. Other Nonmetallic Substrates

Most other LEED investigations on nonmetallic substrates have centered on layer compounds and cubic binary oxides.

Both $MoS_2$ and $NbSe_2$ have been the subject of a R-factor assisted study, though it was somewhat limited in the extent of the database.[C34,C35] Both materials remained unreconstructed except for a small narrowing of the Van der Waals gap.

TABLE 19. LEED results for the (100) surface of some divalent metal oxidesa. [Relaxation and rumple are defined in terms of the fractional anion and cation core displacements $e_1$ and $e_2$ with relaxation $= 0.5(e_1 + e_2)$ and rumple $= (e_1 - e_2)$ as a percentage of the bulk interlayer spacing (from (Ref. 60).]

| | Relaxation (%) | Rumple (%) | Reference |
|---|---|---|---|
| CaO(100) | −1 to −3 | 0 to +2 | C5 |
| MgO(100) | 0 to −3 | 0 to +5 | C32 |
| NiO(100) | 0 to −3 | −5 to +5 | C37 |
| | 0 to −3 | 0 to −3 | C39 |

The (100) surfaces of the oxides of Ca, Mg, and Ni have been examined[C5,C32,C39] using large databases and R-factors. These neutral NaCl-type surfaces might be expected to show differential relaxations or rumplings, driven by the different polarizabilities of the two ions. The LEED calculations were not very sensitive to the choice of starting wavefunction (ionic or neutral atom) or muffin-tin radii used in the construction of the phase shifts compared to small changes in structural parameters. A summary of these results is given in Table 19.

TABLE 20. (Summary Table D) Nonmetal/adsorbate systems

| Substrate | Surface | Ads. | Structure | Ref. | S | Crys. | Anal. meth. | Cont. level | Data coll. | Ang. | Normal | Calc. | Mod. | R-factor | Vor | Rating | d0 | Bond length | Comments |
|---|---|---|---|---|---|---|---|---|---|---|---|---|---|---|---|---|---|---|---|
| C | 0001 | Ar/Kr | — | 1 | — | — | — | — | SP | 1 | 1 | KIN | — | — | — | C+ | 3.2(0.1)Ar<br>3.3(0.1)Kr | — | Physisorbed at 40–50 K. Kr result ambiguous. |
| C | 0001 | K | (1×1) | 2 | — | — | AES | 6% O | SP | 1 | 2(1) | RSP | 3 | — | — | C+ | — | — | K from hot molecular beam sources; 1% step density. Disordered K intercalates and induces shear shift of C layers and a dilation from 3.35 to 5.35 Å in d1. |
| GaAs | 110 | Al | (1×1) | 3 | 2 | — | AES | — | SP | 1 | 10(5) | MI | 5 | 0.30(ZJ)<br>0.25(Rx) | — | A– | — | — | With 450 C anneal, Al replaces Ga in 2nd layer and lower layers with little change in GaAs structure; not chemisorbed. |
| GaAs | 110 | Sb | (1×1) | 4 | 2 | H | AES | Low | SP | 1 | 14(9) | MI | 5 | 0.20(Rx) | −10 | A– | — | 2.6(0.17) Ga–Sb<br>2.7(0.17) As–Sb | Chains of Sb atoms occupy Ba and As sites on unrelaxed surface. No differences between sputter-annealed and cleaved surfaces |
| InP | 110 | Sb | (1×1) | 5 | | H | AES | Low | SP | 1 | 14(9) | MI | 4 | 0.25(Rx) | −9 | A– | — | 2.86 In–Sb<br>2.49 P–Sb | Sb atoms occupy normal In, P sites in top layer on top of unrelaxed InP. Vertical displacement of Sb not clear. |
| Si | 100 | H | (1×1) | 6 | 1 | H(P) | AES | Low | FC | Many | 3(0) | CMTA | — | — | −10 | B– | — | — | Surface unreconstructured ; d1 contracted by 10%. |
| Si | 100 | H | (1×1) | 7 | 1 | — | AES | Low | FC | 2 | 3(0) | RSP | 1 | — | −4 | B– | — | — | Unreconstructed surface. |
| Si | 111 | Ag | $(\sqrt{3}\times\sqrt{3})$R30 | 8 | 1 | H(P) | — | — | SP | Many | 1(0) | CMTA | 3 | — | −11 | C+ | — | — | Ag embedded in topmost Si layer by 0.7Å; Si reconstructed down to 4 layers. |
| Si | 111 | Ag | (3×1) | 8 | 1 | H(P) | — | — | SP | Many | 1(0) | CMTA | 3 | — | −11 | C+ | — | — | Ag atoms adsorbed in unknown site with less reconstruction. |
| Si | 111 | Ni | (1×1) | 9 | 1 | H | AES | — | — | 2 | 4(0) | — | — | — | — | B– | — | — | Below threshold coverage, LEED data same as for quenched Si(111). Above 6 ML $NiSi_2$ forms; top layer contains only Si. Ni in 2nd layer rotated by 180 degrees; d1 contracted by 25%. |

#### 4.5.b. References to Table 20—Nonmetal/adsorbate systems

[1]C.G. Shaw, S.C. Fain, Jr., M.D. Chinn, and M.F. Toney, Surf. Sci. **97**, 128 (1980).
[2]N.J. Wu and A. Ignatiev, Phys. Rev. B **28**, 7288 (1983).
[3]A. Kahn, D. Kanani, J. Carelli, J. L. Yeh, C. B. Duke, R. J. Meyer, and A. Paton, J. Vac. Sci. Technol. **18**, 792 (1981).
[4]C.B. Duke, A. Paton, W.K. Ford, A. Kahn, and J. Carelli, Phys. Rev. **26**, 803 (1982).
[5]C.B. Duke, C. Mailhot, A. Paton, K. Li, C. Bonapace, and A. Kahn, Surf. Sci. **163**, 391 (1985).
[6]S.J. White and D.P. Woodruff, Surf. Sci. **63**, 254 (1977).
[7]S.J. White, D.P. Woodruff, B.W. Holland, and R.S. Zimmer, Surf. Sci. **74**, 34 (1978).
[8]Y. Terada, T. Yoshizuka, K. Oura, and T. Hanawa, Surf. Sci. **114**, 65 (1982).
[9]W.S. Yang, F. Jona, and P.M. Marcus, Phys. Rev. **28**, 7377 (1983).

#### 4.5.c. Notes on Nonmetal/Adsorbate Systems

Compared with the metals, studies of adsorption structures on nonmetals are rare. This may well be due to the difficulty of solving the structures of many clean nonmetal surfaces, e.g., GaAs, Si (see Sec. 4.4). As Table 20 shows, other than a couple of studies on physisorption and intercalation into graphite, investigations of such systems is limited to semiconductor systems. Moreover, many of these systems do not result in chemisorbed structures of the type frequently seen in the metals.

The only investigations which employed reasonably large datasets involve GaAs and InP substrates (Table 20, Refs. 3–5) and refer to epitaxial-type adsorption experiments where atomic adsorbates such as Al, Sb replace surface atoms on top of an unrelaxed substrate. The H–Si studies (Table 20, Ref. 6; Table 20, Ref. 7) really are clean surface studies in that the scattering properties of the H atoms were not included.

## 5. Acknowledgments

The author gratefully acknowledges the help of Ms. Jill Price, Ms. Sharon Lee, and Mr. John Mischenko in locating many of the papers. This work was supported by the National Bureau of Standards Critical Compilation of Physical and Chemical Reference Data Program through Grant No. 60NANB6D0616.

## 6. References

[1]J. B. Pendry, *Low Energy Electron Diffraction* (Academic, London, 1974).
[2]L. J. Clarke, *Surface Crystallography: An Introduction to Low Energy Electron Diffraction* (Wiley, Chichester, 1985).
[3]*The Structure of Surfaces*, edited by M. A. Van Hove, and S. Y. Tong, Springer Series in Surface Sciences Vol. 2 (Springer, Berlin, 1985).
[4]J. A. Strozier, Jr., D. W. Jepsen, and F. Jona, in *Surface Physics of Materials*, edited by J. M. Blakely, (Academic, New York, 1975), Vol. I, p. 1.
[5]S. Y. Tong, Prog. Surf. Sci. **7**, 1 (1975).
[6]P. M. Marcus, in *Advances in Characterization of Metal and Polymer Surfaces*, edited by L. H. Lee (Academic, New York, 1976).
[7]F. Jona and P. M. Marcus, Commun. Solid State Phys. **8**, 1 (1977).
[8]F. Jona, Surface Sci. **68**, 204 (1977).
[9]S. Y. Tong, in *Electron Diffraction 1927–77*, edited by P. J. Dobson *et al.* (The Institute of Physics, London, 1977), p. 270.
[10]F. Jona, J. Phys. C **11**, 4271 (1978).
[11]M. A. Van Hove and S. Y. Tong, *Surface Crystallography by LEED*, Springer Series in Chemical Physics, Vol. 2, (Springer, Berlin, 1978).
[12]M. A. Van Hove, Surf. Sci. **81**, 1 (1979).
[13]G. A. Somorjai and M. A. van Hove, *Adsorbed Monolayers on Surfaces* (Springer, Berlin, 1981).
[14]P. M. Marcus, Appl. Surf. Sci. **13**, 20 (1982).
[15]J. E. Inglesfield, Prog. Surf. Sci. **20**, 105 (1985).
[16]J. M. MacLaren, J. B. Pendry, P. J. Rous, D. K. Saldin, D. D. Vredensky, G. A. Somorjai, and M. A. Van Hove, *Surface Crystallography Information Service* (Kluwer, Norwell, MA , 1987).
[17]P. R. Watson, Ph. D. thesis, University of British Columbia, 1979.
[18]*Methods of Surface Analysis*, edited by A. W. Czanderna (Elsevier, Amsterdam, 1975).
[19]P. C. Stair, T. J. Kaminska, L. L. Kesmodel, and G. A. Somorjai, Phys. Rev. B **11**, 623 (1975).
[20]T. N. Tommet, G. B. Olszewski, P. A. Chadwick, and S. L. Bernasek, Rev. Sci. Instrum. **50**, 147 (1979).
[21]D. C. Frost, K. A. R. Mitchell, F. R. Shepherd, and P. R. Watson, J. Vac. Sci. Technol. **13**, 1196 (1976).
[22]P. Heilmann, E. Lang, K. Heinz, and K. Müller, Appl. Phys. **9**, 247 (1976).
[23]D. G. Welkie and M. G. Lagally, Appl. Surf. Sci. **3**, 272 (1979).
[24]P. C. Stair, Rev. Sci. Instrum. **51**, 132 (1980).
[25]M. B. Webb and M. G. Lagally, Solid State Phys. **28**, 301 (1973).
[26]D. L. Adams and U. Landman, Phys. Rev. Lett. **33**, 585 (1974).
[27]U. Landman and D. L. Adams, J. Vac. Sci. Technol. **11**, 195 (1974).
[28]D. L. Adams, U. Landman, and J. C. Hamilton, J. Vac. Sci. Technol. **12**, 260 (1975).
[29]V. L. Moruzzi, A. F. Janak, and A. R. Williams, *Calculated Electronic Properties of Metals* (Pergamon, New York, 1978).
[30]H. D. Shih, in *Determination of Surface Structures by LEED*, edited by P. M. Marcus and F. Jona (Plenum, New York, 1983), p. 67.
[31]D. W. Jepsen and F. Jona, Phys. Rev. B **5**, 3933 (1972).
[32]K. O. Legg, F. Jona, D. W. Jepsen, and P. M. Marcus, J. Phys. C **10**, 937 (1977).
[33]D. W. Jepsen, Phys. Rev. B **22**, 5701 (1980).
[34]G. E. Laramore and C. B. Duke, Phys. Rev. B **5**, 267 (1972).
[35]R. J. Meyer, C. B. Duke, A. Paton, A. Kahn, E. So, J. L Yeh, and P. Mark, Phys. Rev. B **19**, 5194 (1979).
[36]C. B. Duke and G. E. Laramore, Phys. Rev. B **2**, 4765 (1970).
[37]D. J. Titterington and C. G. Kinniburgh, Comp. Phys. Commun. **20**, 237 (1980).
[38]B. W. Holland and R. S. Zimmer, J. Phys. C **8**, 2395 (1075).
[39]S. Y. Tong and M. A. Van Hove, Phys. Rev. B **16**, 1459 (1977).
[40]M. A. Van Hove, R. Lin, and G. A. Somorjai, Phys. Rev. Lett. **51** 778 (1983).
[41]M. A. Van Hove and G. A. Somorjai, Surf. Sci. **114**, 171 (1982).
[42]T. C. Ngoc, M. G. Lagally, and M. B. Webb, Surf. Sci. **35**, 117 (1973).
[43]C-M. Chan, S. L. Cunningham, M. A. Van Hove, and W. H. Weinberg, Surf. Sci. **67**, 1 (1977).
[44]*Determination of Surface Structures by LEED*, edited bt P. M. Marcus and F. Jona (Plenum, New York, 1984).
[45]G. A. Somorjai, *Chemistry in Two Dimensions: Surfaces* (Cornell University, Ithaca, NY, 1981).
[46]M. A. Van Hove, S. Y. Tong, and M. H. Elconin, Surf. Sci. **64**, 85 (1977).
[47]C. B. Duke, A. Paton, W. K. Ford, A. Kahn, and J. Carelli, Phys. Rev. B **24**, 562 (1981).
[48]E. Zanazzi and F. Jona, Surf. Sci. **62**, 61 (1977).
[49]J. B. Pendry, J. Phys. C **15**, 957 (1980).
[50]D. L. Adams, H. B. Neilsen, and M. A. Van Hove, Phys. Rev. B **20**, 4789 (1979).
[51]J. Phillip and J. Rundgren, in Ref. 44, p. 409.
[52]M. A. Van Hove and R. J. Koestner, in Ref. 44, p. 204.
[53]P. R. Watson, F. R. Shepherd, D. C. Frost, and K. A. R. Mitchell, Surf. Sci. **72**, 562 (1978).
[54]J. B. Pendry and D. K. Saldin, Surf. Sci. **145**, 33 (1984).
[55]R. Feder and J. Kirschner, Surf. Sci. **103**, 75 (1981).
[56]R. J. Koestner, J. C. Frost, P. C. Stair, M. A. Van Hove, and G. A. Somorjai, Surf. Sci. **116**, 85 (1982).
[57]P. R. Watson (submitted).
[58]B. W. Holland, C. B. Duke, and A. Paton, Surf. Sci. **140**, L269 (1984).
[59]A. Kahn, Surf. Sci. **168**, 1 (1986).
[60]M. Prutton, J. A. Walker, M. R. Welton-Cook, and R. C. Felton, Surf. Sci. **89**, 45 (1979).